Scientific Report S-30
September 30, 1974

Prepared for
George C. Marshall Space Flight Center
National Aeronautics and Space Administration
Huntsville, Alabama 35812
Under Contract NAS8-29632/1-3-40-33039(2F)

TELEOPERATOR EQUATIONS

OF MOTION

Principal Investigator: J. C. Hung

Department of Electrical Engineering
The University of Tennessee
Knoxville, Tennessee 37916

(NASA-CR-150043) TELEOPERATOR EQUATIONS OF MOTION (Tennessee Univ.) 126 p N77-70537

Unclas
00/98 55048

126

ACKNOWLEDGMENTS

This volume is a technical report on a study of the equations of motion for a teleoperator system. The study was initiated by the National Aeronautics and Space Administration, George C. Marshall Space Flight Center, and was performed by The University of Tennessee under Contract NAS8-29632 over a period of sixteen months.

The participants of the project at U.T. include Mr. M. H. Kao, Mr. Ali Moazed, and Dr. J. C. Hung. The assistance of Messrs. J. D. Ellsworth, Z. Thompson, and W. G. Thornton, all of NASA/MSFC, are acknowledged.

ABSTRACT

The following contains results of a study on equations of motion for a free-flying teleoperator. Three different kinds of models have been developed and analyzed. Equations for each model were obtained. Computer simulations were performed to demonstrate the adequacy of each model and the correctness of the equations. Very interesting and encouraging results were obtained. Recommendations for further study are given

TABLE OF CONTENTS

LIST OF FIGURES

CHAPTER 1

INTRODUCTION

Extending man's reach in space is one of the goals for the space program. The Space Shuttle, which makes launching of satellites into earth orbit a virtually routine event, will increase man's ability to do work in space while contributing to the economy of space operations. It will be a space transportation system designed to carry out various missions in earth orbit. One possible way to fulfill these mission objectives is to use a teleoperator.

A teleoperator is defined to be a remotely controlled cybernetic man-machine system designed to augment and extend man's sensory, manipulation, and congruitive capabilities to a remote and hostile environment while controlled by a man from a more benign and convenient location such as a nearby spacecraft or a ground based station. The intervention of man in the system can be made "minimal" if the machine possesses sufficient artificial intelligence and dexterity to perform the intended activities. Figure 1-1 shows this concept.[1]

The use of space shuttle and free-flying Teleoperator (FFTO) will allow practical maneuvering of masses in outer space. A satellite that is to be retrieved will generally have some initial angular motion. Before the satellite can be retrieved, it will be necessary to null its angular rates. The angular motion of a satellite can be expressed at any instant as the resultant of a spin component and a tumble component. If one of these components is zero, the satellite is in a state of pure

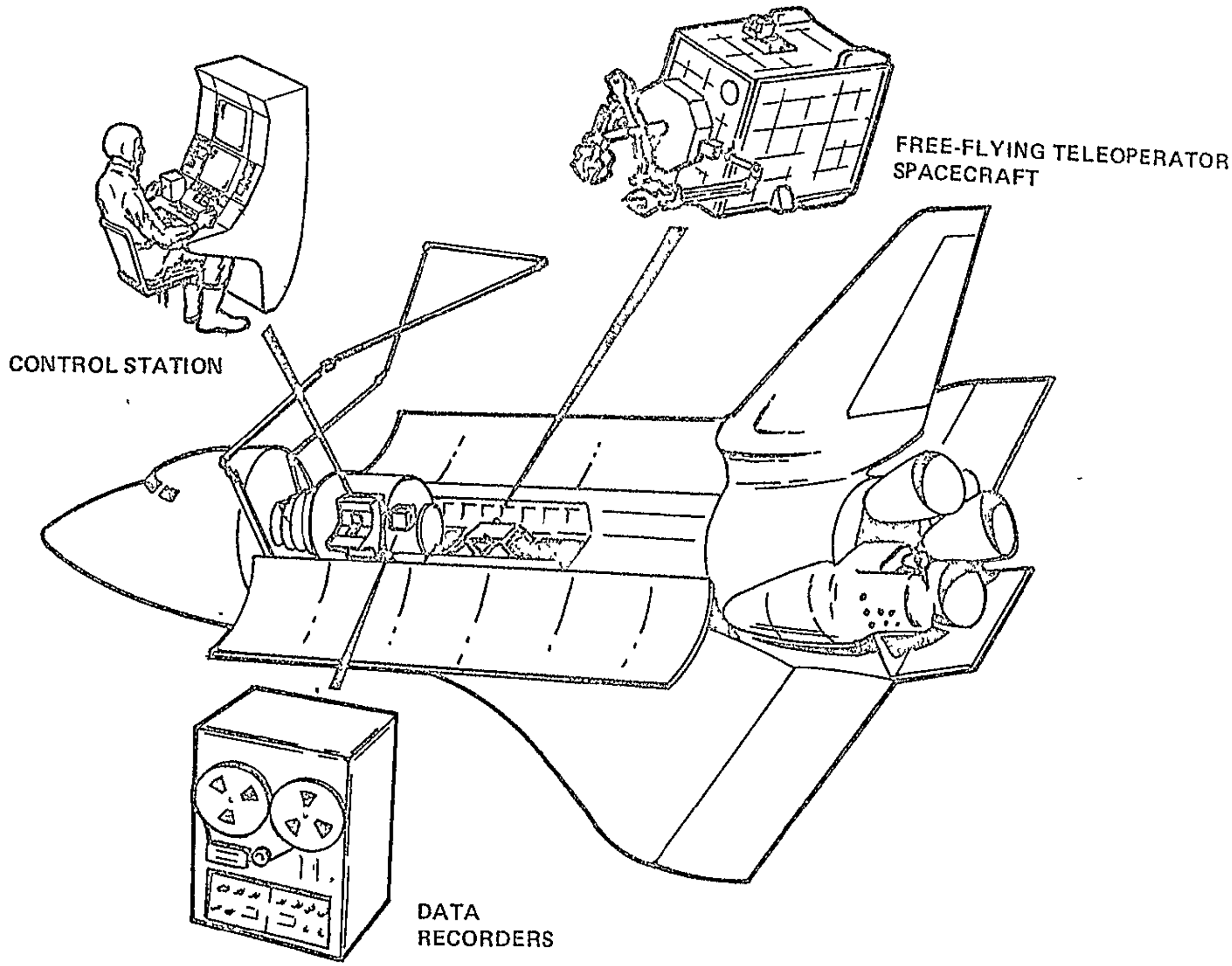

Figure 1-1. Free-Flying Teleoperator Concept

spin or pure tumble. Utilizing a teleoperator to null pure spin or pure tumble is straightforward. The problem is more complicated, however, for the general case where both spin and tumble are present.

If a disturbance-free service is to be performed on a satellite which is functioning normally, the teleoperator needs first to maneuver itself to match to the dynamics of the whole satellite. Furthermore, the arms and hands of the teleoperator also need to catch up with the area on the satellite, where service is to be performed. A detailed knowledge is needed of the required teleoperator maneuvering, including an in-depth analysis of its kinematics and dynamics.

This knowledge is needed of the dynamics of various satellites in their normal operational modes and in their failure modes. For example, when a satellite loses its attitude control, it may have unstabilized three-axis motion such as spinning and tumbling. Knowledge of these dynamics is the prerequisite to the development of teleoperator specifications.

The resulting dynamics of the combined system of teleoperator and satellite, after contact has been made, needs to be studied. The result of this study will determine the attitude requirements for a teleoperator and also provide the information needed for the design of arm and hand mechanisms for successful despinning and detumbling of a satellite.

The purpose of this study is to develop a set of equations which describe the state of the manipulator , the teleoperator, the satellite, and the combination of teleoperator and satellite. These equations will be useful for further study of the teleoperator operation via computer simulations.

Chapter 2 of this report contains the equations relating the position and velocity of the manipulator's hand to its base at teleoperator body.

Chapter 3 describes the nulling of a satellite's initial angular motion under the ideal condition that the teleoperator is stationary.

Chapter 4 presents the set of dynamic equations which describe the combined motion of the teleoperator and the satellite.

Chapter 5 summarizes the results of the study and offers recommendation for further investigation.

All computer programs are written in CSMP (Continuous Simulation Modeling Program). They are included in appendices.

CHAPTER 2

MANIPULATOR KINEMATICS

Manipulator Model

A manipulator model, shown in Figure 2-1, is chosen as the basic model for the present study. This model is composed of two arm sections, a shoulder, and a hand. The manipulator has two bending joints and two swivel joints which are conceptually shown in the figure. Four rotational freedoms exist, they are represented by the angles α_1, α_2, θ_1, and θ_2. Counter-clockwise rotation is considered the positive sense.

Six coordinate frames

$$S_i : (x_i, y_i, z_i) , \quad i = 1 \text{ to } 6 ,$$

are defined in Figure 2-1. Frame S_1 is hand-fixed while frame S_6 is FFTO-fixed. These coordinate frames help to formulate the position and velocity of the hand with respect to various parts of the manipulator.

Position Vectors for Finger Tip and Hand

Referring to Figure 2-1, the finger tip position in coordinate frame S_1 is given by

$$\underline{f}_1 = \begin{bmatrix} x_1 \\ y_1 \\ z_1 \end{bmatrix} = \begin{bmatrix} 0 \\ 0 \\ \ell_1 \end{bmatrix} = \underline{\ell}_1 \qquad (2\text{-}1)$$

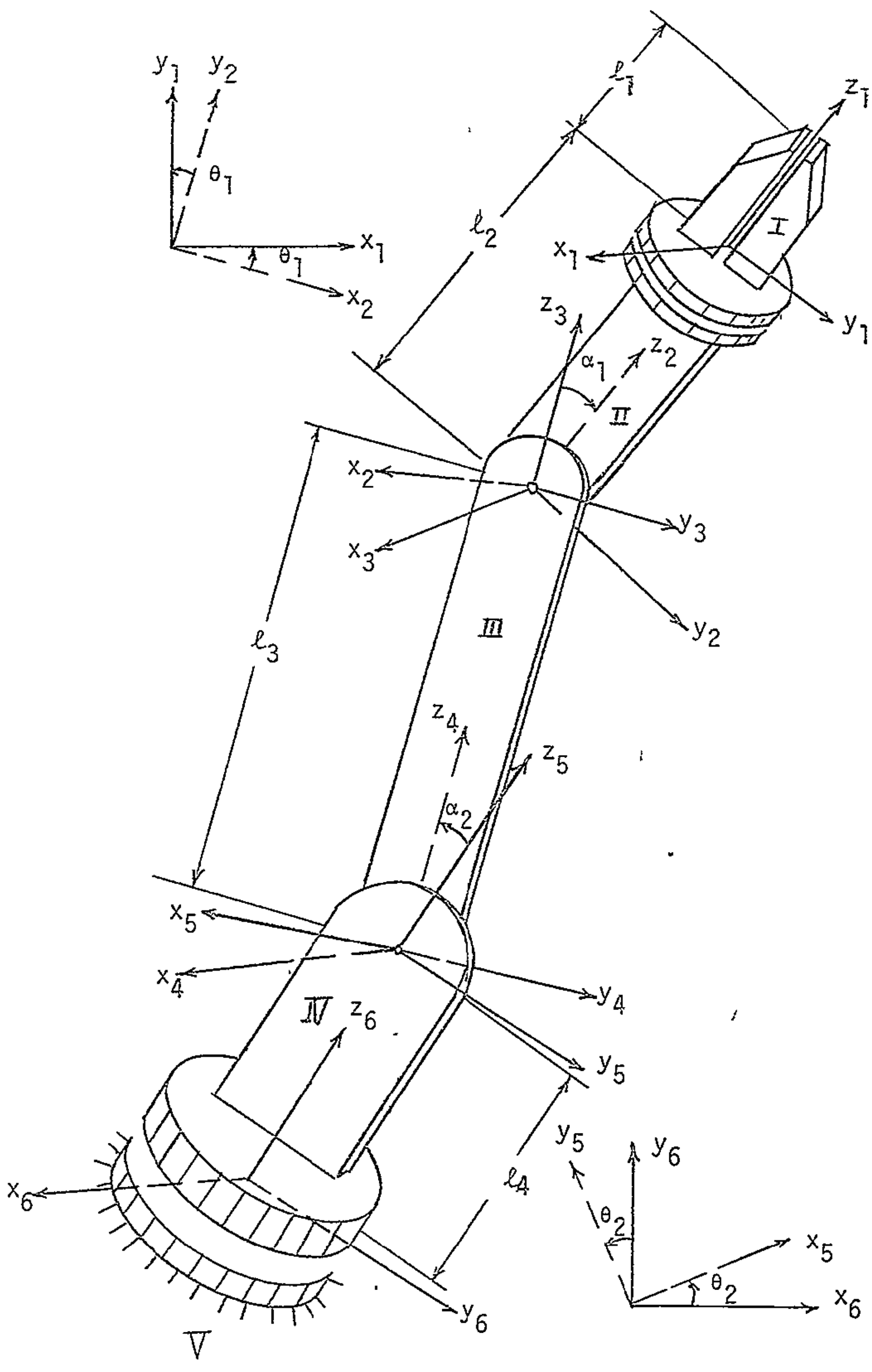

Figure 2-1. The Manipulator

The position in coordinate frame S_2 is obtained from (2-1) through a linear transformation given by

$$\underline{f}_2 = \begin{bmatrix} \cos\theta_1 & -\sin\theta_1 & 0 \\ \sin\theta_1 & \cos\theta_1 & 0 \\ 0 & 0 & 1 \end{bmatrix} \begin{bmatrix} x_1 \\ y_1 \\ z_1+\ell_2 \end{bmatrix}$$

$$= T_{21}\underline{f}_1 + T_{21}\,\underline{\ell}_2 = T_{21}(\underline{\ell}_1 + \underline{\ell}_2) \tag{2-2}$$

where

$$T_{21} = \begin{bmatrix} \cos\theta_1 & -\sin\theta_1 & 0 \\ \sin\theta_1 & \cos\theta_1 & 0 \\ 0 & 0 & 1 \end{bmatrix} \tag{2-3}$$

and

$$\underline{\ell}_2 = [0 \quad 0 \quad \ell_2]^t \tag{2-4}$$

where $[\quad]^t$ represents the transpose of a vector or matrix. The finger tip position in coordinate frame S_3 is

$$\underline{f}_3 = \begin{bmatrix} 1 & 0 & 0 \\ 0 & \cos\alpha_1 & -\sin\alpha_1 \\ 0 & \sin\alpha_1 & \cos\alpha_1 \end{bmatrix} \begin{bmatrix} x_2 \\ y_2 \\ z_2 \end{bmatrix} = T_{32}\underline{f}_2 \tag{2-5}$$

where

$$T_{32} = \begin{bmatrix} 1 & 0 & 0 \\ 0 & \cos\alpha_1 & -\sin\alpha_1 \\ 0 & \sin\alpha_1 & \cos\alpha_1 \end{bmatrix} \tag{2-6}$$

Proceeding in the similar manner we can obtain the finger tip position in coordinate frames S_4, S_5, and S_6 as

$$\underline{f}_4 = \underline{f}_3 + \underline{\ell}_3 \tag{2-7}$$

$$\underline{f}_5 = T_{54}\, \underline{f}_4 \tag{2-8}$$

$$\underline{f}_6 = T_{65}\, (\underline{f}_5 + \underline{\ell}_4) \tag{2-9}$$

where

$$T_{54} = \begin{bmatrix} 1 & 0 & 0 \\ 0 & \cos\alpha_2 & -\sin\alpha_2 \\ 0 & \sin\alpha_2 & \cos\alpha_2 \end{bmatrix} \tag{2-10}$$

$$T_{65} = \begin{bmatrix} \cos\theta_2 & -\sin\theta_2 & 0 \\ \sin\theta_2 & \cos\theta_2 & 0 \\ 0 & 0 & 1 \end{bmatrix} \tag{2-11}$$

$$\underline{\ell}_3 = [0 \quad 0 \quad \ell_3]^t \tag{2-12}$$

and

$$\underline{\ell}_4 = [0 \quad 0 \quad \ell_4]^t \tag{2-13}$$

Combining Equations (2-1) to (2-13), the finger tip position expressed in FFTO-fixed frame is given by

$$\underline{f}_6 = T_{65}T_{54}T_{32}(\underline{\ell}_1 + \underline{\ell}_2) + T_{65}T_{54}\underline{\ell}_3 + T_{65}\underline{\ell}_4 \tag{2-14}$$

By defining

$$\begin{aligned} T_{64} &= T_{65}T_{54} \\ T_{62} &= T_{65}T_{54}T_{32} \end{aligned} \tag{2-15}$$

(2-14) takes the simple form

$$\underline{f}_6 = T_{62}(\underline{\ell}_1 + \underline{\ell}_2) + T_{64}\,\underline{\ell}_3 + T_{65}\underline{\ell}_4 \tag{2-16}$$

Notice that, while $\underline{\ell}_1$, $\underline{\ell}_2$, $\underline{\ell}_3$ and $\underline{\ell}_4$ are constant vectors, all the transformation matrices T_{ij} are variable since they involve variable angles.

The position of hand can be obtained in a similar way. Let $\underline{h}_i$, i = 2 to 6, be the position vector of hand in coordinate frame S_i, we have

$$\underline{h}_2 = \underline{\ell}_2 \tag{2-17}$$

$$\underline{h}_3 = T_{32}\underline{h}_2 \tag{2-18}$$

$$\underline{h}_4 = \underline{h}_3 + \underline{\ell}_3 \tag{2-19}$$

$$\underline{h}_5 = T_{54}\underline{h}_4 \tag{2-20}$$

$$\underline{h}_6 = T_{65}\ (\underline{h}_5 + \underline{\ell}_4) \tag{2-21}$$

Combining (2-17) to (2-21), gives the hand position expressed in FFTO-frame

$$\underline{h}_6 = T_{62}\,\underline{\ell}_2 + T_{64}\,\underline{\ell}_3 + T_{65}\,\underline{\ell}_4 \tag{2-22}$$

Velocity Vectors for Manipulator's Finger Tip and Hand

By taking the derivative of (2-16) and (2-22) the velocity vectors for manipulator's finger tip and hand are given by, respectively,

$$\dot{\underline{f}}_6 = \dot{T}_{62}\ (\underline{\ell}_1 + \underline{\ell}_2) + \dot{T}_{64}\,\underline{\ell}_3 + \dot{T}_{65}\,\underline{\ell}_4 \tag{2-23}$$

and

$$\dot{\underline{h}}_6 = \dot{T}_{62}\,\underline{\ell}_2 + \dot{T}_{64}\,\underline{\ell}_3 + \dot{T}_{65}\,\underline{\ell}_4 \tag{2-24}$$

Both (2-23) and (2-24) are functions of angular rates $\dot{\theta}_2$, $\dot{\alpha}_1$ and $\dot{\alpha}_2$.

Acceleration Vectors for Finger Tip and Hand

By taking the derivative of (2-23) and (2-24) the acceleration vectors for manipulators finger tip and hand are obtained

$$\ddot{\underline{f}}_6 = \ddot{T}_{62}\,(\underline{\ell}_1 + \underline{\ell}_2) + \ddot{T}_{64}\,\underline{\ell}_3 + \ddot{T}_{65}\,\underline{\ell}_4 \tag{2-25}$$

$$\ddot{\underline{h}}_6 = \ddot{T}_{62}\,\underline{\ell}_2 + \ddot{T}_{64}\,\underline{\ell}_3 + \ddot{T}_{65}\,\underline{\ell}_4 \tag{2-26}$$

Uniqueness Consideration

Corresponding to a given set of angles θ_2, α_1 and α_2 the hand position $\underline{h}_6$ and finger tip position $\underline{f}_6$ are unique. On the other hand, given a desired hand or finger tip position, the set of angles is in general not unique. The non-uniqueness creates ambiguity in generating control signals. This difficulty can be eliminated by defining a specific sequence of angular rotations at different joints.

Define a set of polar coordinates for each coordinate frame as shown in Figure 2-2 where the coordinates are represented by (r_i, θ_i, ψ_i), $i = 1$ to 6. Then a possible sequence of angular movement can be established as follows.

1. At the beginning, the manipulator is in a folded position.
2. For a given $\underline{f}_6$, the desired distance f_5 between the shoulder bending joint and the finger tip can be determined from

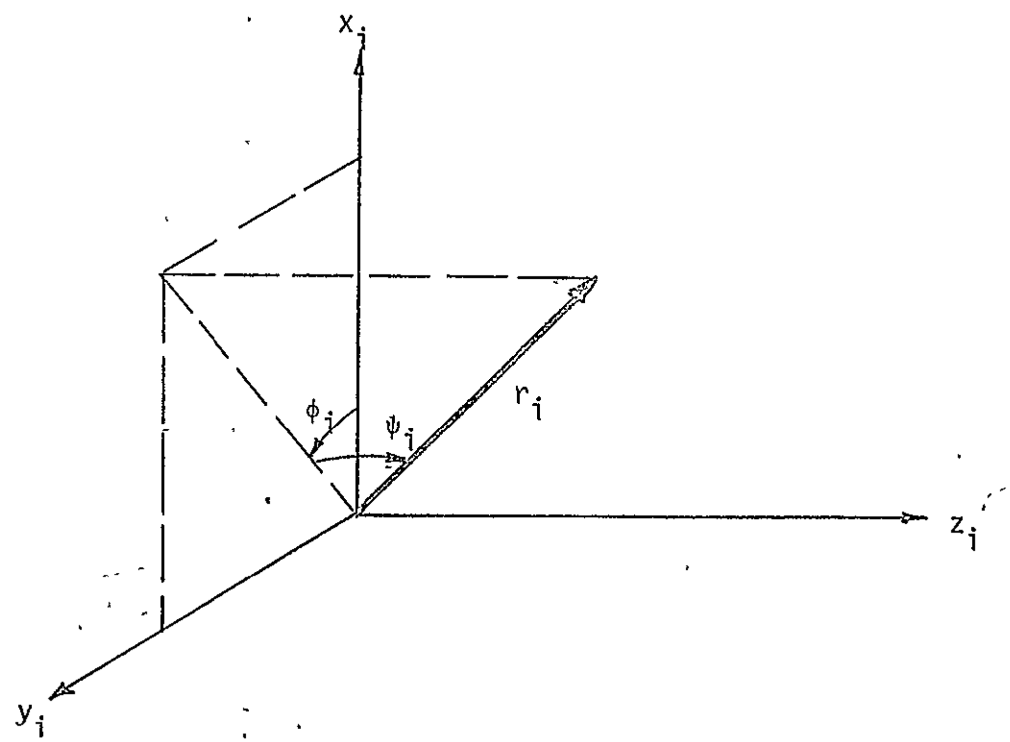

Figure 2-2. Polar Coordinates (i

$$f_5 = \left|\underline{f}_6 - \underline{\ell}_4\right| \tag{2-25}$$

3. Rotate the base swivel joint until $\theta_2 = \phi_6$.
4. Rotate the forearm bending joint, in the direction where α_1 is positive, until the distance f_5 is obtained.
5. Rotate the shoulder bending joint until $\alpha_2 = \psi_5$.

   The finger tip is now at the desired position.

If it is desired to catch the object with the hand oriented in a different direction, the direction of the angle α_1, in Step 4 can be reversed.

If visual aid equipment is available, the control of hand position is made easier with the help of remote human guidance.

CHAPTER 3

SATELLITE'S EQUATIONS OF MOTION

1. PRELIMINARY REMARKS

A satellite is assumed to possess an initial angular velocity which is the combined motion of tumbling and spinning. An external moment is applied on the satellite to despin and detumble until its angular velocity is nulled. There are several ways to accomplish the despin-detumble operation. The dynamics of the satellite during despin-detumble process is studied in this chapter. The study includes the development of the satellite's equations of motion for different cases. Methods of applying external moments are discussed. Then, computer simulations are made to reveal the dynamic properties.

It should be mentioned that some of the results of this chapter are available in Reference 4. But the derivation is different. Furthermore, the inclusion of this study allows a better understanding of the operation of a teleoperator system.

2. EQUATIONS OF ROTATIONAL MOTION

This section presents the general equations of rotational motion for the satellite. Referring to Figure 3-1, two coordinate frames are defined. The inertial coordinates are denoted by (X, Y, Z) while the body coordinates are denoted by (x, y, z). The origin O of the body frame is at the center of mass of the satellite.

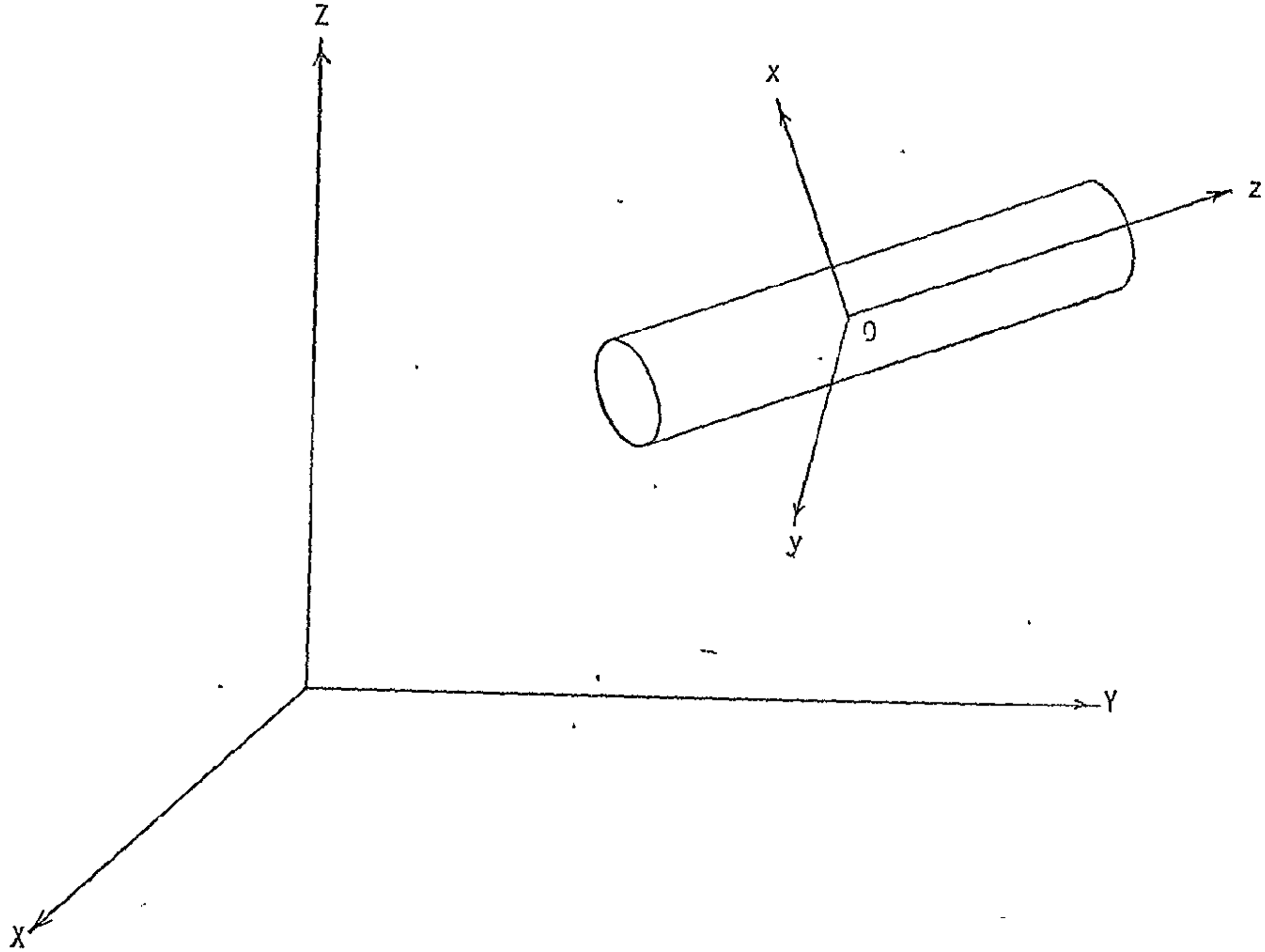

Figure 3-1. Inertial and Body Coordinates

The equations of rotational motion can then be written as[7]

$$M_x = I_{xx}\,\dot{\omega}_x + I_{xy}(\dot{\omega}_y - \omega_x\omega_z) + I_{xz}(\dot{\omega}_z + \omega_x\omega_y)$$

$$+ (I_{zz} - I_{yy})\,\omega_y\omega_z + I_{yz}(\omega_y^2 - \omega_z^2) \qquad (3\text{-}1)$$

$$M_y = I_{xy}(\dot{\omega}_x + \omega_y\omega_z) + I_{yy}\,\dot{\omega}_y + I_{yz}(\dot{\omega}_z - \omega_x\omega_y)$$

$$+ (I_{xx} - I_{zz})\,\omega_x\omega_z + I_{xz}(\omega_z^2 - \omega_x^2) \qquad (3\text{-}2)$$

$$M_z = I_{xz}(\dot{\omega}_x - \omega_y\omega_z) + I_{yz}(\dot{\omega}_y + \omega_x\omega_z) + I_{zz}\,\dot{\omega}_z$$

$$+ (I_{yy} - I_{xx})\,\omega_x\omega_y + I_{xy}(\omega_x^2 - \omega_y^2) \qquad (3\text{-}3)$$

In these equations, ω_x, ω_y, ω_z are absolute body angular rates along body coordinates x, y, z, respectively. I_{xx}, I_{yy}, and I_{zz} are moments of inertia of the satellite, taken with respect to x, y, and z axes. I_{xy}, I_{yz}, and I_{xz} are products of inertia. M_x, M_y, and M_z are applied moments along x, y, and z axes.

For a given set of initial conditions and a known applied moment $\underline{M} = [M_x, M_y, M_z]^t$, one can, in theory, solve for $\underline{\omega} = [\omega_x, \omega_y, \omega_z]$ as a function of time. In general, however, this is a difficult procedure. On the other hand, if the angular rate $\underline{\omega}$ is given, the calculation of the required external moment is usually a straightforward procedure.

It should be noted that the time integrals of ω_x, ω_y, and ω_z do not correspond to any physical angles which might be used to give the orientation of the body. To solve for the orientation, one must transform continuously to another set of coordinates. Or, one may solve the rotational equations in terms of the other coordinates from the beginning. One set of such other coordinates are the set of three Euler angles. They are three successive angular displacements which can carry out the transformation from one Cartesian system of axes to another. The three body angular rates ω_x, ω_y, and ω_z can be expressed in terms of Euler angles and their time derivatives.

The Euler angles used in this study are ψ, θ, and ϕ, in the sequence as shown in Figure 3-2. The transformation from X, Y, Z to ξ', η', ζ' system, representing a rotation of angle ψ about the Z-axis, is

$$\begin{bmatrix} \xi' \\ \eta' \\ \zeta' \end{bmatrix} = \begin{bmatrix} \cos\psi & \sin\psi & 0 \\ -\sin\psi & \cos\psi & 0 \\ 0 & 0 & 1 \end{bmatrix} \begin{bmatrix} X \\ Y \\ Z \end{bmatrix} \tag{3-4}$$

The transformation from ξ', η', ζ' to ξ, η, ζ system representing a rotation of angle θ about ξ'-axis, is

$$\begin{bmatrix} \xi \\ \eta \\ \zeta \end{bmatrix} = \begin{bmatrix} 1 & 0 & 0 \\ 0 & \cos\theta & \sin\theta \\ 0 & -\sin\theta & \cos\theta \end{bmatrix} \begin{bmatrix} \xi' \\ \eta' \\ \zeta' \end{bmatrix} \tag{3-5}$$

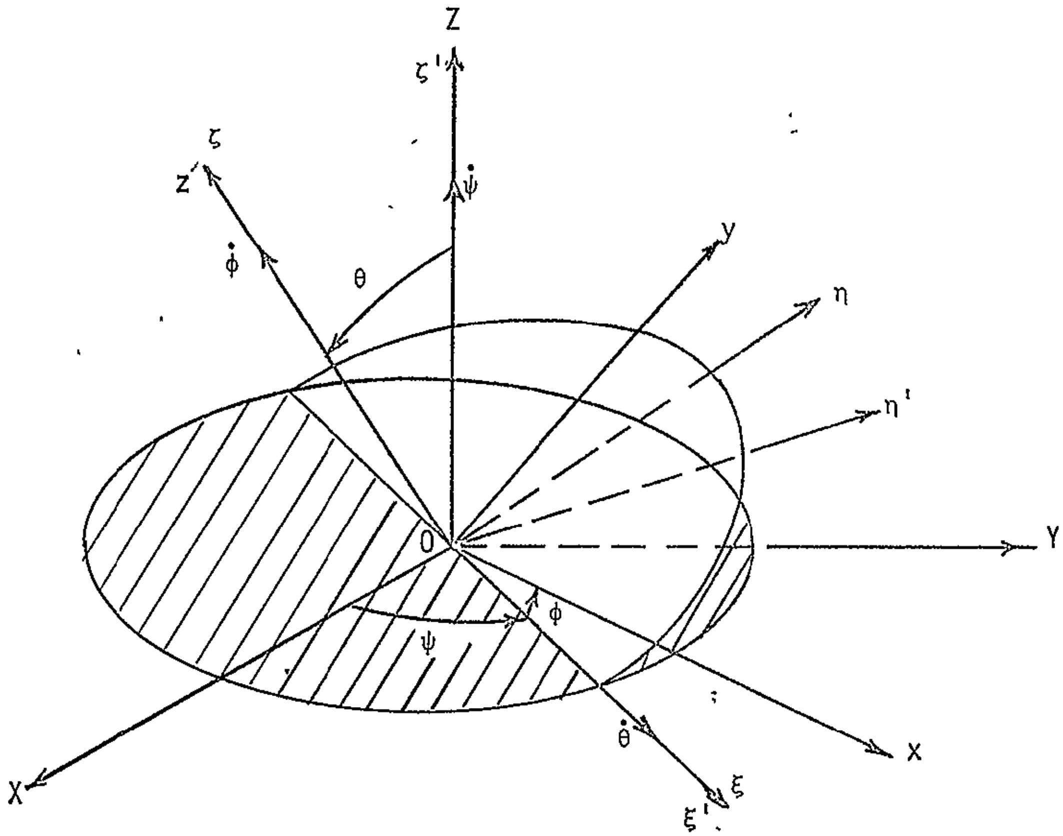

Figure 3-2. Euler Angles

Finally, the transformation from ξ, η, ζ to x, y, z system, representing a rotation of angle ϕ about ζ-axis, is

$$\begin{bmatrix} x \\ y \\ z \end{bmatrix} = \begin{bmatrix} \cos\phi & \sin\phi & 0 \\ -\sin\phi & \cos\phi & 0 \\ 0 & 0 & 1 \end{bmatrix} \begin{bmatrix} \xi \\ \eta \\ \zeta \end{bmatrix} \tag{3-6}$$

Combining (3-4), (3-5) and (3-6) gives the transformation from X, Y, Z to x, y, z system as

$$\begin{bmatrix} x \\ y \\ z \end{bmatrix} = R \begin{bmatrix} X \\ Y \\ Z \end{bmatrix} \tag{3-7}$$

where R is a matrix given by

$$R = \begin{bmatrix} \cos\psi\cos\phi - \sin\psi\cos\theta\sin\phi & \sin\psi\cos\phi + \cos\psi\cos\theta\sin\phi & \sin\theta\sin\phi \\ -\cos\psi\sin\phi - \sin\psi\cos\theta\cos\phi & -\sin\psi\sin\phi + \cos\psi\cos\theta\cos\phi & \sin\theta\cos\phi \\ \sin\psi\sin\theta & -\cos\psi\sin\theta & \cos\theta \end{bmatrix} \tag{3-8}$$

Notice that R is orthogonal, therefore the inverse of (3-7) is

$$\begin{bmatrix} X \\ Y \\ Z \end{bmatrix} = R^t \begin{bmatrix} x \\ y \\ z \end{bmatrix} \tag{3-9}$$

where R^t is the transpose of R.

The directions of Euler angular rates $\dot{\psi}$, $\dot{\theta}$ and $\dot{\phi}$ with respect to satellite body are shown in Figure 3-3. These three angular rates are sometimes called precession, nutation and spin, respectively.

The angular rates ω_x, ω_y, and ω_z can now be written in terms of Euler angles and their rates as

$$\left.\begin{aligned} \omega_x &= \dot{\psi} \sin\theta \sin\phi + \dot{\theta} \cos\phi \\ \omega_y &= \dot{\psi} \sin\theta \cos\phi - \dot{\theta} \sin\phi \\ \omega_z &= \dot{\psi} \cos\theta + \dot{\phi} \end{aligned}\right\} \tag{3-10}$$

The angular rate ω_z is sometimes called the "total spin" which should not be confused with the spin rate $\dot{\phi}$.

To facilitate the analysis, a special case is considered first. Then the analysis of the general case follows.

3. SATELLITE WITH AXIAL SYMMETRY

Consider a satellite body having axial symmetry, and assume that only a spin rate $\dot{\phi}$ exist under nominal condition. The xyz frame is re-defined with its origin at the mass center of the satellite and with its z-axis along the spin direction. Under the nominal condition the xyz frame is stationary with respect to the inertial frame. Thus the xyz frame can be considered as a set of principal axes for the satellite.

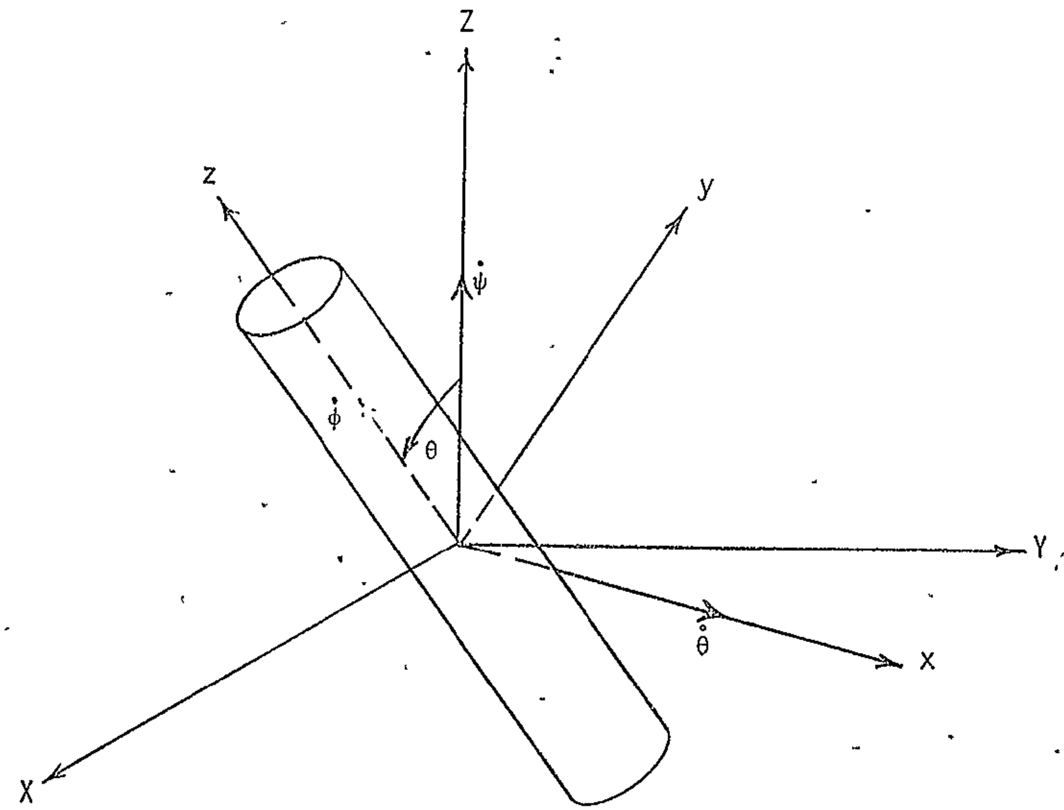

Figure 3-3. The Euler Angle Rates of the Satellite

Hence, an arbitrary rotation of the body relative to this coordinate system will not cause the moments of inertia to change, since the rotation can always be resolved into components about the axes of symmetry. Denoting

$$\left.\begin{aligned} I_{xx} &= I_{yy} = I_t \\ I_{zz} &= I_a \end{aligned}\right\} , \tag{3-11}$$

the components of angular momentum can be written as

$$\left.\begin{aligned} H_x &= I_t\ \omega_x' \\ H_y &= I_t\ \omega_y' \\ H_z &= I_a\ \omega_z' \end{aligned}\right\} \tag{3-12}$$

where ω_x', ω_y', ω_z' are components of the absolute angular rate of the body, expressed along xyz axes. Now suppose that the body rotates about the z-axis with an angular velocity $\dot{\phi}$ measured relative to the xyz system. Let the absolute angular velocity of the xyz coordinate system be $\underline{\omega} = [\omega_x, \omega_y, \omega_z]^t$, which is related to $\underline{\omega}'$ by

$$\left.\begin{aligned} \omega_x' &= \omega_x \\ \omega_y' &= \omega_y \\ \omega_z' &= \omega_z + \dot{\phi} \end{aligned}\right\} \tag{3-13}$$

ıuation (3-12) can then be written as

$$\left.\begin{aligned} H_x &= I_t\ \omega_x \\ H_y &= I_t\ \omega_y \\ H_z &= I_a\ (\omega_z + \dot{\phi}) \end{aligned}\right\} \tag{3-14}$$

›ing the relative angular momentum equation

$$\dot{\underline{H}} = (\dot{\underline{H}})_r + \underline{\omega} \times \underline{H} \tag{3-15}$$

ıd the moment equation

$$\underline{M} = \dot{\underline{H}} \tag{3-16}$$

set of modified Euler equations are obtained

$$\left.\begin{aligned} M_x &= I_t\ \dot{\omega}_x - (I_t - I_a)\ \omega_y\omega_z + I_a\dot{\phi}\omega_y \\ M_y &= I_t\ \dot{\omega}_y + (I_t - I_a)\ \omega_x\omega_z - I_a\dot{\phi}\omega_x \\ M_z &= I_a\ (\dot{\omega}_z + \ddot{\phi}) \end{aligned}\right\} \tag{3-17}$$

where M_x, M_y and M_z are components of the vector moment $\underline{M}$ resolved along xyz coordinates. Assuming there is no rotation of the xyz coordinates along the z direction relative to the XYZ frame, then (3-10) becomes

$$\left.\begin{aligned} \omega_x &= \dot{\theta} \\ \omega_y &= \dot{\psi}\sin\theta \\ \omega_z &= \dot{\psi}\cos\theta \end{aligned}\right\} \qquad (3\text{-}18)$$

Differentiating (3-18) and substituting the result into (3-17), gives

$$\left.\begin{aligned} M_x &= I_t\,\ddot{\theta} + I_a(\dot{\phi} + \dot{\psi}\cos\theta)\dot{\psi}\sin\theta - I_t\,\dot{\psi}^2\sin\theta\cos\theta \\ M_y &= I_t\,(\ddot{\psi}\sin\theta + \dot{\psi}\,\dot{\theta}\cos\theta) + I_t\,\dot{\theta}\,\dot{\psi}\cos\theta - I_a(\dot{\phi} + \dot{\psi}\cos\theta)\dot{\theta} \\ M_z &= I_a\,(\ddot{\phi} + \ddot{\psi}\cos\theta - \dot{\psi}\,\dot{\theta}\sin\theta) \end{aligned}\right\} \qquad (3\text{-}19)$$

The above set of equations will be used to simulate different cases of the operation of angular rate reduction of a satellite.

A. Combined Despinning and Deconing

In this case it is assumed that the satellite is in coning motion which is a combined result of spinning and tumbling. It is further assumed that the coning is without noding. Under this condition, by a suitable choice of x and y coordinates, the total angular momentum of the satellite can be expressed as

$$\underline{H} = \hat{i}\, H_x + \hat{j}\, H_y + \hat{k}\, H_z \tag{3-20}$$

where

$$\left.\begin{aligned} H_x &= 0 \\ H_y &= I_t\, \dot{\psi} \sin\theta \\ H_z &= I_a\, (\dot{\psi} \cos\theta + \dot{\phi}) \end{aligned}\right\} \tag{3-21}$$

and $\hat{i}$, $\hat{j}$, $\hat{k}$ are unit vectors associated with the xyz coordinates.

For this case the external moments are applied in such a way that the spin rate $\dot{\phi}$ and coning rate $\dot{\psi}$ decrease simultaneously while the coning angle θ is maintained constant. (See Figure 3-4(a)) The desired external moments should be

$$\left.\begin{aligned} M_x &= 0 \\ M_y &= -k\, I_t\, \dot{\psi} \sin\theta \\ M_z &= -k\, I_a\, (\dot{\psi} \cos\theta + \dot{\phi}) \end{aligned}\right\} \tag{3-22}$$

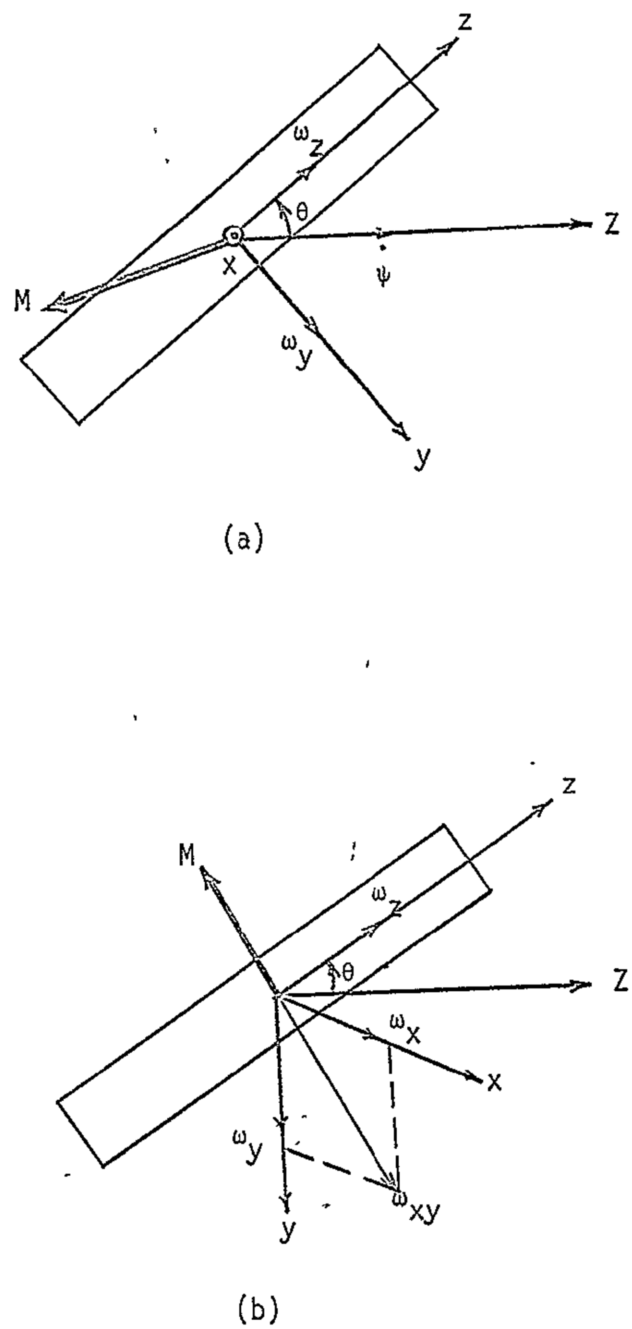

Figure 3-4. Despin and Detumble Moments

where k is a positive proportional constant taken to be

$$k = \frac{M_o}{I_t} \tag{3-23}$$

B. First Detumbling Then Despinning

The tumbling rate is the vector sum of ω_x and ω_y given by

$$\underline{\omega}_{xy} = \hat{i}\,\omega_x + \hat{j}\,\omega_y \tag{3-24}$$

as shown in Figure 3-4(b). To perform detumbling, the external moment should be applied in a direction opposite to $\underline{\omega}_{xy}$. Therefore, with the help of (3-14) and (3-18),

$$\left.\begin{aligned} M_x &= -M_o\,\dot{\theta} \\ M_y &= -M_o\,\dot{\psi}\sin\theta \\ M_z &= 0 \end{aligned}\right\} \tag{3-25}$$

where M_o is a positive proportional constant.

After nulling $\underline{\omega}_{xy}$, a moment is applied to zero the total spin rate ω_z. The applied moment is given by

$$\left.\begin{aligned} M_x &= 0 \\ M_y &= 0 \\ M_z &= -M\,\dot{\phi} \end{aligned}\right\} \tag{3-26}$$

where k_3 is a positive proportional constant.

It has been found, through simulation, that the applied moments could be a linear functions of $\dot{\psi}$, $\dot{\phi}$, or θ, in order to avoid producing new rates which are opposite to the nulled ones. However, the best detumbling results were obtained for a moment which was a linear function of the coning angle θ. Further discussion will be presented in the simulation section of this chapter.

C. First Despin Then Detumble

The analysis for this case and the way external moments are applied are similar to those discussed for Procedure B, except that the operation is done in reverse order.

4. THE GENERAL CASE

The moment equations for the general case are obtained by substituting (3-10) and its derivatives into (3-1), (3-2) and (3-3), giving

$$\begin{aligned}
M_x = I_{xx} [&\ddot{\psi} \sin\theta \sin\phi + \dot{\psi}\, \dot{\theta} \cos\theta \sin\phi \\
&+ \dot{\psi}\, \dot{\phi} \sin\theta \cos\phi + \ddot{\theta} \cos\phi - \dot{\theta}\, \dot{\phi} \sin\phi] \\
+ I_{xy} [&\ddot{\psi} \sin\theta \cos\phi + \dot{\psi}\, \dot{\theta} \cos\theta \cos\phi \\
&- \dot{\psi}\, \dot{\phi} \sin\theta \sin\phi - \ddot{\theta} \sin\phi - \dot{\theta}\, \dot{\phi} \cos\phi \\
&- (\dot{\psi} \sin\theta \sin\phi + \dot{\theta} \cos\phi)(\dot{\psi} \cos\theta + \dot{\phi})]
\end{aligned}$$

$$+ I_{xz} [\ddot{\psi} \cos\theta - \dot{\psi}\,\dot{\theta} \sin\theta + \ddot{\phi}$$

$$+ (\dot{\psi} \sin\theta \sin\phi + \dot{\theta} \cos\phi)\,(\dot{\psi} \sin\theta \cos\phi - \dot{\theta} \sin\phi)]$$

$$+ (I_{zz} - I_{yy})\,[\dot{\psi} \sin\theta \cos\phi - \dot{\theta} \sin\phi]\,(\dot{\psi} \cos\theta + \dot{\phi})$$

$$+ I_{yz} [(\dot{\psi} \sin\theta \cos\phi - \dot{\theta} \sin\phi)^2 - (\dot{\psi} \cos\theta + \dot{\phi})^2] \tag{3-27}$$

$$M_y = I_{yy} [\ddot{\psi} \sin\theta \cos\phi + \dot{\psi}\,\dot{\theta} \cos\theta \cos\phi$$

$$- \dot{\psi}\,\dot{\phi} \sin\theta \sin\phi - \ddot{\theta} \sin\phi - \dot{\theta}\,\dot{\phi} \cos\phi]$$

$$+ I_{\ z} [\ddot{\psi} \cos\theta - \dot{\psi}\,\dot{\theta} \sin\theta + \ddot{\phi}$$

$$- (\dot{\psi} \sin\theta \sin\phi + \dot{\theta} \cos\phi)\,(\dot{\psi} \sin\theta \cos\phi - \dot{\theta} \sin\phi)]$$

$$+ I_{yx} [\ddot{\psi} \sin\theta \sin\phi + \dot{\psi}\,\dot{\theta} \cos\theta \sin\phi$$

$$+ \dot{\psi}\,\dot{\phi} \sin\theta \cos\phi + \ddot{\theta} \cos\phi - \dot{\theta}\,\dot{\phi} \sin\phi$$

$$+ (\dot{\psi} \sin\theta \cos\phi - \dot{\theta} \sin\phi)\,(\dot{\psi} \cos\theta + \dot{\phi})]$$

$$+ (I_{xx} - I_{zz})\,[\dot{\psi} \sin\theta \sin\phi + \dot{\theta} \cos\phi]\,(\dot{\psi} \cos\theta + \dot{\phi})$$

$$+ I_{zx} [(\dot{\psi} \cos\theta + \dot{\phi})^2 - (\dot{\psi} \sin\theta \sin\phi + \dot{\theta} \cos\phi)^2] \tag{3-28}$$

$$M_z = I_{zz} [\ddot{\psi} \cos\theta - \dot{\psi} \dot{\theta} \sin\theta + \ddot{\phi}]$$

$$+ I_{zx} [\ddot{\psi} \sin\theta \sin\phi + \dot{\psi} \dot{\theta} \cos\theta \sin\phi$$

$$+ \dot{\psi} \dot{\phi} \sin\theta \cos\phi + \ddot{\theta} \cos\phi - \dot{\theta} \dot{\phi} \sin\phi$$

$$- (\dot{\psi} \sin\theta \cos\phi - \dot{\theta} \sin\phi) (\dot{\psi} \cos\theta + \dot{\phi})]$$

$$+ I_{zy} [\ddot{\psi} \sin\theta \cos\phi + \dot{\psi} \dot{\theta} \cos\theta \cos\phi$$

$$- \dot{\psi} \dot{\phi} \sin\theta \sin\phi - \ddot{\theta} \sin\phi - \dot{\theta} \dot{\phi} \cos\phi$$

$$+ (\dot{\psi} \sin\theta \sin\phi + \dot{\theta} \cos\phi) (\dot{\psi} \cos\theta + \dot{\phi})]$$

$$+ (I_{yy} - I_{xx}) [\dot{\psi} \sin\theta \sin\phi + \dot{\theta} \cos\phi]$$

$$\times (\dot{\psi} \sin\theta \cos\phi - \dot{\theta} \sin\phi)$$

$$+ I_{xy} [(\dot{\psi} \sin\theta \sin\phi + \dot{\theta} \cos\phi)^2 - (\dot{\psi} \sin\theta \cos\phi - \dot{\theta} \sin\phi)^2] \qquad (3\text{-}29)$$

Note that is is difficult to apply moments expressed along xyz coordinates. To get around this difficulty the nodal coordinates ξ, η, and ζ are used for expressing the components of applied moment. Using the inverse of the transformation (3-6), one has

$$\begin{bmatrix} M_\xi \\ M_\eta \\ M_\zeta \end{bmatrix} = \begin{bmatrix} \cos\phi & -\sin\phi & 0 \\ \sin\phi & \cos\phi & 0 \\ 0 & 0 & 1 \end{bmatrix} \begin{bmatrix} M_x \\ M_y \\ M_z \end{bmatrix} \tag{3-30}$$

Substituting (3-30) into (3-27), (3-28) and (3-29), gives the set of rotational equations of motion in nodal coordinates.

5. SIMULATION BY COMPUTER

Simulation Condition

The satellite dynamics for the axial symmetry case has been simulated using digital computer. First, equations in (3-19) are solved for $\ddot{\theta}$, $\ddot{\psi}$, and $\ddot{\phi}$. The resulted three equations are used for simulation. The initial condition is so chosen that the coning angle is constant, that is

$$\ddot{\theta}_0 = \dot{\theta}_0 = 0 \tag{3-31}$$

Solving the first equation of (3-19), gives

$$\dot{\psi}_0 \sin\theta_0 \, [I_a \, \dot{\phi}_0 + \dot{\psi}_0 \cos\theta_0 \, (I_a - I_t)] = 0$$

Since $\dot{\psi}_0 \sin\theta_0 \neq 0$, it requires

$$I_a \, \dot{\phi}_0 + \dot{\psi}_0 \, \cos\theta_0 (I_a - I_t) = 0 \tag{3-32}$$

Thus, $\dot{\phi}_0$ can be solved if $\dot{\psi}_0$ is known, vice versa.

The set of initial conditions and parameter values used for the simulation are shown below.

Initial Conditions

$$\theta_o = 1.1486 \text{ radians} = 65.81°$$

$$\psi_o = 0$$

$$\phi_o = 0$$

$$\dot{\theta}_o = 0$$

$$\dot{\psi}_o = 0.4809 \text{ radian/second}$$

$$\dot{\phi}_o = 4.19 \text{ radians/second}$$

Moments of Inertia

$$\left.\begin{aligned} I_a &= 9529 \text{ kg-m}^2 \\ I_t &= 212129 \text{ kg-m}^2 \end{aligned}\right\} \tag{3-34}$$

Proportional Constant

$$M_o = 800 \text{ kg-m} \tag{3-35}$$

The following quantities are computed and/or recorded during the simulation.

1. The magnitude of the total angular momentum $\underline{H}$, given by

$$H = \sqrt{H_x^2 + H_y^2 + H_z^2}.$$

$$= \sqrt{I_t^2 (\dot{\theta}^2 + \dot{\psi}^2 \sin^2\theta) + I_a^2 (\dot{\phi} + \dot{\psi} \cos\theta)^2} \tag{3-36}$$

2. The drift angle β that $\underline{H}$ makes with the Z-axis, given by

$$\tan\beta = \frac{|H_{XY}|}{H_Z}.$$

where H_{XY} is the component of $\underline{H}$ in the XY-plane and H_Z is the component of $\underline{H}$ along the Z-axis. Since

$$H_Z = H_z \cos\theta + H_y \sin\theta$$

$$H_{XY} = \sqrt{H_x^2 + (H_y \cos\theta - H_z \sin\theta)^2}$$

therefore

$$\tan\beta = \frac{\sqrt{(I_t\,\dot{\theta})^2 + [I_t\,\dot{\psi}\,\sin\theta\,\cos\theta - I_a\,(\dot{\phi} + \dot{\psi}\cos\theta)\,\sin\theta]^2}}{I_a\,(\dot{\phi} + \dot{\psi}\,\cos\theta)\,\cos\theta + I_t\,\dot{\psi}\,\sin^2\theta} \tag{3-37}$$

3. The tumbling rate ω_{xy} where

$$\omega_{xy} = \sqrt{\omega_x^2 + \omega_y^2} = \sqrt{\dot{\theta}^2 + \dot{\psi}^2\,\sin^2\theta} \tag{3-38}$$

4. The total spinning rate ω_z given by

$$\omega_z = \dot{\phi} + \dot{\psi}\,\cos\theta \tag{3-39}$$

5. Total work W_T at each instant.
6. Coning rate $\dot{\psi}$.
7. Spin rate $\dot{\phi}$, which is related to the total spin rate ω_z via

$$\omega_z = \dot{\phi} + \dot{\psi}\,\cos\theta \tag{3-40}$$

8. Coning angle θ.

Results of Simulation

The results of simulation plotted in Figures 3-5 to 3-15. Contents of each figure is listed below.

Figure 3-5. Time responses for the "detumble-then-despin" case.

Tumble rate ω_{xy}

Total spin rate ω_z

Spin rate $\dot{\phi}$

Figure 3-6. Time response for the "detumble-then-despin" case. (Continuation)

Coning angle θ

Coning rate $\dot{\psi}$

Total angular momentum H

Drift angle β

Figures 3-7 and 3-8. Similar to Figures 3-5 and 3-6, but for the "simultaneous despin and decone" case.

Figures 3-9 and 3-10. Similar to Figures 3-5 and 3-6, but for the "despin-then-detumble" case.

Figure 3-11. A plot of the values of the drift angle β versus the proportional constant M_0 for all three cases having the same end condition.

Figure 3-12. A plot of the values of proportional constant M_0 versus t for all three cases having the same end condition.

Figure 3-13. A plot of total work at any time versus time for all three cases having nearly the same end condition.

Figure 3-14. A plot of total spin rate ω_z versus the total work for all three cases.

Figure 3-15. A plot of tumble rate ω_{xy} versus the total work for all three cases.

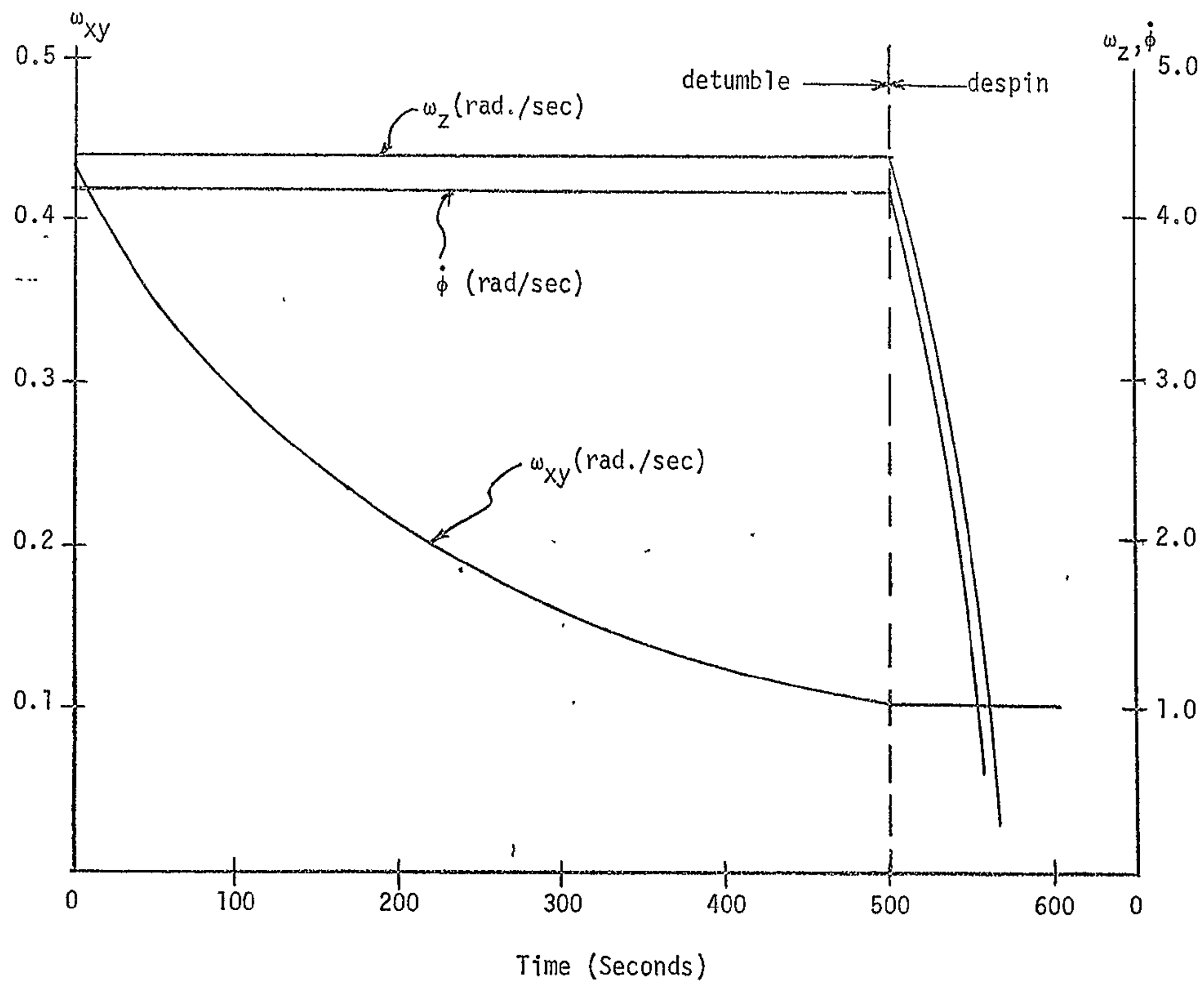

Figure 3-5. Time Response for "Detumble-then-Despin" Case

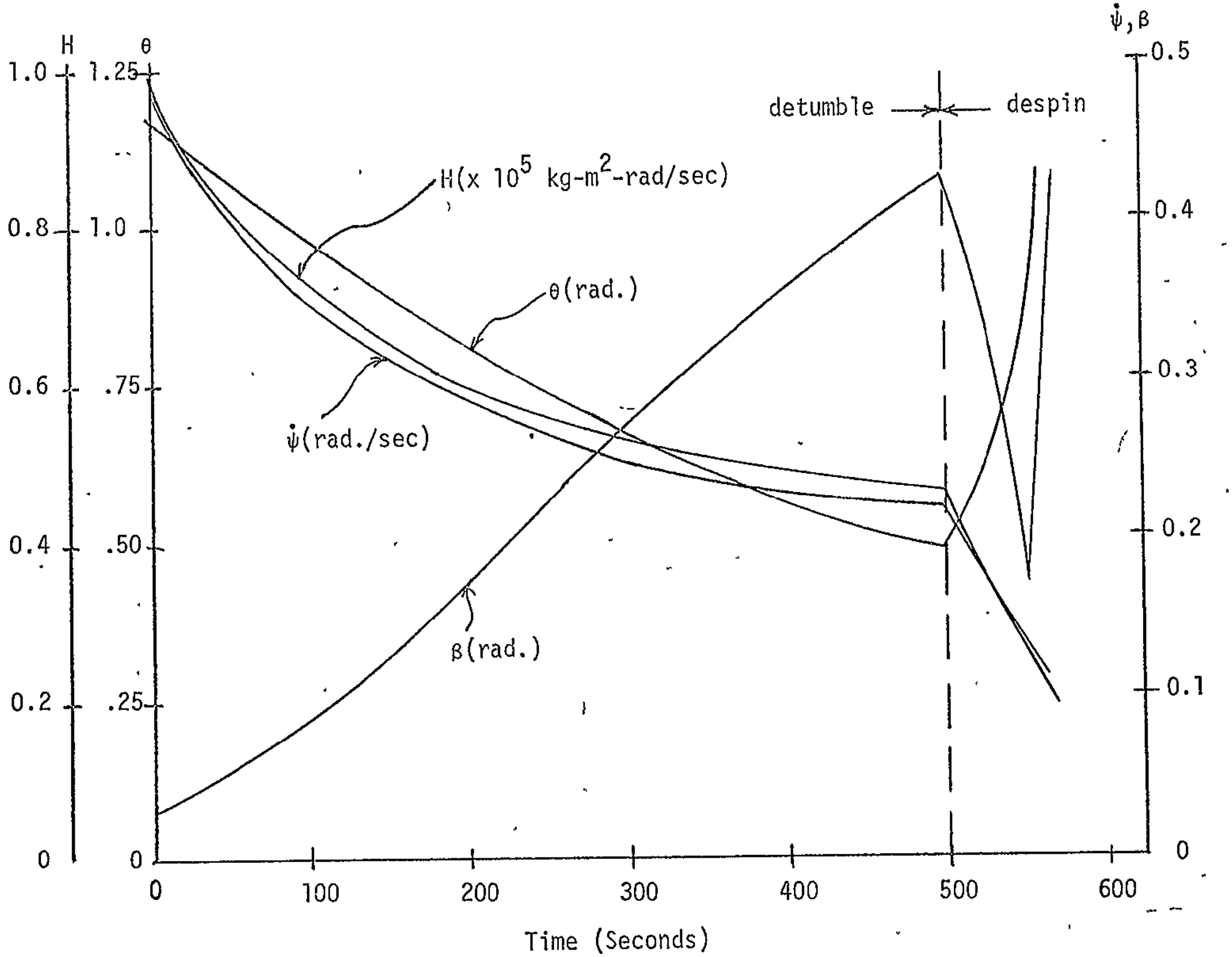
H
θ
$\dot{\psi}$, β
1.0
1.25
0.8
1.0
0.6
.75
0.4
.50
0.2
.25
0
0
0.5
0.4
0.3
0.2
0.1
0
detumble
despin
H(x 10^5 kg-m^2-rad/sec)
θ(rad.)
$\dot{\psi}$(rad./sec)
β(rad.)
0
100
200
300
400
500
600
Time (Seconds)

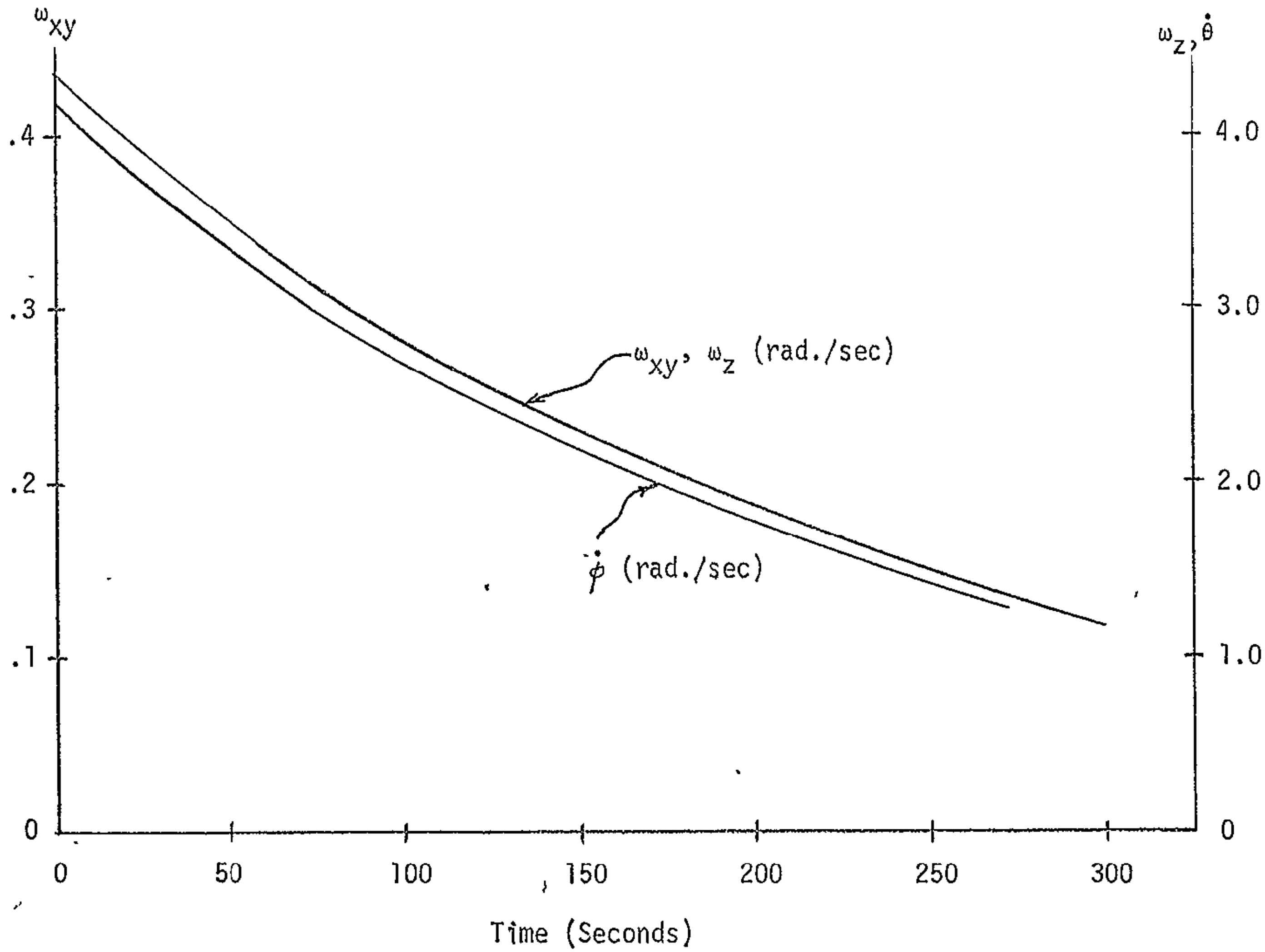

Figure 3-7. Time Response for "Simultaneous Despin and Decone" Case

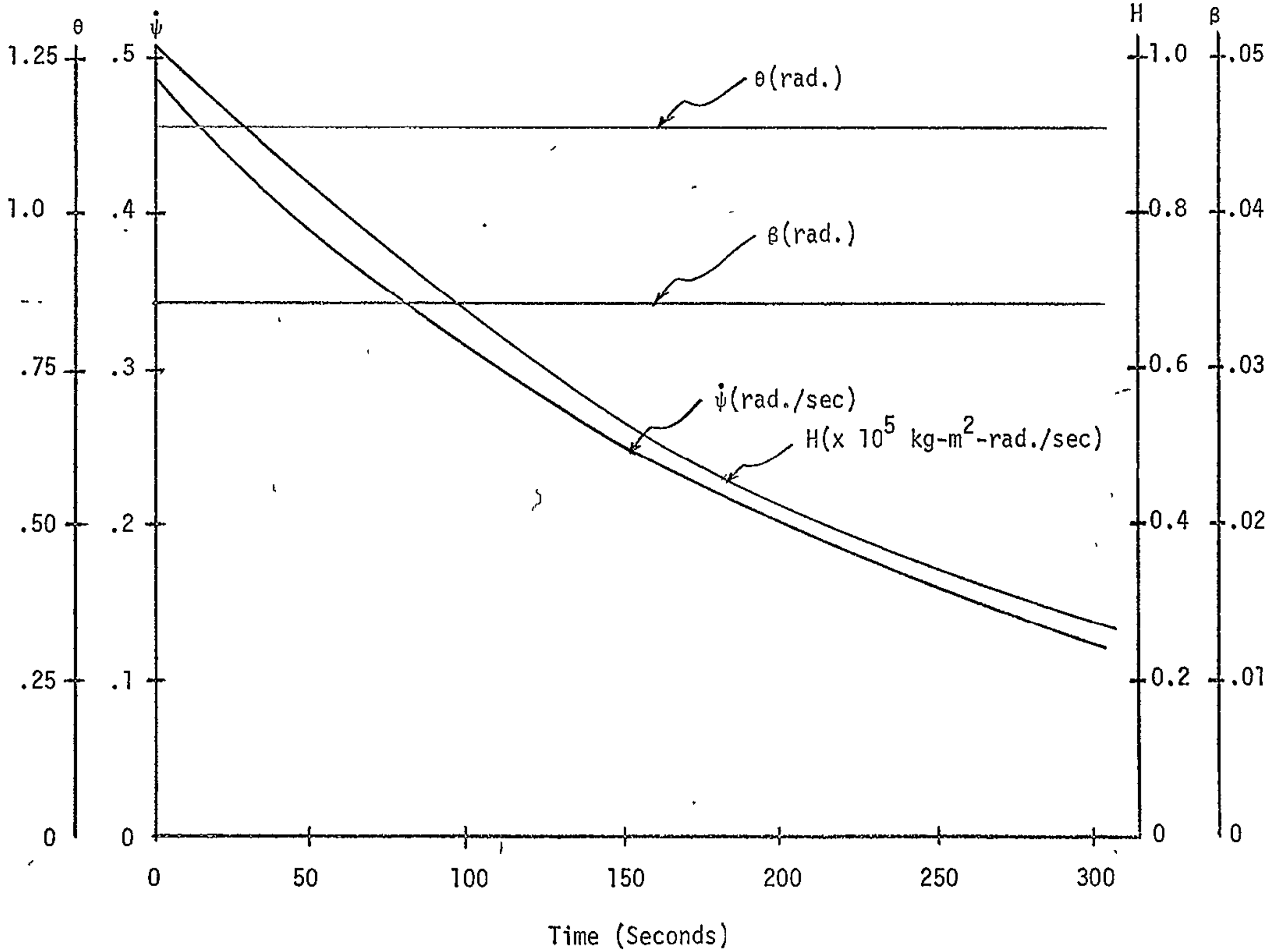

Figure 3-8. Time Response for "Simultaneous Despin and Detumble" Case

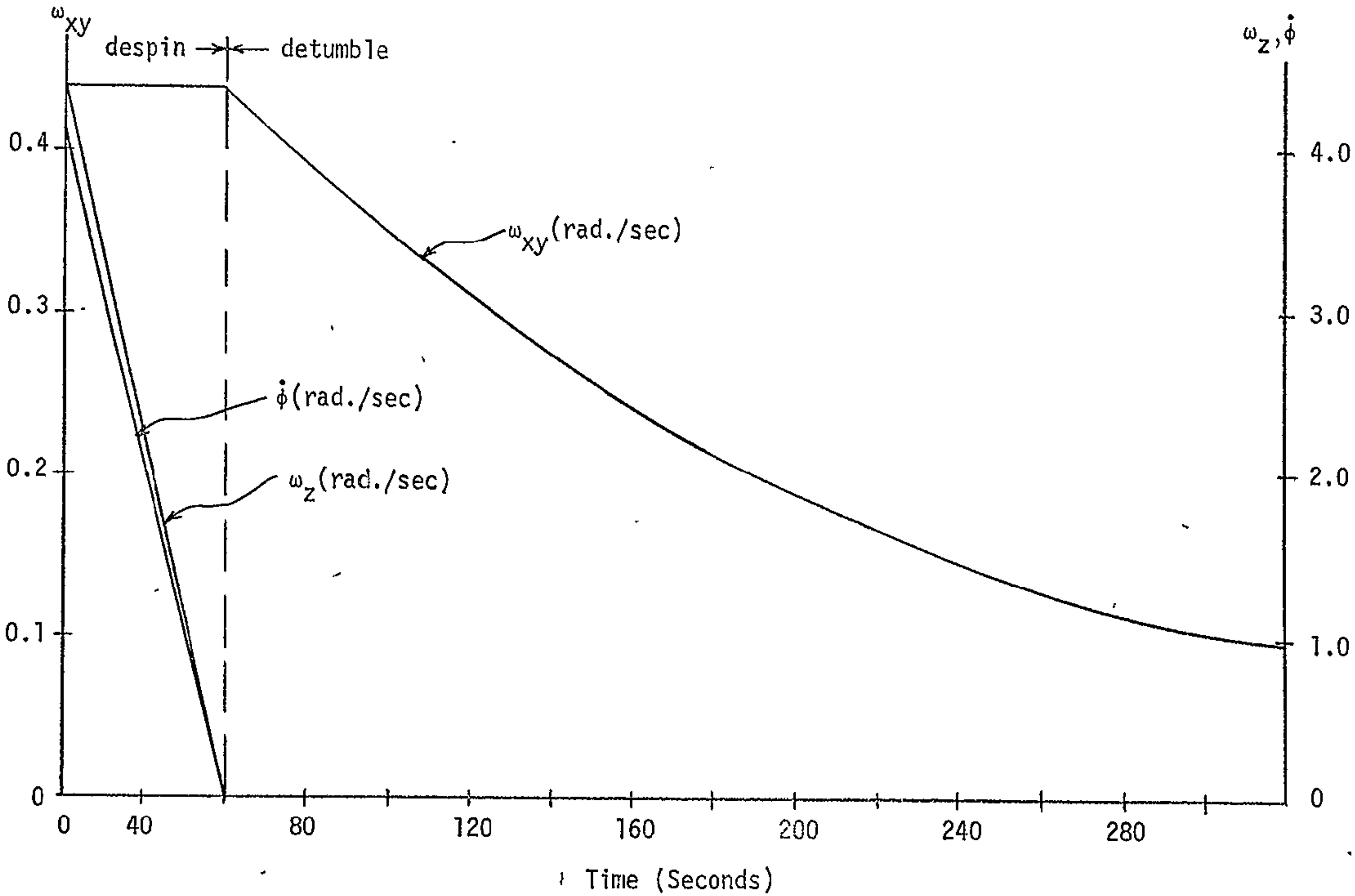

Figure 3-9. Time Response for "Despin-then-Detumble" Case

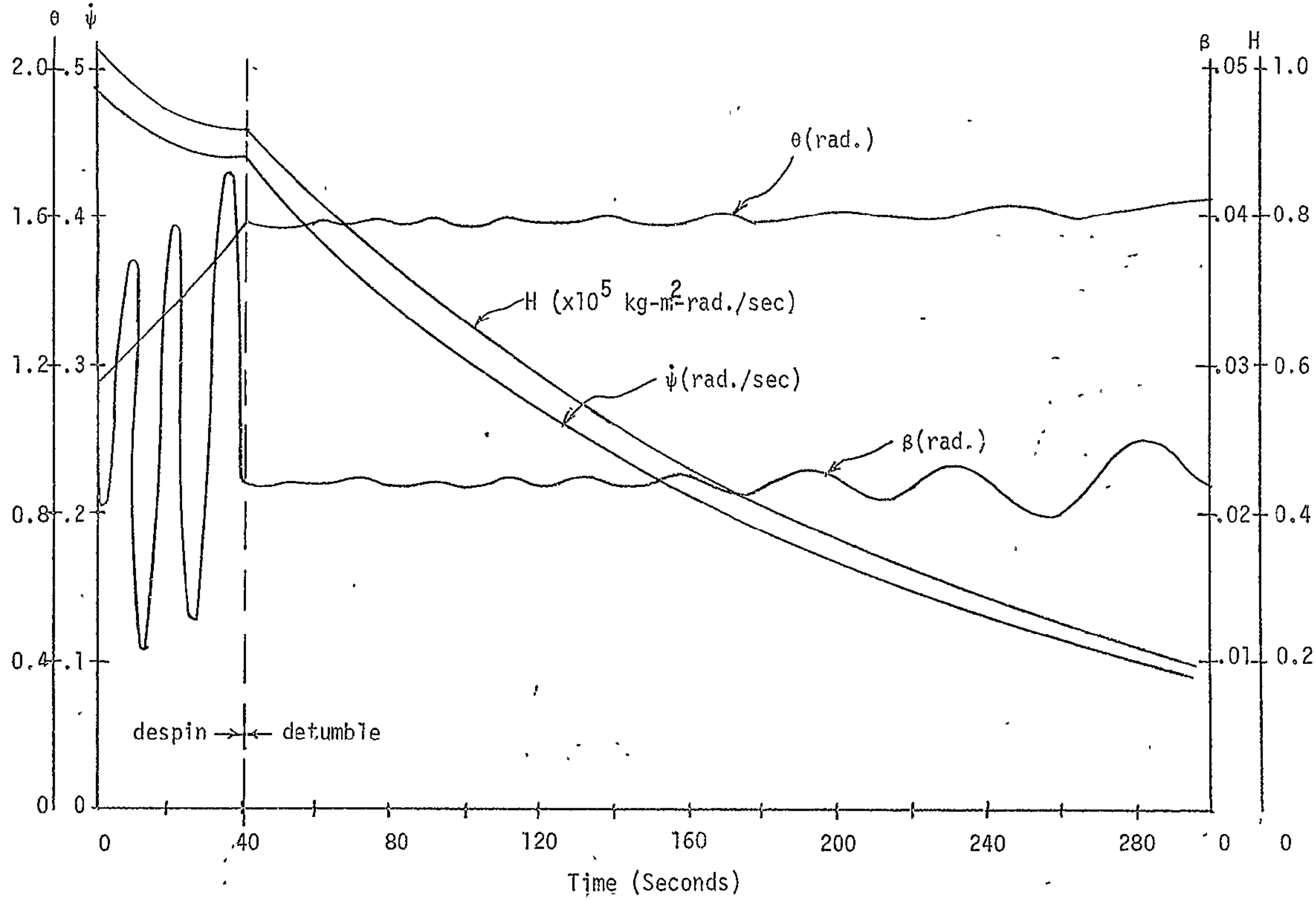

Figure 3-10. Time Response for "Despin-then-Detumble" Case

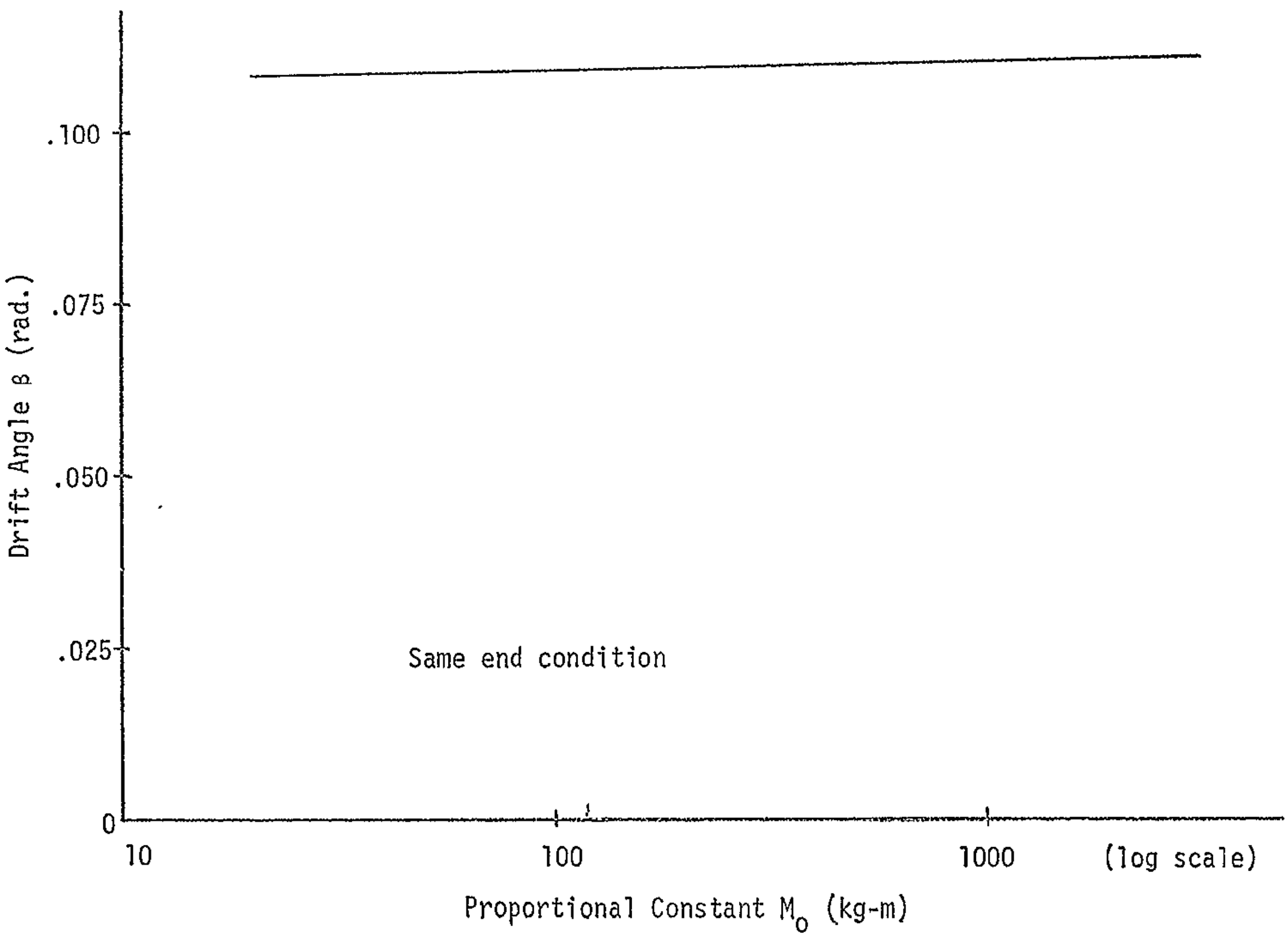

Figure 3-11. Drift Angle Versus M_o

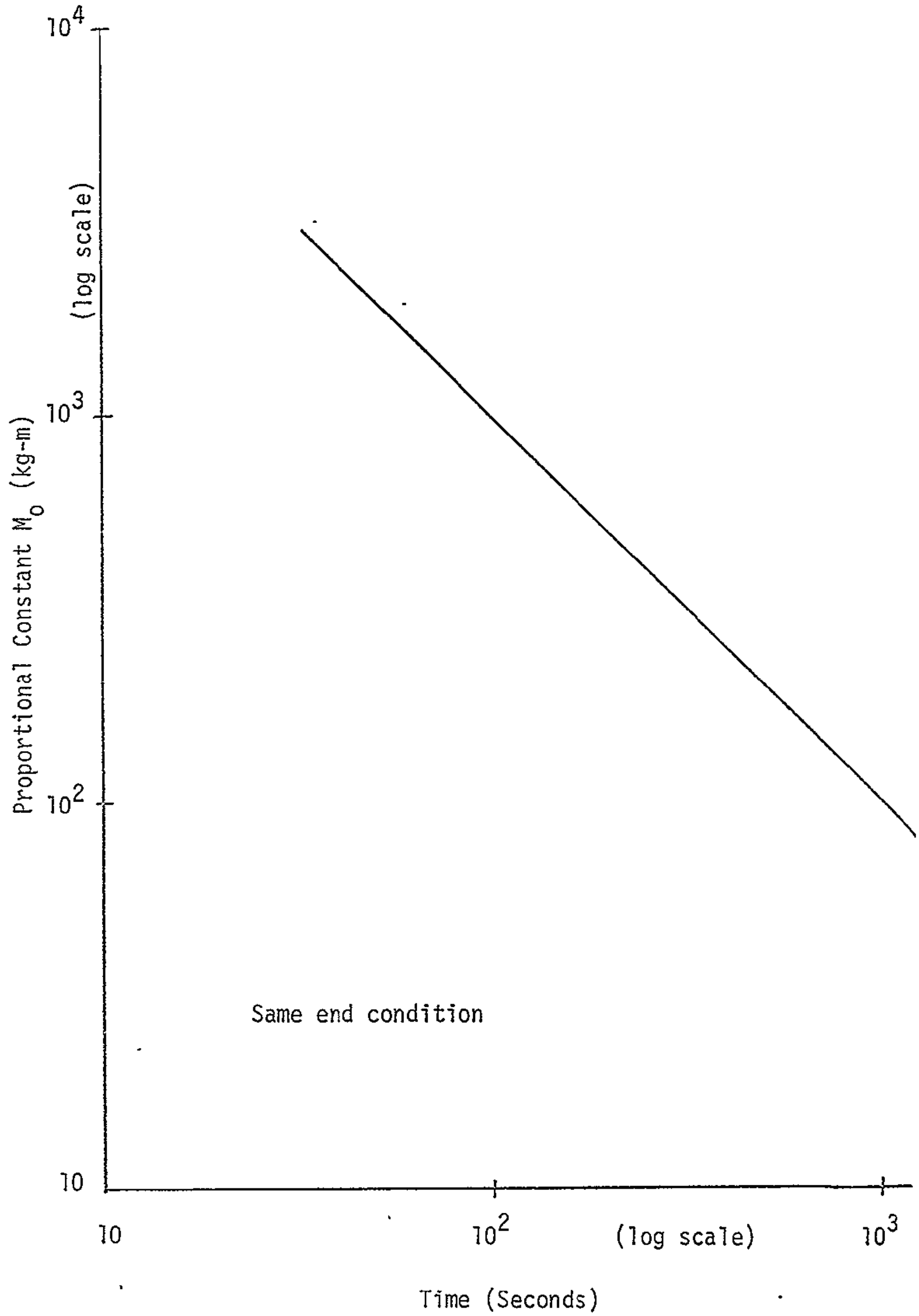

Figure 3-12. Proportional Constant Versus Time.

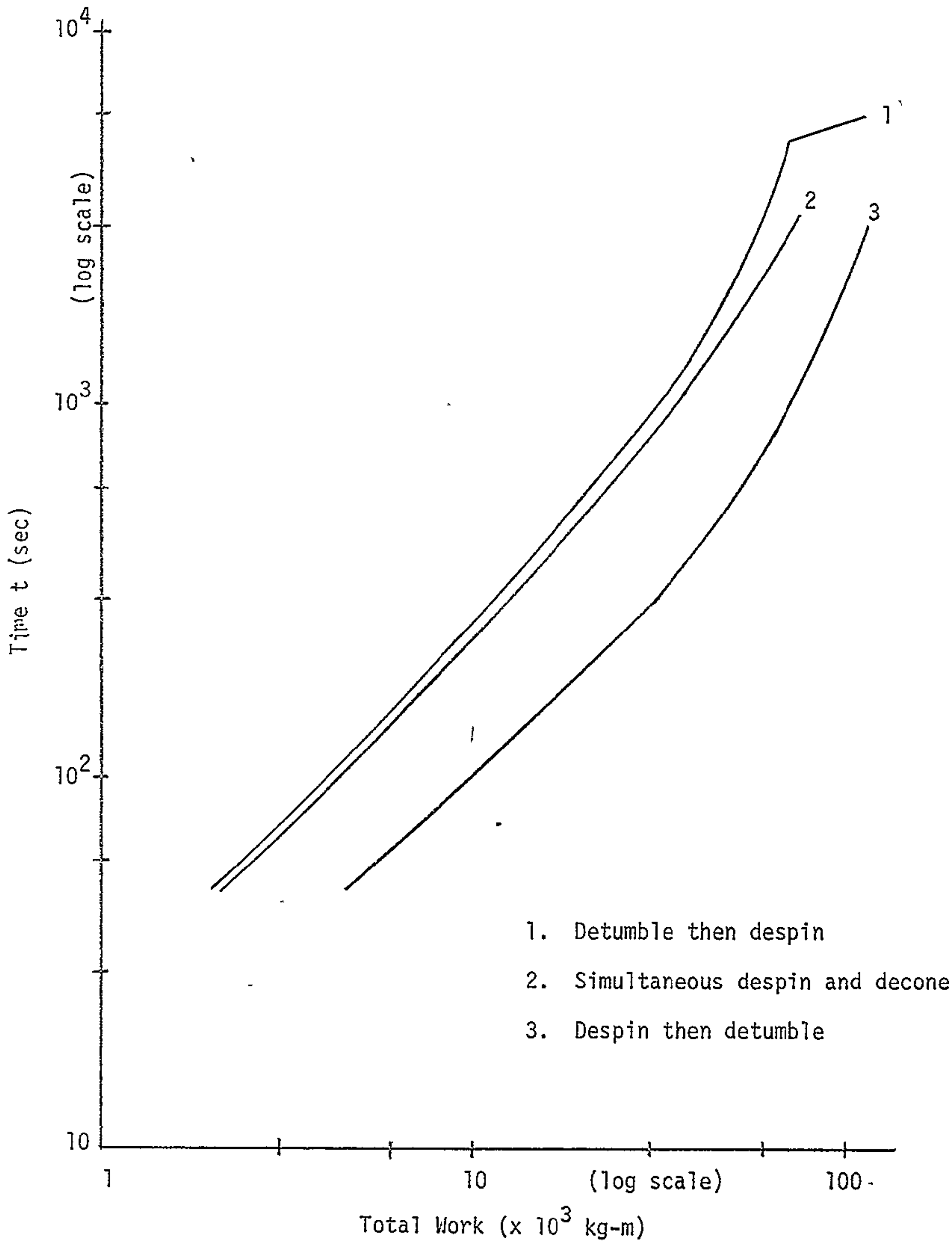

Figure 3-13. Time Versus Work

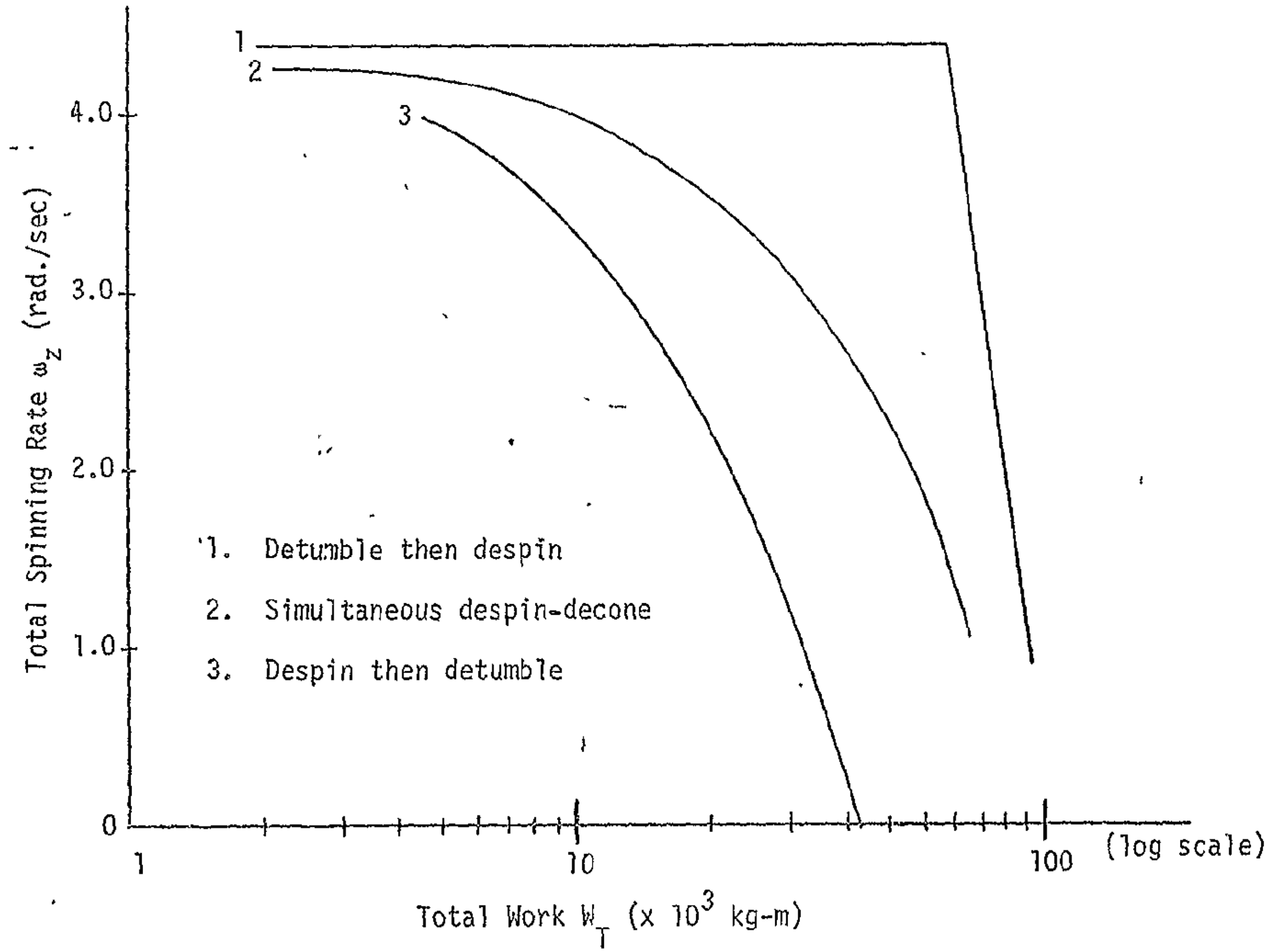

Figure 3-14. Total Spin Rate Versus Work

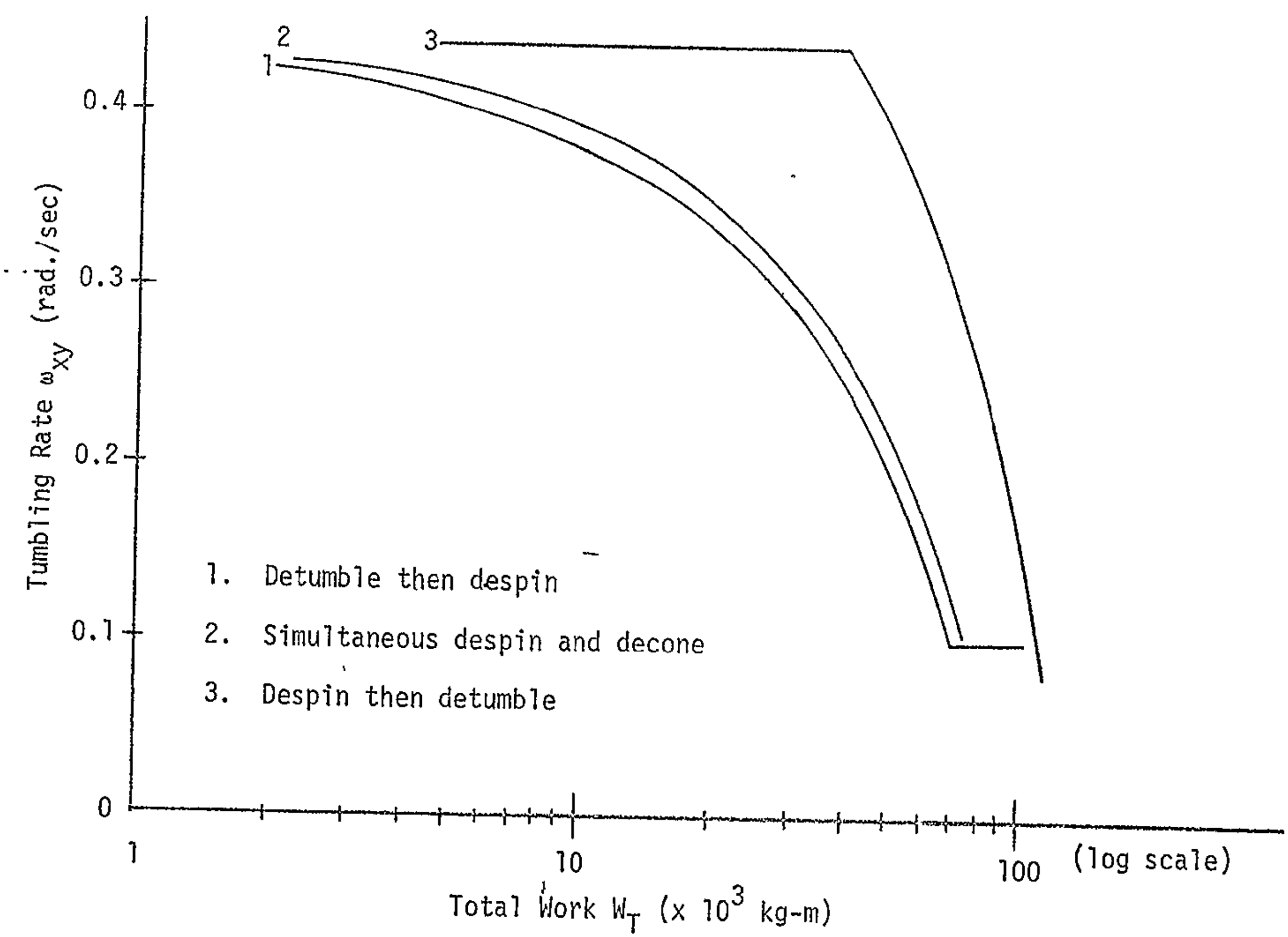

Figure 3-15. Tumble Rate Versus Work

Discussion of Results

The simulation shows that detumbling results in a decrease in coning angle. On the other hand, despinning results in an increase coning angle. This can be explained by noting that detumbling alone reduces H_{xy} while H_z stays constant, therefore the angle between $\underline{H}_z$ $\underline{H}$, which is the coning angle, is reduced. Despinning alone reduces while H_{xy} stays constant, therefore increases the coning angle.

The change of coning angle causes a drift of coning axis. It possible to exert torque at suitable instants for drift correction[4]. However, in the present simulation, no drift correction torque is use This is due to the fact that, although it is a simple matter to do sc theory, the practical application of this procedure is difficult. Th drift correction involves the application of torque at particular positions and these positions are hard to detect.

In one detumbling simulation, different values of the proporti constant M_0 were used to determine the behavior of the drift angle β. The result is plotted in Figure 3-11 showing that no noted increase i β due to the increase of M_0. Also recorded from this simulation is t time required for detumbling to reach a specified state versus values M_0. The result is plotted in Figure 3-12 showing that the relationsh between M_0 and t is such that $M_0 t$ = constant. Therefore the detumbli time and the proportional constant for moment could be determined fron one another when one of the two is specified. Table 3-1 lists the num ical data obtained from this simulation.

Table 3-1. Data for Detumble Simulation

(Same end condition)

M_o kg-m	t seconds	β radians	W_T kg-m
20	4950	0.10833	35897
200	495	0.10848	35904
800	125	0.10170	35700
1600	67.5	0.12030	38000
3000	33	0.11334	35907

The total works required for nulling the motion of the satelli versus time are different for different detumble-despin procedures as shown in Figure 3-13. The detumble-then-despin and the simultaneous despin and decone cases are very close. The least work case is the despin-then-detumble procedure.

Computer Programs

All the computer programs are written in CSMP (Continuous Simulation Modeling Program). They are contained in Appendix 1.

CHAPTER 4

STABILIZATION OF FREE-FLYING TELEOPERATOR DURING DESPIN AND DECONE OPERATION

1. SYSTEM CONFIGURATION

Figure 4-1 shows a combined system of a FFTO and a satellite for despin-decone operation. The despin and decone torques are applied simultaneously to the satellite by the FFTO through the wrist and shoulder brakes. During the despin-decone operation the arm angle α_1 and α_2 are locked rigid. Other symbols shown in the figure are defined as follows:

ℓ_1 = distance between the wrist brake and the satellite's center of mass o_s.

ℓ_2 = length of FFTO's forearm.

ℓ_3 = length of FFTO's rear-arm.

ℓ_4 = length of FFTO's shoulder.

ℓ_5 = distance from the shoulder brake to the FFTO's center of mass o.

$\theta = \alpha_2 - \alpha_1$

ℓ_{sf} = distance between o_s and o.

The reaction torque received by the FFTO during the despin-decone operation is counteracted by a set of control jets produced by clusters of thrusters mounted on the FFTO as shown in Figure 4-1. However, the

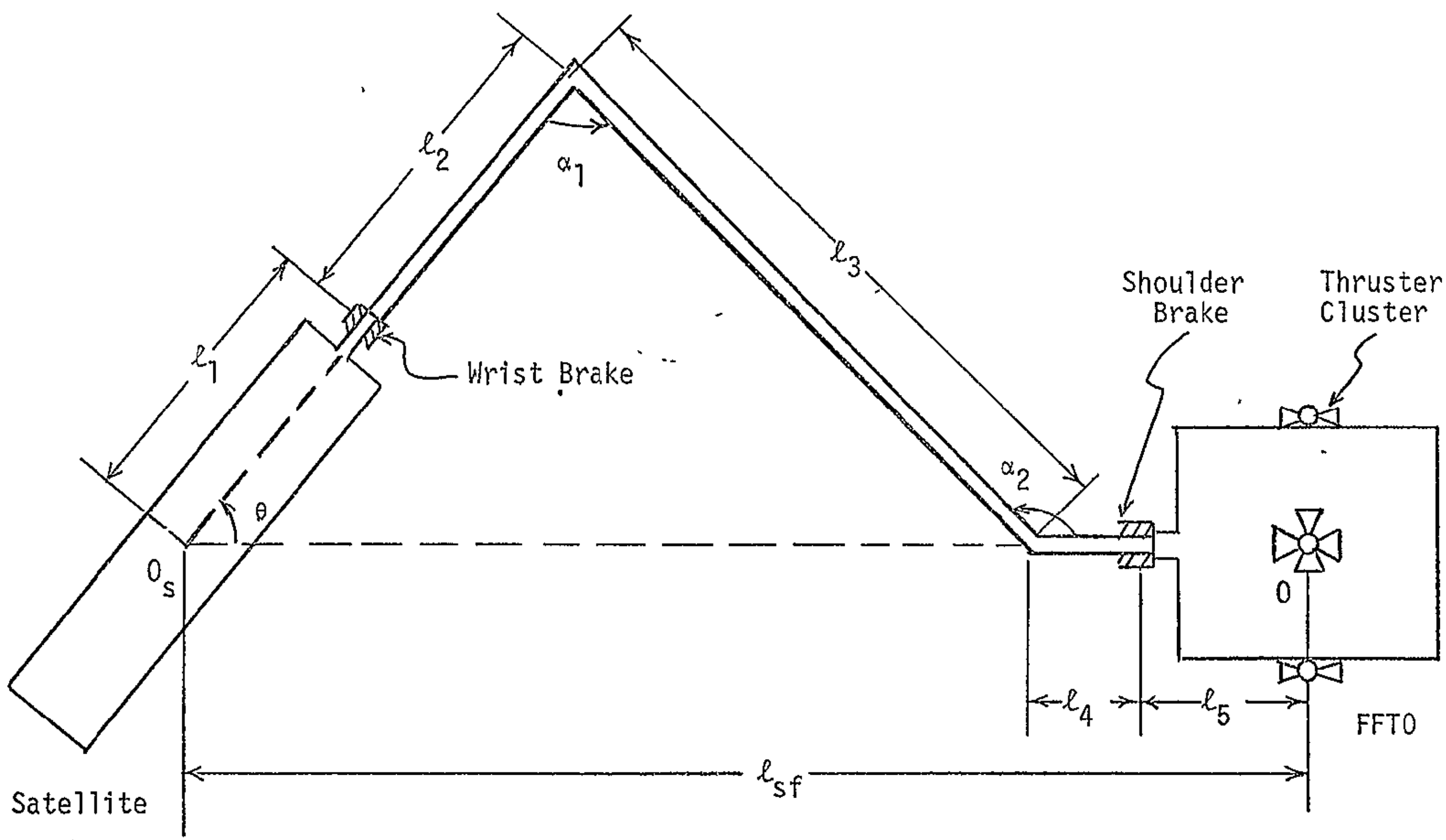

Figure 4-1. System Configuration

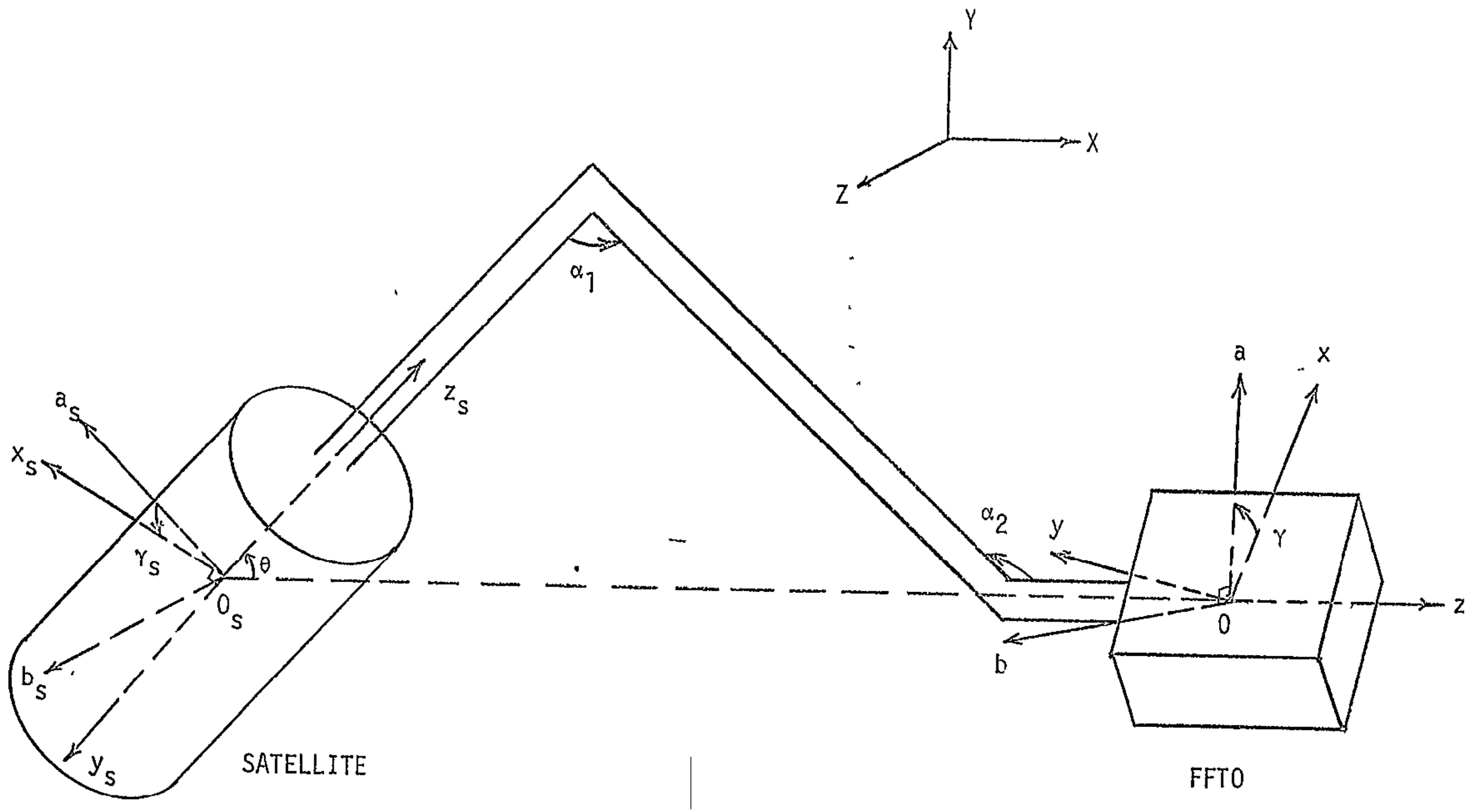

Figure 4-2. Coordinate Systems

thrust level of each thruster is limited, therefore an effective stab zation of the FFTO requires the simultaneous control of the control j and the brake forces.

2. COORDINATE SYSTEMS

Five coordinate systems are defined here, with the help of Fig 4-2, for the convenience of the ensuing analysis.

XYZ-system: This is an inertially fixed coordinate system who X, Y, and Z coordinates are fixed with respect to distant stars.

xyz-system: This coordinate system is fixed to the body of th FFTO. The x, y and z coordinates are along three principal axes of tl body, with the origin 0 of the coordinates located at the mass center of the body.

$x_s y_s z_s$-system: This system is fixed to the body of the satell The x_s, y_s, and z_s axes are along three principal axes of the satelli with the origin 0_s of the coordinates located at the mass center of tl satellite body.

abz-system: This system has its origin coincided with the ori of the xyz-system, but the orientation of its three axes are fixed wi respect to the FFTO's arm. The a-coordinate lies in the arm plane wh is formed by three arm sections. The z-coordinate is the same as tha for xyz-system. The b-coordinate is perpendicular to the arm plane. The relationship between xyz and abz systems is therefore a rotation c angle γ along the z-axis as shown in Figure 4-3(a).

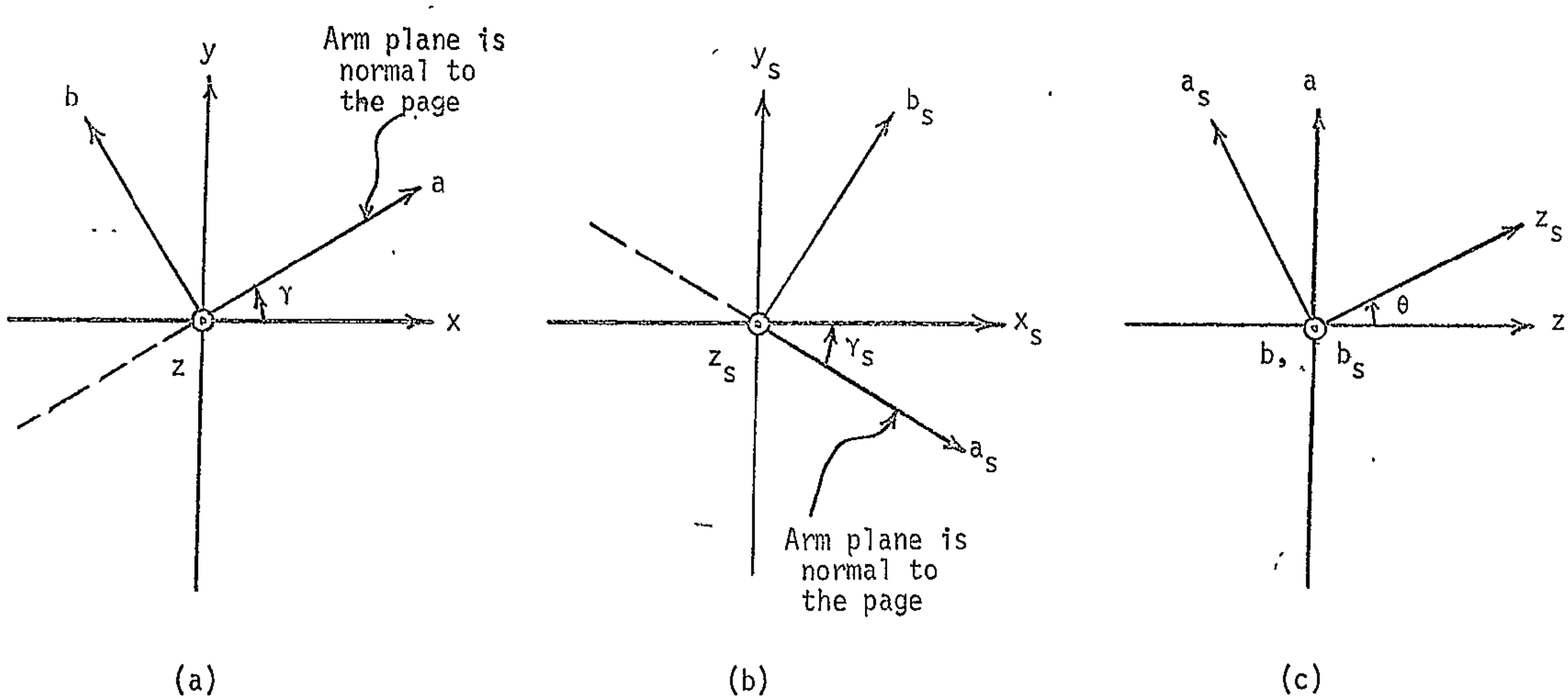

Figure 4-3. Relationships Among Coordinate Systems

$a_s b_s z_s$-system: This system has its origin coincided with the origin of the $x_s y_s z_s$-system, but the orientation of its three axes are also fixed with respect to the FFTO's arm. The a_s-coordinate also lie in the arm plane, the z_s coordinate is the same as that for $x_s y_s z_s$-sys and the b_s coordinate is perpendicular to the arm plane. The relation ship between $x_s y_s z_s$ and $a_s b_s z_s$ systems is a rotation of angle γ_s along the z_s-axis as shown in Figure 4-3(b). Since both b and b_s axes are normal to the arm plane the orientation relationship between abz and $a_s b_s z_s$ systems can be denoted by an angle θ as shown in Figure 4-3(c).

If V is a vector in space, its representations in various coord nate systems are related by the following sets of transformations:

$$\begin{bmatrix} V_x \\ V_y \\ V_z \end{bmatrix} = \begin{bmatrix} \cos\gamma & -\sin\gamma & 0 \\ \sin\gamma & \cos\gamma & 0 \\ 0 & 0 & 1 \end{bmatrix} \begin{bmatrix} V_a \\ V_b \\ V_z \end{bmatrix} = T_{xyz}^{abz} \begin{bmatrix} V_a \\ V_b \\ V_z \end{bmatrix} \quad (4$$

$$\begin{bmatrix} V_a \\ V_b \\ V_z \end{bmatrix} = \begin{bmatrix} \cos\gamma & \sin\gamma & 0 \\ -\sin\gamma & \cos\gamma & 0 \\ 0 & 0 & 1 \end{bmatrix} \begin{bmatrix} V_x \\ V_y \\ V_z \end{bmatrix} = T_{abz}^{xyz} \begin{bmatrix} V_x \\ V_y \\ V_z \end{bmatrix} \quad (4$$

$$\begin{bmatrix} V_{xs} \\ V_{ys} \\ V_{zs} \end{bmatrix} = \begin{bmatrix} \cos\gamma_s & \sin\gamma_s & 0 \\ -\sin\gamma_s & \cos\gamma_s & 0 \\ 0 & 0 & 1 \end{bmatrix} \begin{bmatrix} V_{as} \\ V_{bs} \\ V_{zs} \end{bmatrix} = T_{x_s y_s z_s}^{a_s b_s z_s} \begin{bmatrix} V_{as} \\ V_{bs} \\ V_{zs} \end{bmatrix} \quad (4$$

$$\begin{bmatrix} V_{as} \\ V_{bs} \\ V_{zs} \end{bmatrix} = \begin{bmatrix} \cos\gamma_s & -\sin\gamma_s & 0 \\ \sin\gamma_s & \cos\gamma_s & 0 \\ 0 & 0 & 1 \end{bmatrix} \begin{bmatrix} V_{xs} \\ V_{ys} \\ V_{zs} \end{bmatrix} = T^{x_s y_s z_s}_{a_s b_s z_s} \begin{bmatrix} V_{xs} \\ V_{ys} \\ V_{zs} \end{bmatrix} \tag{4-2b}$$

$$\begin{bmatrix} V_{a} \\ V_{b} \\ V_{z} \end{bmatrix} = \begin{bmatrix} \cos\theta & 0 & \sin\theta \\ 0 & 1 & 0 \\ -\sin\theta & 0 & \cos\theta \end{bmatrix} \begin{bmatrix} V_{as} \\ V_{bs} \\ V_{zs} \end{bmatrix} = T^{a_s b_s z_s}_{abz} \begin{bmatrix} V_{as} \\ V_{bs} \\ V_{zs} \end{bmatrix} \tag{4-3a}$$

$$\begin{bmatrix} V_{as} \\ V_{bs} \\ V_{zs} \end{bmatrix} = \begin{bmatrix} \cos\theta & 0 & -\sin\theta \\ 0 & 1 & 0 \\ \sin\theta & 0 & \cos\theta \end{bmatrix} \begin{bmatrix} V_{a} \\ V_{b} \\ V_{z} \end{bmatrix} = T^{abz}_{a_s b_s z_s} \begin{bmatrix} V_{a} \\ V_{b} \\ V_{z} \end{bmatrix} \tag{4-3b}$$

$$\begin{bmatrix} V_{x} \\ V_{y} \\ V_{z} \end{bmatrix} = \begin{bmatrix} C_{11} & C_{21} & C_{31} \\ C_{12} & C_{22} & C_{32} \\ C_{13} & C_{23} & C_{33} \end{bmatrix} \begin{bmatrix} V_{X} \\ V_{Y} \\ V_{Z} \end{bmatrix} = T^{XYZ}_{xyz} \begin{bmatrix} V_{X} \\ V \\ V \end{bmatrix} \tag{4-4a}$$

$$\begin{bmatrix} V_{X} \\ V_{Y} \\ V_{Z} \end{bmatrix} = \begin{bmatrix} C_{11} & C_{12} & C_{13} \\ C_{21} & C_{22} & C_{23} \\ C_{31} & C_{32} & C_{33} \end{bmatrix} \begin{bmatrix} V_{x} \\ V_{y} \\ V_{z} \end{bmatrix} = T^{xyz}_{XYZ} \begin{bmatrix} V_{x} \\ V_{y} \\ V_{z} \end{bmatrix} \tag{4-4b}$$

In these equations the subscripts denote the coordinates along which the vector components are resolved. Matrix element C_{ij} represents direction consine.

3. KINEMATIC RELATIONSHIPS

In this section the kinematic relationships between various variables of the satellite and that of the FFTO are developed.

Let $(\omega_x, \omega_y, \omega_z)$ and $(\omega_a, \omega_b, \omega_z)$ be the absolute angular velocities of the FFTO resolved along xyz and abz coordinates, respectively. They are related by the transformation (4-1b), that is,

$$\begin{bmatrix} \omega_a \\ \omega_b \\ \omega_z \end{bmatrix} = \begin{bmatrix} \cos\gamma & \sin\gamma & 0 \\ -\sin\gamma & \cos\gamma & 0 \\ 0 & 0 & 1 \end{bmatrix} \begin{bmatrix} \omega_x \\ \omega_y \\ \omega_z \end{bmatrix} \tag{4-5}$$

Similarly, let $(\nu_{xs}, \nu_{ys}, \nu_{zs})$ and $(\nu_{as}, \nu_{bs}, \nu_{zs})$ be the absolute angular velocities of the satellite resolved along $x_s y_s z_s$ and $a_s b_s z_s$ coordinates, respectively. They are related by the transformation (4-2b), that is,

$$\begin{bmatrix} \nu_{as} \\ \nu_{bs} \\ \nu_{zs} \end{bmatrix} = \begin{bmatrix} \cos\gamma_s & -\sin\gamma_s & 0 \\ \sin\gamma_s & \cos\gamma_s & 0 \\ 0 & 0 & 1 \end{bmatrix} \begin{bmatrix} \nu_{xs} \\ \nu_{ys} \\ \nu_{zs} \end{bmatrix} \tag{4-6}$$

Finally, let (μ_a, μ_b, μ_z) and $(\mu_{as}, \mu_{bs}, \mu_{zs})$ be the absolute angular velocities of the arm resolved along the abz and $a_s b_s z_s$ coordinates. Since the az-plane (arm plane) leads xz-plane by the time varying angle γ as shown in Figure 4-3(a), the arm rotates with respect to the FFTO at an angular velocity $\dot{\gamma}$ along the z-axis. Thus we have

$$\underbrace{\begin{bmatrix} \mu_a \\ \mu_b \\ \mu_z \end{bmatrix}}_{\text{arm}} = \underbrace{\begin{bmatrix} \omega_a \\ \omega_b \\ \omega_z \end{bmatrix}}_{\text{FFTO}} + \underbrace{\begin{bmatrix} 0 \\ 0 \\ \dot{\gamma} \end{bmatrix}}_{\substack{\text{arm w.r.t.} \\ \text{FFTO}}} \tag{4-7}$$

Also, since the $a_x z_s$-plane (also the arm plane) lags $x_s z_s$-plane by the time varying angle γ_s as shown in Figure 4-3(b), the arm rotates with respect to the satellite at an angular velocity $-\dot{\gamma}_s$ along the z_s-axis, giving

$$\underbrace{\begin{bmatrix} \mu_{as} \\ \mu_{bs} \\ \mu_{zs} \end{bmatrix}}_{\text{arm}} = \underbrace{\begin{bmatrix} \nu_{as} \\ \nu_{bs} \\ \nu_{zs} \end{bmatrix}}_{\text{satellite}} + \underbrace{\begin{bmatrix} 0 \\ 0 \\ -\dot{\gamma}_s \end{bmatrix}}_{\substack{\text{arm w.r.t.} \\ \text{satellite}}} \tag{4-8}$$

Notice that the two angular velocity vectors (μ_a, μ_b, μ_z) and (μ_{as}, μ_{bs}, μ_{zs}) are related by the transformation (4-3a). That is,

$$\begin{bmatrix} \mu_a \\ \mu_b \\ \mu_z \end{bmatrix} = \begin{bmatrix} \cos\theta & 0 & \sin\theta \\ 0 & 1 & 0 \\ -\sin\theta & 0 & \cos\theta \end{bmatrix} \begin{bmatrix} \mu_{as} \\ \mu_{bs} \\ \mu_{zs} \end{bmatrix} \tag{4-9}$$

What we are after is the relationship between $(\omega_x, \omega_y, \omega_z)$, the angular velocity of the FFTO, and $(\nu_{xs}, \nu_{ys}, \nu_{zs})$, the angular velocity of the satellite. This is accomplished by substituting (4-5) into (4-7) and (4-6) into (4-8), and then substitute the two resulting equations into (4-9). The final expression is

$$\begin{bmatrix} \cos\gamma & \sin\gamma & 0 \\ -\sin\gamma & \cos\gamma & 0 \\ 0 & 0 & 1 \end{bmatrix} \begin{bmatrix} \omega_x \\ \omega_y \\ \omega_z \end{bmatrix} + \begin{bmatrix} 0 \\ 0 \\ \dot{\gamma} \end{bmatrix}$$

$$\begin{bmatrix} \cos\theta & 0 & \sin\theta \\ 0 & 1 & 0 \\ -\sin\theta & 0 & \cos\theta \end{bmatrix} \left\{ \begin{bmatrix} \cos\gamma_s & -\sin\gamma_s & 0 \\ \sin\gamma_s & \cos\gamma_s & 0 \\ 0 & 0 & 1 \end{bmatrix} \begin{bmatrix} \nu_{xs} \\ \nu_{ys} \\ \nu_{zs} \end{bmatrix} + \begin{bmatrix} 0 \\ 0 \\ -\dot{\gamma}_s \end{bmatrix} \right\} . \quad (4-1$$

Or, in the expanded form,

$$\dot{\gamma}_s = \nu_{zs} - (\omega_x \cos\gamma + \omega_y \sin\gamma) \csc\theta$$

$$+ (\nu_{xs} \cos\gamma_s - \nu_{ys} \sin\gamma_s) \cot\theta \quad (4-$$

$$\dot{\gamma} = -\omega_z + (\omega_x \cos\gamma + \omega_y \sin\gamma) \cot\theta$$

$$- (\nu_{xs} \cos\gamma_s - \nu_{ys} \sin\gamma_s) \csc\theta \quad (4-$$

$$-\omega_x \sin\gamma + \omega_y \cos\gamma = \nu_{xs} \sin\gamma_s + \nu_{ys} \cos\gamma_s \tag{4-13}$$

Since the rotational and translational motions are coupled, it is necessary to include the kinematic equations for translational motion. Let (X_f, Y_f, Z_f) be the position of the FFTO's mass center and (X_s, Y_s, Z_s) be that of satellite's mass center. The following relationship exists.

$$X_s = X_f - \ell_{sf} C_{13} \tag{4-14}$$

$$Y_s = Y_f - \ell_{sf} C_{23} \tag{4-15}$$

$$Z_s = Z_f - \ell_{sf} C_{33} \tag{4-16}$$

In summary, for this Satellite-FFTO system, there are eight degrees of freedom. Among them ω_x, ω_y, ω_z and X_f, Y_f, Z_f are used to describe the rotation and translation motion of the FFTO, respectively. The other two are γ and γ_s which are used to describe the spinning and coning motion of the satellite with respect to the FFTO. For this eight-degrees-of-freedom system, which will have fourteen variables (including ω_x, ω_y, ω_z, ν_{xs}, ν_{ys}, ν_{zs}, X_f, Y_f, Z_f, X_s, Y_s, Z_s, γ and γ_s), Equations (4-11), (4-12), (4-13), (4-14), (4-15) and (4-16) are the necessary 14 - 8 = 6 constraint equations. The fourteen variables will be involved in the formulation of dynamic equations later.

4. THE BRAKE MODEL

The brake model which is used as wrist brake and shoulder brake is shown in Figure 4-4, in which mass A is lined up with mass B with the brake works between them. Assuming linear friction, the torque results from the brake is proportional to the relative axial angular velocity between them, that is

$$M_{brake} = K(\dot{\theta}_1 - \dot{\theta}_2) \tag{4-17}$$

where K is the frictional torque constant which can be adjusted by the tightness of the brake. From the Newton's law of action and reaction, the frictional brake torques resulted on mass A and B are equal in magnitude and opposite in direction as shown in the figure.

5. FREE-BODY DIAGRAMS

For the convenience of setting up the dynamic equations, free body diagrams are used. Figure 4-5 gives the free-body diagrams for the satellite, the arm of FFTO, and the body of FFTO. In the figure, all forces and moments acting on each body are indicated.

Based on the brake model discussed in the last section, the brake torque exerted by the shoulder brake to the arm is given by

$$M_z' = K\,\dot{\gamma} \tag{4-18}$$

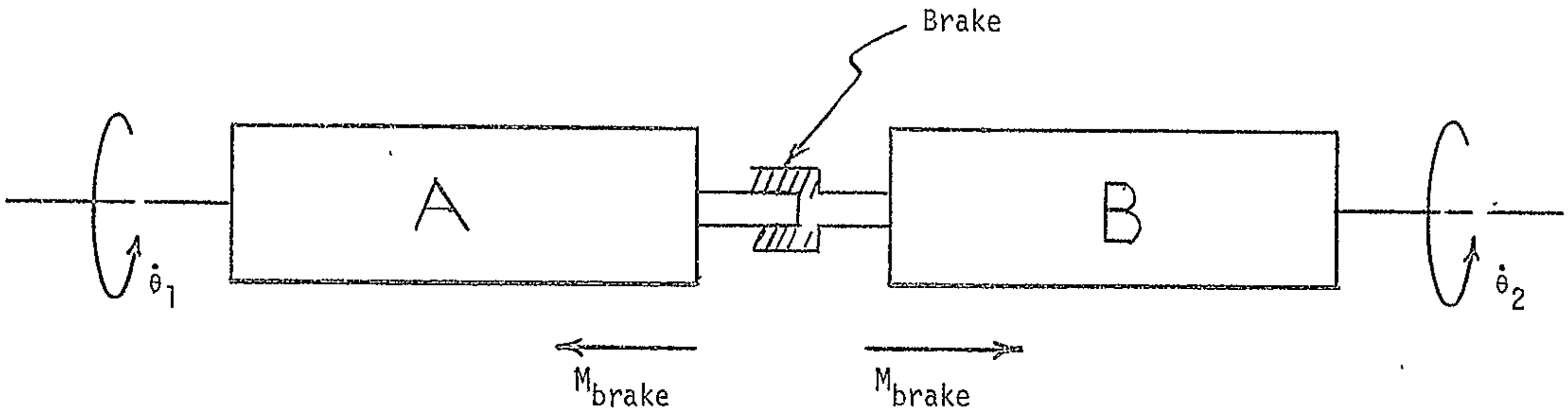

Figure 4-4. Brake Model

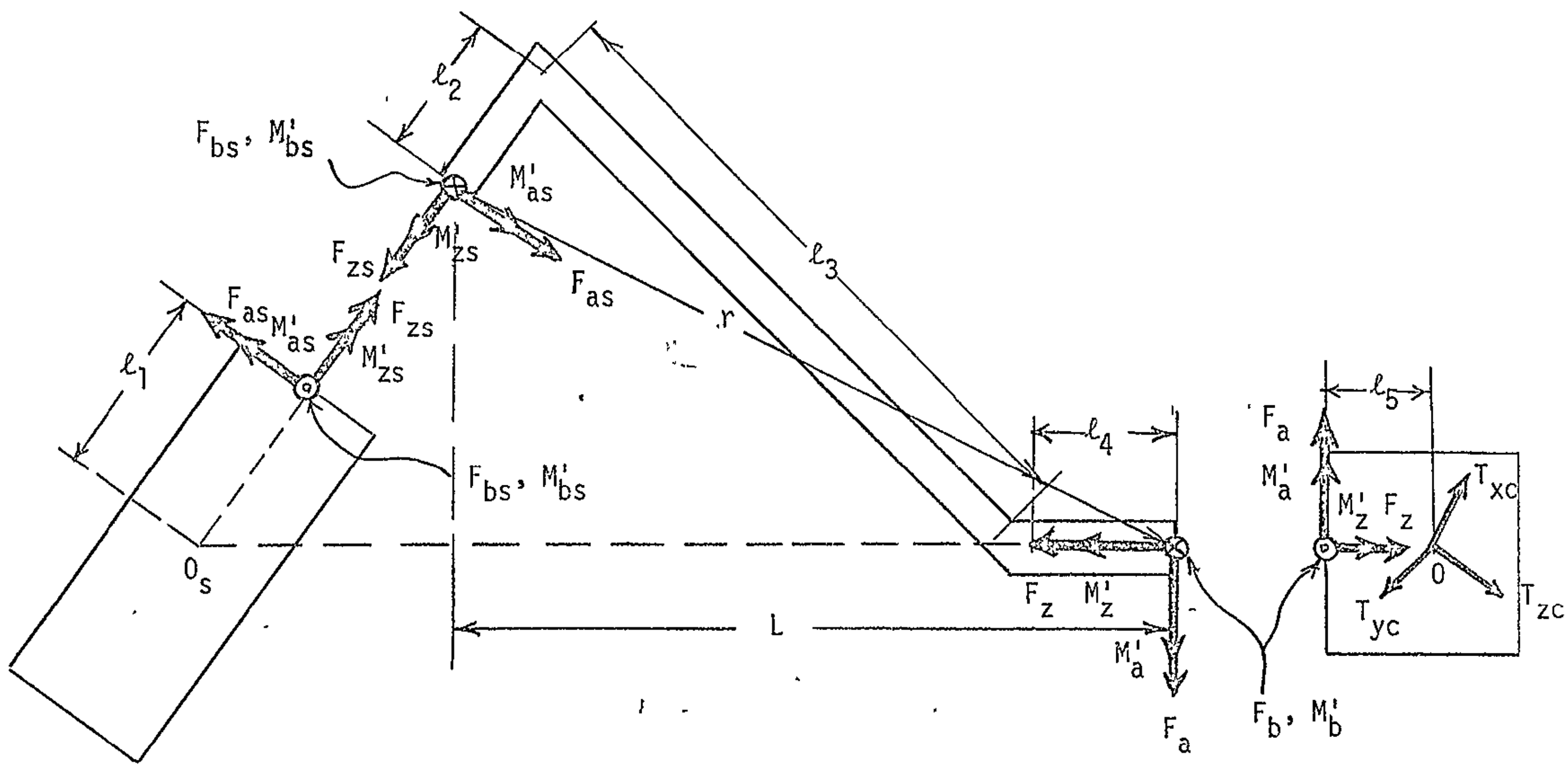

Figure 4-5. Free Body Diagrams

where K is a proportional factor and $\dot{\gamma}$ is the relative angular velocity between two sides of the shoulder brake. Similarly, the brake torque exerted by wrist brake to the satellite is given by

$$M'_{zs} = -K_s\dot{\gamma}_s \tag{4-19}$$

where K_s is a proportional factor and $\dot{\gamma}_s$ is the relative angular velocity between two sides of the wrist brake.

Besides the frictional torque due to the brake there is interaction torque at each brake junction. The interaction torque is in a direction normal to the brake torque. In Figure 4-5, M'_{as}, M'_{bs}, M'_a and M'_b are interacting torque components.

In addition to the interacting moments effected through the brakes, there are interacting forces among bodies at each end of the arm. At the shoulder end the interacting force components are (F_a, F_b, F_z), which are expressed along the abz coordinates. At the wrist end the interacting force components are (F_{as}, F_{bs}, F_{zs}), which are expressed along the $a_sb_sz_s$ coordinates.

Also control thrust torques T_{xc}, T_{yc} and T_{zc} along x, y, z axes are applied on the FFTO in order to stabilize the whole system during the decone-despin process.

It should be noted that all inertial forces and moments are not shown explicitly in Figure 4-5.

6. DYNAMIC EQUATIONS FOR FFTO

The moment equilibrium equations of FFTO expressed along xyz coordinates are given by, assuming an axially symmetrical body.

$$\begin{bmatrix} M_x \\ M_y \\ M_z \end{bmatrix} = \begin{bmatrix} I_{11}\dot{\omega}_x + (I_{33} - I_{22})\,\omega_y\omega_z \\ I_{22}\dot{\omega}_y + (I_{11} - I_{33})\,\omega_z\omega_x \\ I_{33}\dot{\omega}_z + (I_{22} - I_{11})\,\omega_x\omega_y \end{bmatrix} \tag{4-20}$$

where I_{11}, I_{22} and I_{33} are the moments of inertia of the FFTO about its body axes x, y, and z, respectively. The total external moments M_x, M_y and M_z are due to control thrust torques, forces and moments from the shoulder brake, which are obtained from moments M_a, M_b and M_z through the transformation (4-1a).

$$\begin{bmatrix} M_x \\ M_y \\ M_z \end{bmatrix} = \begin{bmatrix} \cos\gamma & -\sin\gamma & 0 \\ \sin\gamma & \cos\gamma & 0 \\ 0 & 0 & 1 \end{bmatrix} \begin{bmatrix} M_a \\ M_b \\ M_z \end{bmatrix} + \begin{bmatrix} T_{xc} \\ T_{yc} \\ T_{zc} \end{bmatrix} \tag{4-21}$$

With the help of Figure 4-5, we find

$$\begin{bmatrix} M_a \\ M_b \\ M_z \end{bmatrix} = \begin{bmatrix} M_a' + F_b\ell_5 \\ M_b' - F_a\ell_5 \\ M_z' \end{bmatrix} = \begin{bmatrix} M_a' + F_b\ell_5 \\ M_b' - F_a\ell_5 \\ K\,\dot{\gamma} \end{bmatrix} \tag{4-22}$$

where moments (M_a, M_b, M_z) are the total external moments from brake end taken with respect to the center of mass, o, of the FFTO.. Successive substitution of (4-22) into (4-21) and then into (4-20) gives

$$\begin{bmatrix} I_{11}\dot{\omega}_x + (I_{33} - I_{22})\omega_y\omega_z \\ I_{22}\dot{\omega}_y + (I_{11} - I_{33})\omega_z\omega_x \\ I_{33}\dot{\omega}_z + (I_{22} - I_{11})\omega_x\omega_y \end{bmatrix} = \begin{bmatrix} M_a'\cos\gamma + F_b\ell_5\cos\gamma - M_b'\sin\gamma + F_a\ell_5\sin\gamma + T_{xc} \\ M_a'\sin\gamma + F_b\ell_5\sin\gamma + M_b'\cos\gamma - F_a\ell_5\cos\gamma + T_{yc} \\ K\dot{\gamma} + T_{zc} \end{bmatrix} \tag{4-23}$$

The external force exerted on the FFTO is the interaction force $[F_a, F_b, F_z]^t$ between FFTO and the arm. This force, when expressed along XYZ coordinates, is given by

$$\begin{bmatrix} F_X \\ F_Y \\ F_Z \end{bmatrix} = T_{XYZ}^{xyz}\, T_{xyz}^{abz} \begin{bmatrix} F_a \\ F_b \\ F_z \end{bmatrix} \tag{4-24}$$

The force equilibrium equation for the mass center of FFTO is thus

$$M \begin{bmatrix} \ddot{X}_f \\ \ddot{Y}_f \\ \ddot{Z}_f \end{bmatrix} = T_{XYZ}^{xyz}\, T_{xyz}^{abz} \begin{bmatrix} F_a \\ F_b \\ F_z \end{bmatrix} \tag{4-25}$$

where M is the mass of the FFTO.

7. DYNAMIC EQUATIONS FOR SATELLITE

In a similar manner, the moment equilibrium equations of the satellite expressed along $x_s y_s z_s$ coordinates are given by

$$\begin{bmatrix} M_{xs} \\ M_{ys} \\ M_{zs} \end{bmatrix} = \begin{bmatrix} J_{11}\,\dot{\nu}_{xs} + (J_{33} - J_{22})\,\nu_{ys}\ \ \nu_{zs} \\ J_{22}\,\dot{\nu}_{ys} + (J_{11} - J_{33})\,\nu_{zs}\ \ \nu_{xs} \\ J_{33}\,\dot{\nu}_{zs} + (J_{22} - J_{11})\,\nu_{xs}\ \ \nu_{ys} \end{bmatrix} \tag{4-26}$$

where J_{11}, J_{22} and J_{33} are the moments of inertia of the satellite about its body axes x_s, y_s and z_s, respectively. The external moment M_{xs}, M_{ys}, and M_{zs} are due to forces and moments from the wrist brake, which are obtained from M_{as}, M_{bs}, and M_{zs} through the transformation (4-2a).

$$\begin{bmatrix} M_{xs} \\ M_{ys} \\ M_{zs} \end{bmatrix} = \begin{bmatrix} \cos\gamma_s & \sin\gamma_s & 0 \\ -\sin\gamma_s & \cos\gamma_s & 0 \\ 0 & 0 & 1 \end{bmatrix} \begin{bmatrix} M_{as} \\ M_{bs} \\ M_{zs} \end{bmatrix} \tag{4-27}$$

Again, with the help of Figure 4-5, we find

$$\begin{bmatrix} M_{as} \\ M_{bs} \\ M_{zs} \end{bmatrix} = \begin{bmatrix} M'_{as} - F_{bs}\ell_1 \\ M'_{bs} + F_{as}\ell_1 \\ M'_{zs} \end{bmatrix} = \begin{bmatrix} M'_{as} - F_{bs}\ell_1 \\ M'_{bs} + F_{as}\ell_1 \\ -K_s\dot{\gamma}_s \end{bmatrix} \tag{4-28}$$

where moments (M_{as}, M_{bs}, M_{zs}) are the total external moments taken with respect to the center of mass, 0_s, of the satellite. Successive substitution of (4-28) into (4-27) and then into (4-26) gives

$$\begin{bmatrix} J_{11}\dot{\nu}_{xs}+(J_{33}-J_{22})\nu_{ys}\nu_{zs} \\ J_{22}\dot{\nu}_{ys}+(J_{11}-J_{33})\nu_{zs}\nu_{xs} \\ J_{33}\dot{\nu}_{zs}+(J_{22}-J_{11})\nu_{xs}\nu_{ys} \end{bmatrix} = \begin{bmatrix} M'_{as}\cos\gamma_s-F_{bs}\ell_1\cos\gamma_s+M'_{bs}\sin\gamma_s+F_{as}\ell_1\sin\gamma_s \\ -M'_{as}\sin\gamma_s+F_{bs}\ell_1\sin\gamma_s+M'_{bs}\cos\gamma_s+F_{as}\ell_1\cos\gamma_s \\ -K_s\dot{\gamma}_s \end{bmatrix} \tag{4-29}$$

The external force exerted on the satellite is the interaction force $[F_{as}, F_{bs}, F_{zs}]^t$ between satellite and the arm. This force, when expressed along XYZ coordinates, is given by

$$\begin{bmatrix} F_{Xs} \\ F_{Ys} \\ F_{Zs} \end{bmatrix} = T_{XYZ}^{xyz}\, T_{xyz}^{abz}\, T_{abz}^{a_s b_s z_s} \begin{bmatrix} F_{as} \\ F_{bs} \\ F_{zs} \end{bmatrix} \tag{4-30}$$

The force equilibrium equation for the mass center of satellite is thus

$$M_s \begin{bmatrix} \ddot{X}_s \\ \ddot{Y}_s \\ \ddot{Z}_s \end{bmatrix} = T_{XYZ}^{xyz}\, T_{xyz}^{abz}\, T_{abz}^{a_s b_s z_s} \begin{bmatrix} F_{as} \\ F_{bs} \\ F_{zs} \end{bmatrix} \tag{4-31}$$

where M_s is the mass of the satellite.

8. DYNAMIC EQUATIONS FOR THE ARM

Assuming that the mass of the arm is much less as compared to FFTO and the satellite so we may consider the arm massless. As a result of the masslessness, the total external forces exerted on the arm must equal to zero. Referring to Figure 4-6 and resolving all forces along a_s, b_s, and z_s axes, we get

$$\begin{bmatrix} F_{as} + F_a \cos\theta - F_z \sin\theta \\ F_{bs} + F_b \\ F_{zs} + F_a \sin\theta + F_z \cos\theta \end{bmatrix} = 0$$

or

$$\begin{bmatrix} F_{as} \\ F_{bs} \\ F_{zs} \end{bmatrix} + \begin{bmatrix} \cos\theta & 0 & -\sin\theta \\ 0 & 1 & 0 \\ \sin\theta & 0 & \cos\theta \end{bmatrix} \begin{bmatrix} F_a \\ F_b \\ F_z \end{bmatrix} = 0$$

or

$$\begin{bmatrix} F_{as} \\ F_{bs} \\ F_{zs} \end{bmatrix} = -T^{abz}_{a_s b_s z_s} \begin{bmatrix} F_a \\ F_b \\ F_z \end{bmatrix} \qquad (4\text{-}32)$$

Similarly, the total external torques acted on a massless body must be zero about any point. Choosing point A as the reference point as shown in Figure 4-6 and resolving all torques along the a, b, and z axes, gives

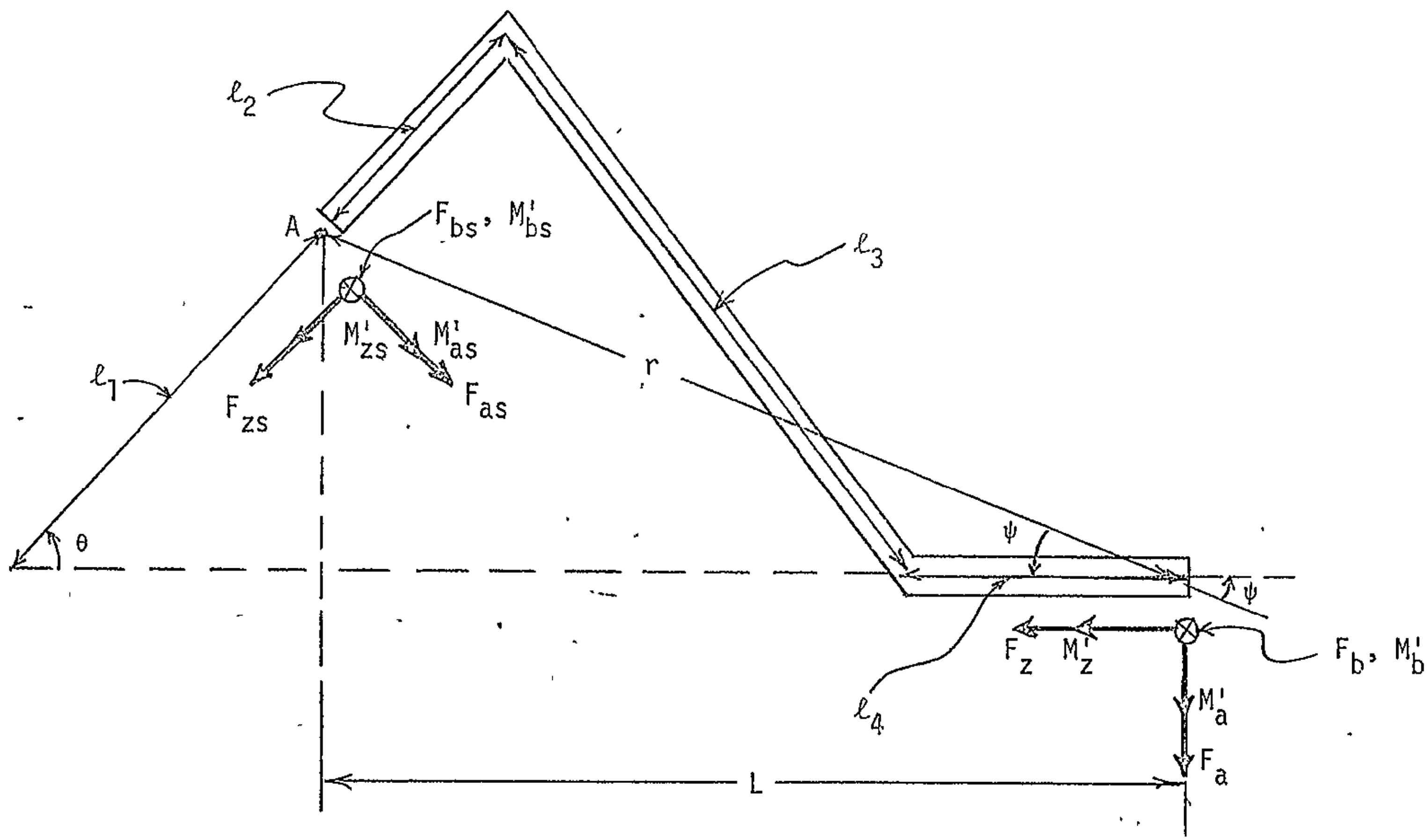

Figure 4-6. Free Body Diagram of the Arm

$$\begin{bmatrix} -M_a' - M_{zs}' \sin\theta - M_{as}' \cos\theta + F_b\, r \cos\psi \\ -M_b' - M_{bs}' - F_a\, r \cos\psi - F_z\, r \sin\psi \\ -M_z' - M_{zs}' \cos\theta + M_{as}' \sin\theta + F_b\, r \sin\psi \end{bmatrix} = 0 \qquad (4\text{-}33)$$

In this equation, $\sin\psi$ and $\cos\psi$ can be eliminated by using the relationship

$$\sin\psi = \frac{\ell_1 \sin\theta}{r}$$

$$\cos\psi = \frac{L}{r}$$

where r and L are distances as shown in Figure 4-6, M_z' and M_{zs}' are given by (4-18) and (4-19). Then (4-33) becomes

$$\begin{bmatrix} -K\dot{\gamma} + K_s\dot{\gamma}_s \cos\theta + M_{as}' \sin\theta + F_b \ell_1 \sin\theta \\ F_b L - M_a' - M_{as}' \cos\theta + K_s \dot{\gamma}_s \sin\theta \\ M_b' + M_{bs}' + F_a L + F_z l_1 \sin\theta \end{bmatrix} = 0 \qquad (4\text{-}34)$$

9. DYNAMIC EQUATIONS FOR TOTAL SYSTEM

The set of vector equations (4-23), (4-25), (4-29), (4-31), (4-32) and (4-34) describe the dynamics of the combined Satellite-FFTO system. Since each vector equation represents three equations, there are a total of eighteen equations. As mentioned before, the fourteen dynamic variables involved in these equations are not all independent; instead, they are subject to the constraint equations (4-11), (4-12), (4-13), (4-14), (4-15), and (4-16).

10. THE CONTROL LAW

From the analysis of the past sections, applying decone and despin brakes, the FFTO will be reacted with forces and moments which tend to make it rotate. In order to achieve the stability of the whole system, proper control torques appeared in (4-23) should be applied on the FFTO to keep it to the inertial directions as stiffly as possible.

For this system, the angular velocities ω_x, ω_y and ω_z of the FFTO are measured by a set of rate gyros. In order to apply the proper control thrust torques, the direction cosine algorithm is selected to study the relationship between the inertial coordinate frame and the FFTO body coordinate frame. The control law will then be studied.

Direction Cosine Algorithm

Let the XYZ axes frame with unit vectors $\hat{i}$, $\hat{j}$, $\hat{k}$ be stationary, and the xyz axes frame with unit vectors $\hat{i}'$, $\hat{j}'$, $\hat{k}'$ be the rotating FFTO body axes frame. Also let

$$\underline{\omega} = \begin{bmatrix} \omega_x \\ \omega_y \\ \omega_z \end{bmatrix} \tag{4-35}$$

be the angular velocity of the xyz frame with respect to the XYZ frame expressed along xyz axes, and C be the "direction cosine matrix" transforming xyz coordinates to XYZ coordinates, i.e.,

$$\underline{V} = C\,\underline{V}' \tag{4-36}$$

where $\underline{V}$ is any vector expressed in XYZ coordinates and $\underline{V}'$ is the same vector expressed in xyz coordinates. C is expressed as

$$C = \begin{bmatrix} C_{11} & C_{12} & C_{13} \\ C_{21} & C_{22} & C_{23} \\ C_{31} & C_{32} & C_{33} \end{bmatrix} = \begin{bmatrix} \hat{i} \cdot \hat{i}' & \hat{i} \cdot \hat{j}' & \hat{i} \cdot \hat{k}' \\ \hat{j} \cdot \hat{i}' & \hat{j} \cdot \hat{j}' & \hat{j} \cdot \hat{k}' \\ \hat{k} \cdot \hat{i}' & \hat{k} \cdot \hat{j}' & \hat{k} \cdot \hat{k}' \end{bmatrix} \tag{4-37}$$

Hence, the derivatives of elements of C are

$$\dot{C}_{11} = \hat{i} \cdot \frac{d\hat{i}'}{d_t} = \hat{i} \cdot (\hat{j}'\omega_z - \hat{k}'\omega_y) = C_{12}\omega_z - C_{13}\omega_y$$

$$\dot{C}_{12} = \hat{i} \cdot \frac{d\hat{j}'}{d_t} = \hat{i} \cdot (\hat{k}'\omega_x - \hat{i}'\omega_z) = C_{13}\omega_x - C_{11}\omega_z$$

$$\dot{C}_{13} = \hat{i} \cdot \frac{d\hat{k}'}{d_t} = \hat{i} \cdot (\hat{i}'\omega_y - \hat{j}'\omega_x) = C_{11}\omega_y - C_{12}\omega_x$$

$$\dot{C}_{21} = \hat{j} \cdot \frac{d\hat{i}'}{d_t} = \hat{j} \cdot (\hat{j}'\omega_z - \hat{k}'\omega_y) = C_{22}\omega_z - C_{23}\omega_y$$

$$\dot{C}_{22} = \hat{j} \cdot \frac{d\hat{j}'}{d_t} = \hat{j} \cdot (\hat{k}'\omega_x - \hat{i}'\omega_z) = C_{23}\omega_x - C_{21}\omega_z$$

$$\dot{C}_{23} = \hat{j} \cdot \frac{d\hat{k}'}{d_t} = \hat{j} \cdot (\hat{i}'\omega_y - \hat{j}'\omega_x) = C_{21}\omega_y - C_{22}\omega_x$$

$$\dot{C}_{31} = \hat{k} \cdot \frac{d\hat{i}'}{d_t} = \hat{k} \cdot (\hat{j}'\omega_z - \hat{k}'\omega_y) = C_{32}\omega_z - C_{33}\omega_y$$

$$\dot{C}_{32} = \hat{k} \cdot \frac{d\hat{j}'}{d_t} = \hat{k} \cdot (\hat{k}'\omega_x - \hat{i}'\omega_z) = C_{33}\omega_x - C_{31}\omega_z$$

$$\dot{C}_{33} = \hat{k} \cdot \frac{d\hat{k}'}{d_t} = \hat{k} \cdot (\hat{i}'\omega_y - \hat{j}'\omega_x) = C_{31}\omega_y - C_{32}\omega_x$$

The derivative of C is therefore

$$\dot{C} = \begin{bmatrix} \dot{C}_{11} & \dot{C}_{12} & \dot{C}_{13} \\ \dot{C}_{21} & \dot{C}_{22} & \dot{C}_{23} \\ \dot{C}_{31} & \dot{C}_{32} & \dot{C}_{33} \end{bmatrix}$$

$$= \begin{bmatrix} C_{12}\omega_z - C_{13}\omega_y & C_{13}\omega_x - C_{11}\omega_z & C_{11}\omega_y - C_{12}\omega_x \\ C_{22}\omega_z - C_{23}\omega_y & C_{23}\omega_x - C_{21}\omega_z & C_{21}\omega_y - C_{22}\omega_x \\ C_{32}\omega_z - C_{33}\omega_y & C_{33}\omega_x - C_{31}\omega_z & C_{31}\omega_y - C_{32}\omega_x \end{bmatrix}$$

$$= \begin{bmatrix} C_{11} & C_{12} & C_{13} \\ C_{21} & C_{22} & C_{23} \\ C_{31} & C_{32} & C_{33} \end{bmatrix} \begin{bmatrix} 0 & -\omega_z & \omega_y \\ \omega_z & 0 & -\omega_x \\ -\omega_y & \omega_x & 0 \end{bmatrix} \tag{4-38}$$

Let

$$\Omega = \begin{bmatrix} 0 & -\omega_z & \omega_y \\ \omega_z & 0 & -\omega_x \\ -\omega_y & \omega_x & 0 \end{bmatrix}$$

be the matrix characterizing the angular velocity of the FFTO xyz frame with respect to the XYZ frame. (4-38) becomes

$$\dot{C} = C\Omega \tag{4-39}$$

Since, in the Satellite-FFTO system, the angular velocities ω_x, ω_y and ω_z of the FFTO are measured by a set of rate gyros, the orientation of the FFTO can then be found by (4-39) whose block diagram is shown in Figure 4-7.

<u>Control Thrust Torques</u>

Control torques are chosen to be proportional to angular displacements as well as angular rates. They are chosen to be

$$T_{xc} = -k_1\omega_x + k_2C_{11}(C_{23} - C_{32}) \tag{4-40}$$

$$T_{yc} = -k_3\omega_y + k_4C_{22}(C_{31} - C_{13}) \tag{4-41}$$

$$T_{zc} = -k_5\omega_z + k_6C_{33}(C_{12} - C_{21}) \tag{4-42}$$

The first term in each of these equations is the part proportional to angular rate and the second term is the part proportional to angular displacement. The second term is obtained through a study of the geometrical relationship between XYZ and xyz frames. All k_i's in these equations are proportional constants.

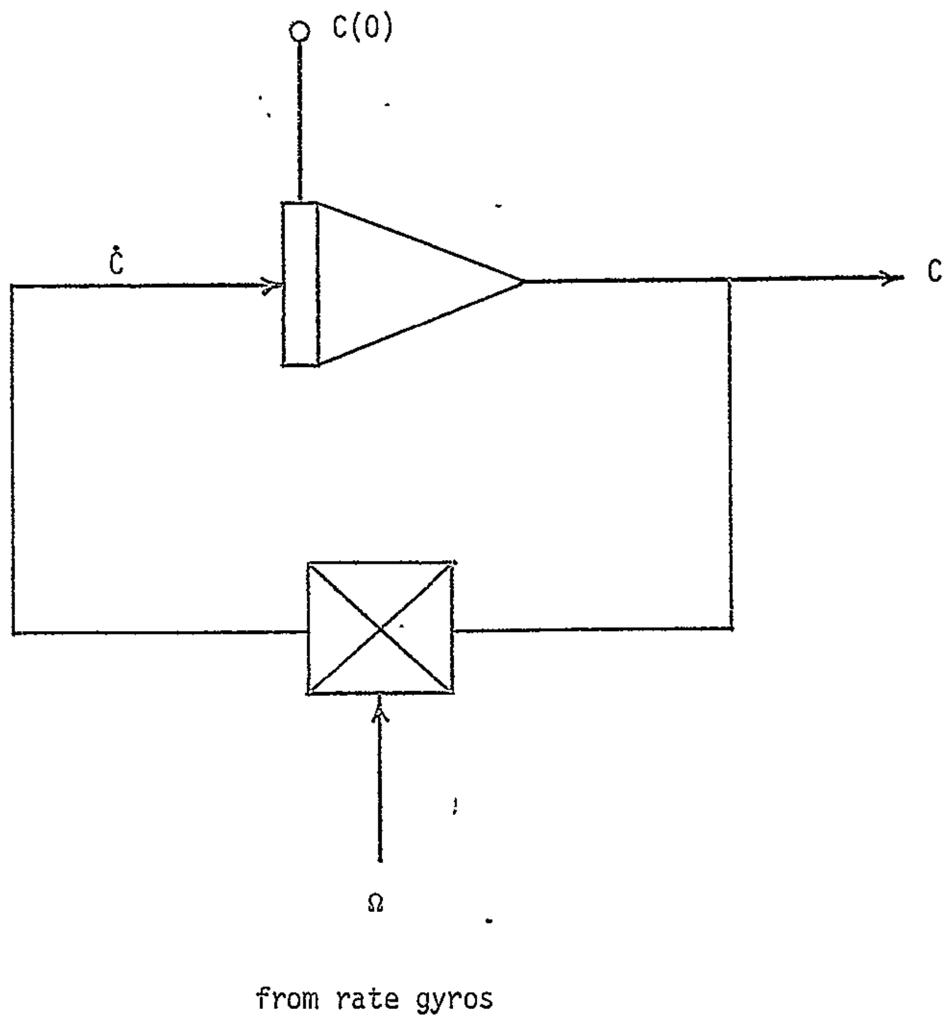

Figure 4-7. Direction Cosine Transformation

It should be mentioned that, while control law development and stabilization techniques are not intended activities of this project, a method of stabilization control is needed to maintain the dynamics of the combined FFTO-satellite system in a reasonable state. Thus the chosen control law represented by (4-40), (4-41) and (4-42) is by no means optimal. However, it is effective for the intended purpose.

11. SIMULATION

Now there are eighteen dynamic equations represented by (4-23), (4-25), (4-29), (4-31), (4-32) and (4-34); there are six constraint equations represented by (4-11), (4-12), (4-13), (4-14), (4-15) and (4-16); there are three control thrust equations (4-40), (4-41), (4-42); and there are nine direction cosine equations represented by (4-39). All these 35 equations describe the FFTO-Satellite system considered. For the convenience of computer simulation, a number of substitutions are made among these equations to eliminate some of them.

Equation Elimination

Substituting (4-32), (4-14), (4-15), and (4-16) into (4-31), gives

$$M_s \begin{bmatrix} \ddot{X}_f - \ell_{sf}\,\ddot{C}_{13} \\ \ddot{Y}_f - \ell_{sf}\,\ddot{C}_{23} \\ \ddot{Z}_f - \ell_{sf}\,\ddot{C}_{33} \end{bmatrix} = T^{xyz}_{XYZ}\; T^{abz}_{xyz}\; T^{a_s b_s z_s}_{abz} \left(-T^{abz}_{a_s b_s z_s} \begin{bmatrix} F_a \\ F_b \\ F_z \end{bmatrix} \right)$$

$$= -T^{xyz}_{XYZ} \; T^{abz}_{xyz} \begin{bmatrix} F_a \\ F_b \\ F_z \end{bmatrix} \tag{4-43}$$

Dividing (4-25) by M, dividing (4-43) by M_s, taking their difference, and rearranging the result with the help of (4-39),

$$\ell_{sf} \begin{bmatrix} \ddot{C}_{13} \\ \ddot{C}_{23} \\ \dot{C}_{33} \end{bmatrix} = \left(\frac{1}{M} + \frac{1}{M_s}\right) T^{xyz}_{XYZ} \; T^{abz}_{xyz} \begin{bmatrix} F_a \\ F_b \\ F_z \end{bmatrix}$$

By inverting the transformation, gives

$$\begin{bmatrix} F_a \\ F_b \\ F_z \end{bmatrix} = \frac{MM_s}{M + M_s} \; \ell_{sf} \; T^{xyz}_{abz} \; T^{XYZ}_{xyz} \begin{bmatrix} \ddot{C}_{13} \\ \ddot{C}_{23} \\ \ddot{C}_{33} \end{bmatrix}$$

$$= D_1 \cdot T^{xyz}_{abz} \; T^{XYZ}_{xyz} \; \frac{d}{dt} \begin{bmatrix} \dot{C}_{13} \\ \dot{C}_{23} \\ \dot{C}_{33} \end{bmatrix}$$

$$= D_1 \begin{bmatrix} \cos\gamma & \sin\gamma & 0 \\ -\sin\gamma & \cos\gamma & 0 \\ 0 & 0 & 1 \end{bmatrix} \begin{bmatrix} C_{11} & C_{21} & C_{31} \\ C_{12} & C_{22} & C_{32} \\ C_{13} & C_{23} & C_{33} \end{bmatrix} \times$$

$$\begin{bmatrix} C_{11}\dot{\omega}_y - C_{12}\dot{\omega}_x + \dot{C}_{11}\omega_y - \dot{C}_{12}\omega_x \\ C_{21}\dot{\omega}_y - C_{22}\dot{\omega}_x + \dot{C}_{21}\omega_y - \dot{C}_{22}\omega_x \\ C_{31}\dot{\omega}_y - C_{32}\dot{\omega}_x + \dot{C}_{31}\omega_y - \dot{C}_{32}\omega_x \end{bmatrix}$$

$$= D_1 \begin{bmatrix} \dot{\omega}_y \cos\gamma - \dot{\omega}_x \sin\gamma + D_5 \\ -\dot{\omega}_y \sin\gamma - \dot{\omega}_x \cos\gamma + D_6 \\ D_7 \end{bmatrix} \tag{4-44}$$

where D_i, i = 1 to 7, are auxiliary equations as defined below.

$$D_1 = \frac{MM_s}{M + M_s} \ell_{sf}$$

$$D_2 = \dot{C}_{11} \omega_y - \dot{C}_{12} \omega_x$$

$$D_3 = \dot{C}_{21} \omega_y - \dot{C}_{22} \omega_x$$

$$D_4 = \dot{C}_{31} \omega_y - \dot{C}_{32} \omega_x$$

$$\begin{aligned} D_5 = {} & D_2 (C_{11} \cos\gamma + C_{12} \sin\gamma) \\ & + D_3 (C_{21} \cos\gamma + C_{22} \sin\gamma) \\ & + D_4 (C_{31} \cos\gamma + C_{32} \sin\gamma) \end{aligned}$$

$$D_6 = D_2 \, (-C_{11} \sin\gamma + C_{12} \cos\gamma)$$

$$+ D_3 \, (-C_{21} \sin\gamma + C_{22} \cos\gamma)$$

$$+ D_4 \, (-C_{31} \sin\gamma + C_{32} \cos\gamma)$$

$$D_7 = D_2 \, C_{13} + D_3 \, C_{23} + D_4 \, C_{33} \quad .$$

Substituting (4-44) into (4-32),

$$\begin{bmatrix} F_{as} \\ F_{bs} \\ F_{zs} \end{bmatrix} = - \begin{bmatrix} \cos\theta & 0 & -\sin\theta \\ 0 & 1 & 0 \\ \sin\theta & 0 & \cos\theta \end{bmatrix} \begin{bmatrix} \dot{\omega}_y \cos\gamma - \dot{\omega}_x \sin\gamma + D_5 \\ -\dot{\omega}_y \sin\gamma - \dot{\omega}_x \cos\gamma + D_6 \\ D_7 \end{bmatrix} D_1 \, .$$

$$= D_1 \begin{bmatrix} \dot{\omega}_x \cos\theta \sin\gamma - \dot{\omega}_y \cos\theta \cos\gamma + D_7 \sin\theta - D_5 \cos\theta \\ \dot{\omega}_x \cos\gamma + \dot{\omega}_y \sin\gamma - D_6 \\ \dot{\omega}_x \sin\theta \sin\gamma - \dot{\omega}_y \sin\theta \cos\gamma - D_7 \cos\theta - D_5 \sin\theta \end{bmatrix} . \qquad (4\text{-}45)$$

Next, using (4-18), (4-19), (4-44) and (4-45) in (4-34) gives

$$M'_{as} = \dot{\omega}_x D_1 \ell_1 \cos\gamma + \dot{\omega}_y D_1 \ell_1 \sin\gamma + D_{13} \qquad (4\text{-}46)$$

$$M'_a = -\dot{\omega}_x D_9 - \dot{\omega}_y D_{10} + D_{11} \qquad (4\text{-}47)$$

$$M'_b = -M'_{bs} + \dot{\omega}_x D_1 L \sin\gamma - \dot{\omega}_y D_1 L \cos\gamma - D_{12} \qquad (4\text{-}48)$$

where D_j, j = 8 to 12, are defined by the following auxiliary equations

$$D_8 = (\ell_1 \cos\theta + L)\, D_1$$

$$D_9 = D_8 \cos\gamma$$

$$D_{10} = D_8 \sin\gamma$$

$$D_{11} = D_6\, D_8 + K_s\, \dot{\gamma}_s \csc\theta - K\, \dot{\gamma} \cot\theta$$

$$D_{12} = L\, D_1\, D_5 + \ell_1\, D_1\, D_7 \sin\theta$$

Multiplying the first equation of (4-29) by $\cos\gamma_s$ and the second one by $\sin\gamma_s$, then taking the difference,

$$\dot{\nu}_{xs} (J_{11} \cos\gamma_s) - \dot{\nu}_{ys} (J_{22} \sin\gamma_s)$$

$$= D_{13} + \ell_1\, D_1\, D_6 - (J_{33} - J_{22})\, \nu_{ys}\, \nu_{zs} \cos\gamma_s$$

$$+ (J_{11} - J_{33})\, \nu_{xs}\, \nu_{zs} \sin\gamma_s \qquad (4\text{-}49)$$

where

$$D_{13} = -D_1\, D_6\, \ell_1 + (K\dot{\gamma} - K_s\, \dot{\gamma}_s \cos\theta)/\sin\theta$$

Multiplying the first equation of (4-29) by $\sin\gamma_s$ and the second one by $\cos\gamma_s$, then taking the sum,

$$J_{11}\,\dot{\nu}_{xs}\sin\gamma_s + J_{22}\,\dot{\nu}_{ys}\cos\gamma_s + (J_{33} - J_{22})\,\nu_{ys}\,\nu_{zs}\sin\gamma_s$$

$$+ (J_{11} - J_{33})\,\nu_{xs}\,\nu_{zs}\cos\gamma_s = M'_{bs} + F_{as}\,\ell_1$$

Substituting the detail of F_{as} given by (4-45) into this equation, gives

$$M'_{bs} = -\dot{\omega}_x\,\ell_1\,D_1\cos\theta\sin\gamma + \dot{\omega}_y\,\ell_1\,D_1\cos\theta\cos\gamma$$

$$+ \dot{\nu}_{xs}\,J_{11}\sin\gamma_s + \dot{\nu}_{ys}\,J_{22}\cos\gamma_s + D_{14} \qquad (4\text{-}50)$$

where

$$D_{14} = (J_{33} - J_{22})\,\nu_{ys}\,\nu_{zs}\sin\gamma_s + (J_{11} - J_{33})\,\nu_{xs}\,\nu_{zs}\cos\gamma_s$$

$$+ \ell_1\,D_1\,(D_5\cos\theta - D_7\sin\theta)$$

Substituting (4-50) into (4-48),

$$M'_b = \dot{\omega}_x\,D_{15} - \dot{\omega}_y\,D_{16} - \dot{\nu}_{xs}\,J_{11}\sin\gamma_s - \dot{\nu}_{ys}\,J_{22}\cos\gamma_s - D_{12} - D_{14} \qquad (4\text{-}51)$$

Substituting details of F_a, F_b, M'_a, M'_b, given by (4-44), (4-47) and (4-51) into the first equation of (4-23),

$$\dot{\omega}_x (I_{11} + D_9 \cos\gamma + \ell_5 D_1 + D_{15} \sin\gamma) + \dot{\omega}_y (D_{10} \cos\gamma$$

$$- D_{16} \sin\gamma) - \dot{v}_{xs} J_{11} \sin\gamma_s \sin\gamma - \dot{v}_{ys} J_{22} \cos\gamma_s \sin\gamma$$

$$= - (I_{33} - I_{22}) \omega_y \omega_z + D_{11} \cos\gamma + (D_{12} + D_{14}) \sin\gamma$$

$$+ \ell_5 D_1 D_6 \cos\gamma + \ell_5 D_1 D_5 \sin\gamma + T_{xc} \qquad (4\text{-}52)$$

where

$$D_{15} = D_8 \sin\gamma$$

$$D_{16} = D_8 \cos\gamma$$

Similarly, from the second equation of (4-23),

$$\dot{\omega}_x (D_9 \sin\gamma - D_{15} \cos\gamma) + \dot{\omega}_y (I_{22} + D_{10} \sin\gamma + D_{16} \cos\gamma$$

$$+ \ell_5 D_1) + \dot{v}_{xs} J_{11} \sin\gamma_s \cos\gamma + \dot{v}_{ys} J_{22} \cos\gamma_s \cos\gamma$$

$$= - (I_{11} - I_{33}) \omega_x \omega_z + D_{11} \sin\gamma - (D_{12} + D_{14}) \cos\gamma$$

$$+ \ell_5 D_1 D_6 \sin\gamma - \ell_5 D_1 D_5 \cos\gamma + T_{yc} \qquad (4\text{-}53)$$

From the third equation of (4-23)

$$\dot{\omega}_z = [K\,\dot{\gamma} + T_{zc} - (I_{22} - I_{11})\,\omega_x\,\omega_y]/I_{33} \tag{4-54}$$

From the third equation of (4-29)

$$\dot{\nu}_{zs} = [-K_s\,\dot{\gamma}_s - (J_{22} - J_{11})\,\nu_{xs}\,\nu_{ys}]\,/\,J_{33} \tag{4-55}$$

Differentiating (4-13)

$$\begin{aligned} &-\dot{\omega}_x \sin\gamma + \dot{\omega}_y \cos\gamma - \dot{\nu}_{xs} \sin\gamma_s - \dot{\nu}_{ys} \cos\gamma_s \\ &= (\omega_x \cos\gamma + \omega_y \sin\gamma)\,\dot{\gamma} + (\nu_{xs} \cos\gamma_s - \nu_{ys} \sin\gamma_s)\dot{\gamma}_s \end{aligned} \tag{4-56}$$

Summary

The set of simulation equations is summarized as follows

$$\begin{aligned} \dot{\gamma}_s &= \nu_{zs} - (\omega_x \cos\gamma + \omega_y \sin\gamma) \csc\theta \\ &\quad + (\nu_{xs} \cos\gamma_s - \nu_{ys} \sin\gamma_s) \cot\theta \end{aligned} \tag{4-11}$$

$$\begin{aligned} \dot{\gamma} &= -\omega_z + (\omega_x \cos\gamma + \omega_y \sin\gamma) \cot\theta \\ &\quad -(\nu_{xs} \cos\gamma_s - \nu_{ys} \sin\gamma_s) \csc\theta \end{aligned} \tag{4-12}$$

$$\dot{\omega}_z = [K\,\dot{\gamma} + T_{zc} - (I_{22} - I_{11})\,\omega_x\,\omega_y] \,/\, I_{33} \tag{4-54}$$

$$\dot{\nu}_{zs} = [-K_s\,\dot{\gamma}_s - (J_{22} - J_{11})\,\nu_{xs}\,\nu_{ys}] \,/\, J_{33} \tag{4-55}$$

Grouping (4-49), (4-52), (4-53) and (4-56) into a single matrix equation,

$$\begin{bmatrix} I_{11} + D_9 \cos\gamma + \ell_5 D_1 + D_{15} \sin\gamma & D_{10} \cos\gamma - D_{16} \sin\gamma & -J_{11} \sin\gamma_s \sin\gamma & -J_{22} \cos\gamma_s \sin\gamma \\ D_9 \sin\gamma - D_{15} \cos\gamma & I_{22} + D_{10} \sin\gamma + \ell_5 D_1 + D_{16} \cos\gamma & J_{11} \sin\gamma_s \cos\gamma & J_{22} \cos\gamma_s \cos\gamma \\ 0 & 0 & J_{11} \cos\gamma_s & J_{22} \sin\gamma_s \\ -\sin\gamma & \cos\gamma & -\sin\gamma_s & -\cos\gamma_s \end{bmatrix} \begin{bmatrix} \dot{\omega}_x \\ \dot{\omega}_y \\ \dot{\nu}_{xs} \\ \dot{\nu}_{ys} \end{bmatrix}$$

$$= \begin{bmatrix} -(I_{33} - I_{22})\,\omega_y\,\omega_z + D_{11} \cos\gamma + \ell_5 D_1 D_6 \cos\gamma \\ + (D_{12} + D_{14}) \sin\gamma + \ell_5 D_1 D_5 \sin\gamma + T_{xc} \\ \\ -(I_{11} - I_{33})\,\omega_x\,\omega_z + D_{11} \sin\gamma + \ell_5 D_1 D_6 \sin\gamma \\ - (D_{12} + D_{14}) \cos\gamma - \ell_5 D_1 D_5 \cos\gamma + T_{yc} \\ \\ D_{13} + \ell_1 D_1 D_6 - (J_{33} - J_{22})\,\nu_{ys}\,\nu_{zs} \cos\gamma_s \\ + (J_{11} - J_{33})\,\nu_{xs}\,\nu_{zs} \sin\gamma_s \\ \\ (\omega_x \cos\gamma + \omega_y \sin\gamma)\,\dot{\gamma} + (\nu_{xs} \cos\gamma_s - \nu_{ys} \sin\gamma_s)\,\dot{\gamma}_s \end{bmatrix}$$

Among the eight angular variables, γ_s, γ, ω_z and ν_{zs} can be obtained by integrating (4-11), (4-12), (4-54) and (4-55) directly. While ω_x, ω_y, ν_{xs} and ν_{ys} have to be obtained by solving the above four simultaneous linear equations for $\dot{\omega}_x$, $\dot{\omega}_y$, $\dot{\nu}_{xs}$ and $\dot{\nu}_{ys}$ and then integrating them. A subroutine named "SIMQ" is used in simulation program to solve these simultaneous linear equations. Also,

$$T_{xc} = -k_1 \omega_x + k_2 C_{11} (C_{23} - C_{32}) \tag{4-40}$$

$$T_{yc} = -k_3 \omega_y + k_4 C_{22} (C_{31} - C_{13}) \tag{4-41}$$

$$T_{zc} = -k_5 \omega_z + k_6 C_{33} (C_{12} - C_{21}) \tag{4-42}$$

The direction cosine elements C_{ij}'s are obtained by integrating the set of nine equations given by (4-39), that is,

$$\dot{C}_{11} = C_{12} \omega_z - C_{13} \omega_y$$

$$\dot{C}_{12} = C_{13} \omega_x - C_{11} \omega_z$$

$$\dot{C}_{13} = C_{11} \omega_y - C_{12} \omega_x$$

$$\dot{C}_{21} = C_{22} \omega_z - C_{23} \omega_y$$

$$\dot{C}_{22} = C_{23} \omega_x - C_{21} \omega_z$$

$$\dot{C}_{23} = C_{21}\,\omega_y - C_{22}\,\omega_x$$

$$\dot{C}_{31} = C_{32}\,\omega_z - C_{33}\,\omega_y$$

$$\dot{C}_{32} = C_{33}\,\omega_x - C_{31}\,\omega_z$$

$$\dot{C}_{33} = C_{31}\,\omega_y - C_{32}\,\omega_x$$

Simulation Parameters and Initial Conditions

Values of parameters and initial conditions used for the simulation are shown below.

Parameter Values (Figure 4-8)

FFTO:

$$M = 200 \text{ kg}$$

$$I_{11} = \frac{M}{12}\,(0.8^2 + 1.5^2) = 48.17 \text{ kg-m}^2$$

$$I_{22} = \frac{M}{12}\,(1.2^2 + 1.5^2) = 61.5 \text{ kg-m}^2$$

$$I_{33} = \frac{M}{12}\,(0.8^2 + 1.2^2) = 34.67 \text{ kg-m}^2$$

$$I_{12} = I_{23} = I_{31} = 0$$

$$\ell_5 = \frac{1.5}{2} = 0.75 \text{ m}$$

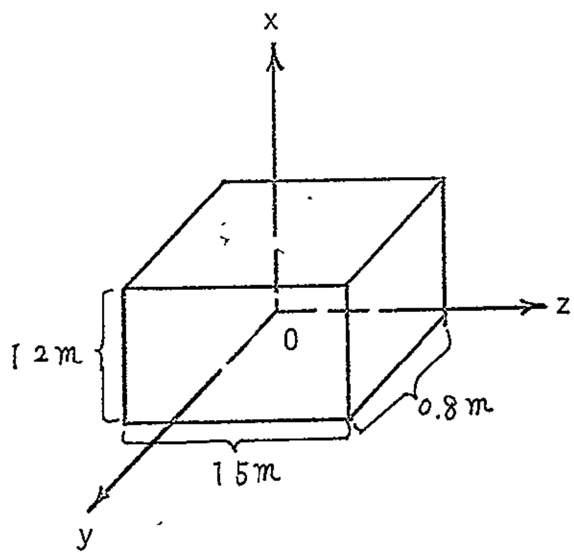

(a) FFTO

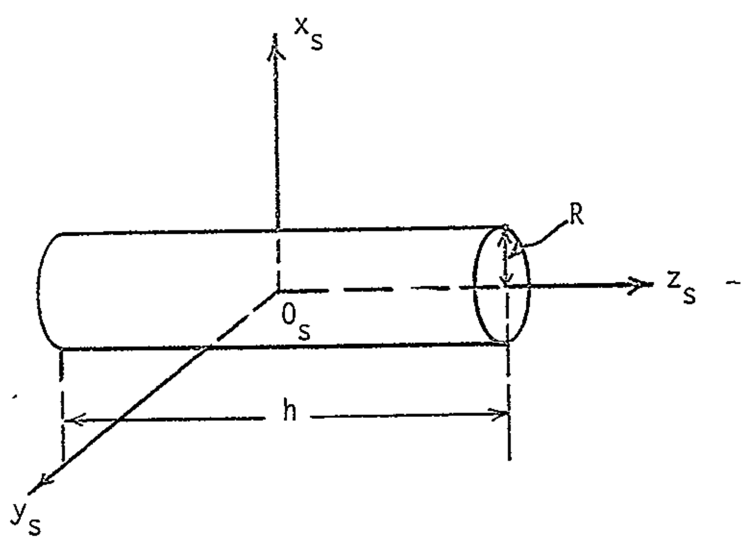

(b) SATELLITE

Figure 4-8. Dimensions for FFTO and Satellite

Satellite:

$M_s = 6{,}600$ kg

$R = 1.741$ m.

$h = 6\ R = 10.446$ m

$\ell_1 = 0.5\ h = 5.223$ m

$$J_{33} = \frac{1}{2} MR^2 = 10{,}000 \text{ kg-m}^2$$

$$J_{11} = J_{22} = \frac{M}{12} (3R^2 + h^2) = 65{,}016.7 \text{ kg-m}^2$$

$$J_{12} = J_{23} = J_{31} = 0$$

Arm of FFTO:

Assume Massless

$\ell_2 = 1.277$ m

$\ell_3 = 5.0$ m

$\ell_4 = 0.5$ m

Initial Conditions

$$\alpha_1 = \alpha_2 = \theta = 60°$$

$$\omega_{xo} = \omega_{yo} = \omega_{zo} = 0$$

$$\nu_{xso} = -0.3464 \text{ rad/sec}$$

$$\nu_{yso} = 0$$

$$\nu_{zso} = 1.300334 \text{ rad/sec.}$$

$$\gamma = 0$$

$$\gamma_s = 0$$

$$C_{11} = C_{22} = C_{33} = 1$$

$$C_{12} = C_{21} = C_{23} = C_{32} = C_{13} = C_{31} = 0$$

The initial condition data shows that

$$\frac{|H_{zs}|}{|H_{as}|} = \frac{J_{33}\,\nu_{zs}}{J_{11}\,\nu_{as}} = \frac{10{,}000 \times 1.3003}{65{,}016.7 \times 0.3464} = \frac{1}{\sqrt{3}} = \cot 60°$$

Hence, $\underline{H}$ is initially along the z-direction as shown in Figure 4-9.

Brake Forces. The brake force factors are chosen to be ramp functions are shown below.

$$K = K_s = 1000\ t \qquad \text{(t in seconds)}$$

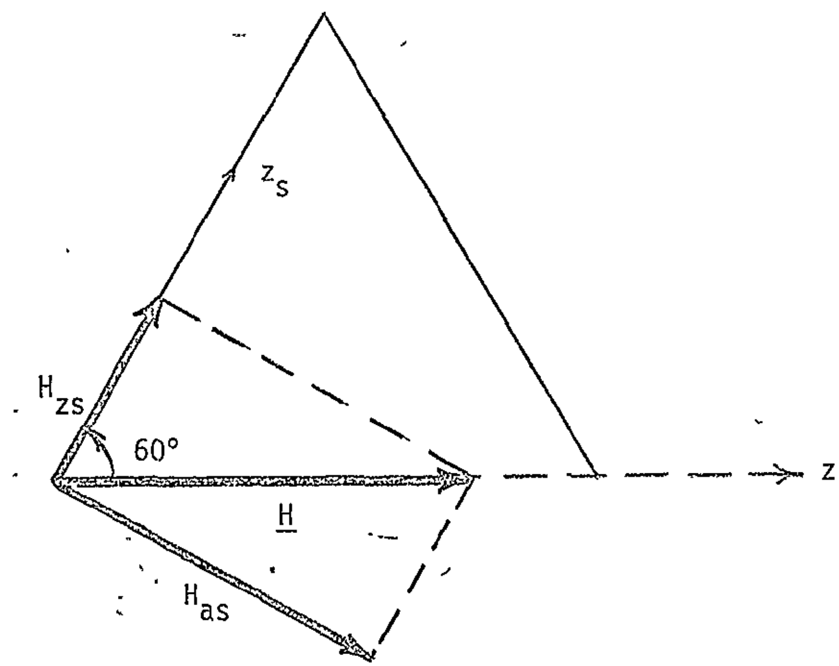

Figure 4-9. Initial Angular Momentum of Satellite

Thrust Torques

$$k_1 = k_3 = k_5 = 10{,}000$$

$$k_2 = k_4 = k_6 = 100{,}000$$

Simulation Results and Discussion

Results of the simulation are plotted in Figures 4-10 to 4-16. The simulation revealed a stable joint dynamics of the FFTO-satellite system. The results are very encouraging.

Figure 4-10 shows the time responses of FFTO's reaction angular rates. The reaction angular rates decrease as expected. The oscillation in each angular rate, though may not be objectionable, can be removed by adopting a different control law or by increasing the rate control constant k_i ($i = 1, 3, 5$) of the present control law.

Figure 4-11 depicts the time response of direction cosines C_{ii}, $i = 1$ to 3, of the FFTO. Their values are not constant, but the variations are small. The maximum deviation of the values of direction cosines from unity is 0.014. This deviation practically disappears completely after 15 seconds, indicating an effective stabilization effort.

Figure 4-12 contains time responses of the satellite's angular rate during the detumble-despin operation. It is shown that, after 15 seconds, the satellite lost most of its dynamics from an initial rate of 1.3 rad./sec to less than 0.1 rad./sec along the z_s-axis. Similar behavior is for other axes.

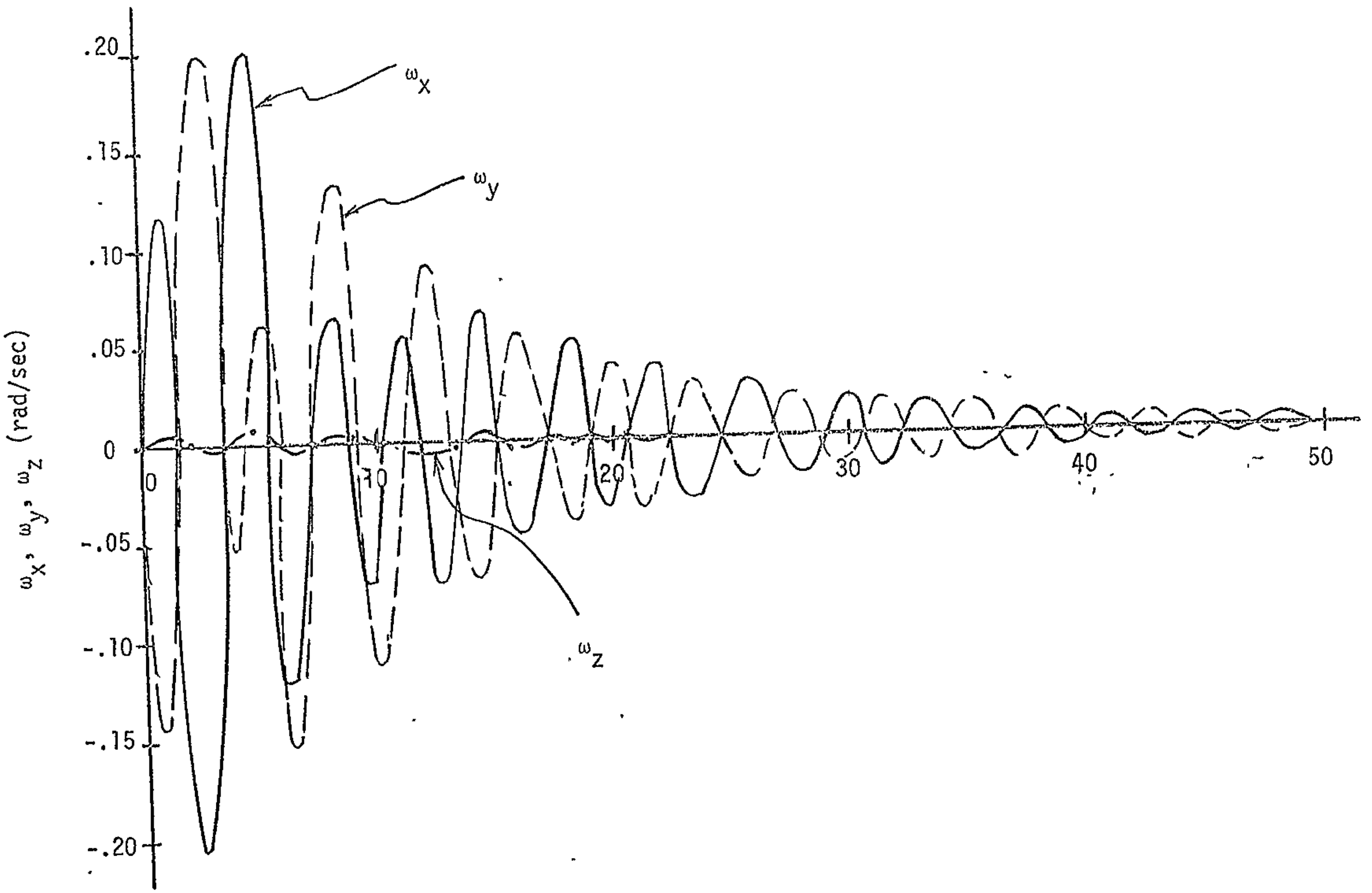

Figure 4-10. Time Response of FFTO

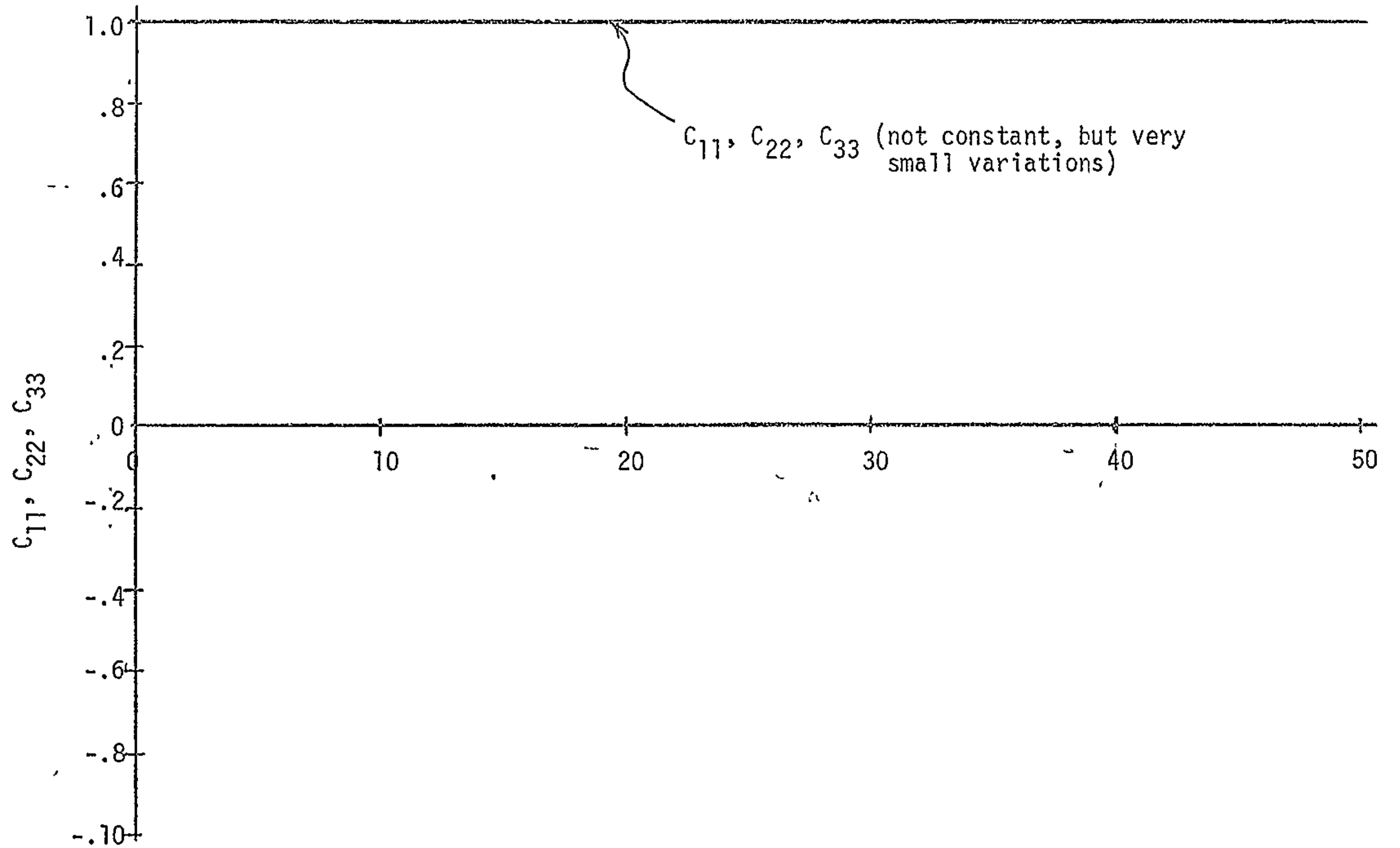

Figure 4-11. Direction Cosine of FFTO

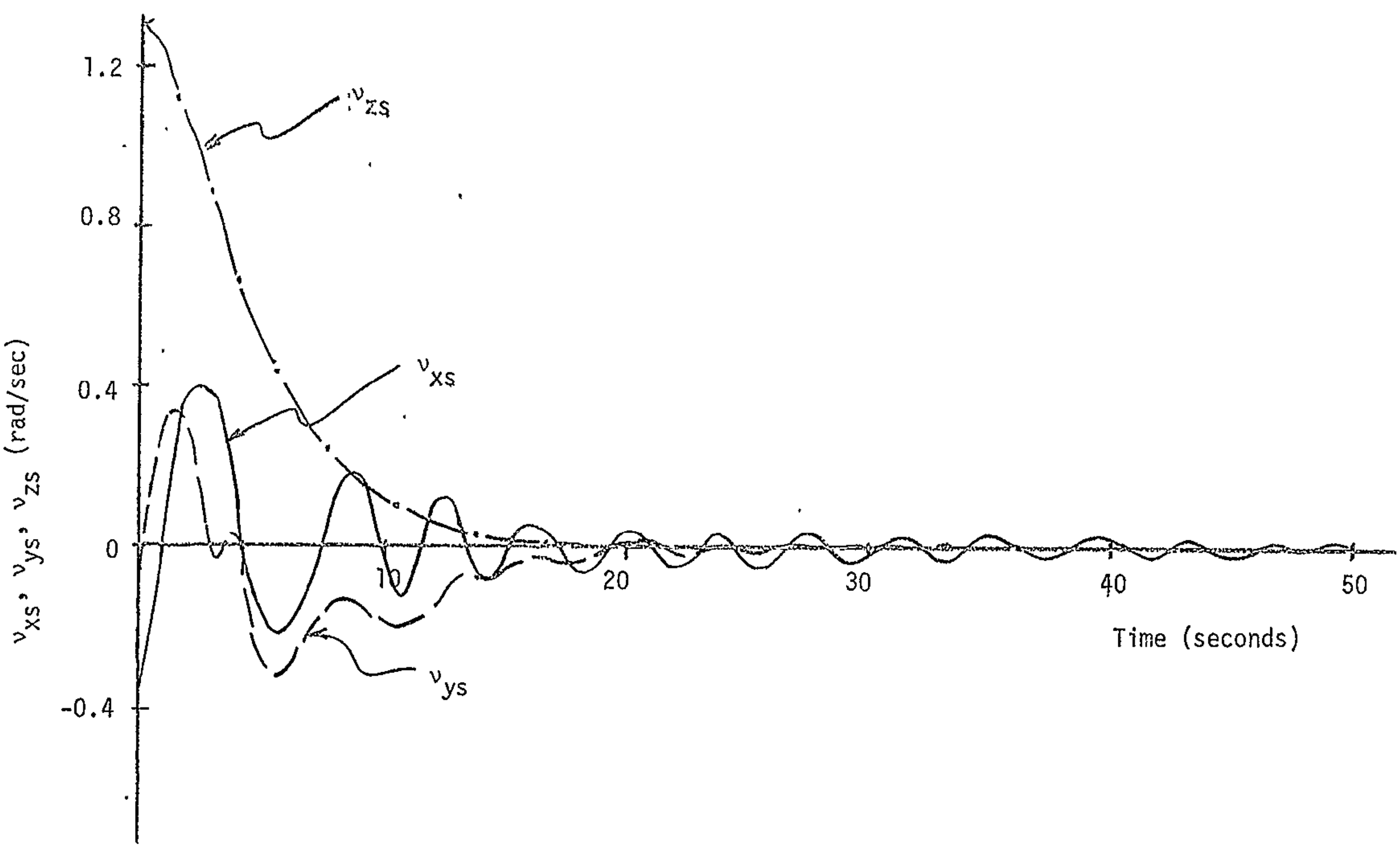

Figure 4-12. Time Response of Satellite

Figure 4-13 plots the angular momentum of the satellite. The momentum is reduced in 15 seconds from its initial value of 2.6×10^4 kg-m^2-rad./sec to 2.8×10^2 kg-m^2-rad./sec which is about 1% of the initial value.

Figure 4-14 shows the relative angular rates at two brake junctions. The angular rate $\dot{\gamma}_s$ decreases nonotomically while $\dot{\gamma}$ decreases with a small oscillation at the beginning.

Figure 4-15 shows the relative angles at two brake junctions. Both angles become constant after about 15 seconds indicating the diminishing of relative motion between the FFTO and satellite.

Figure 4-16 gives the time responses of thrust torques in three orthogonal directions. The maximum torque value is about 2.6×10^4 newton-meters in the x any y directions and about 2.2×10^3 newton-meters in z-direction. The oscillations in torques require oscillation in thrusts which may be objectionable. However, by using a different control law the oscillatory behavior can be removed.

Simulation Program

The simulation is written in CSMP which is included in Appendix 2.

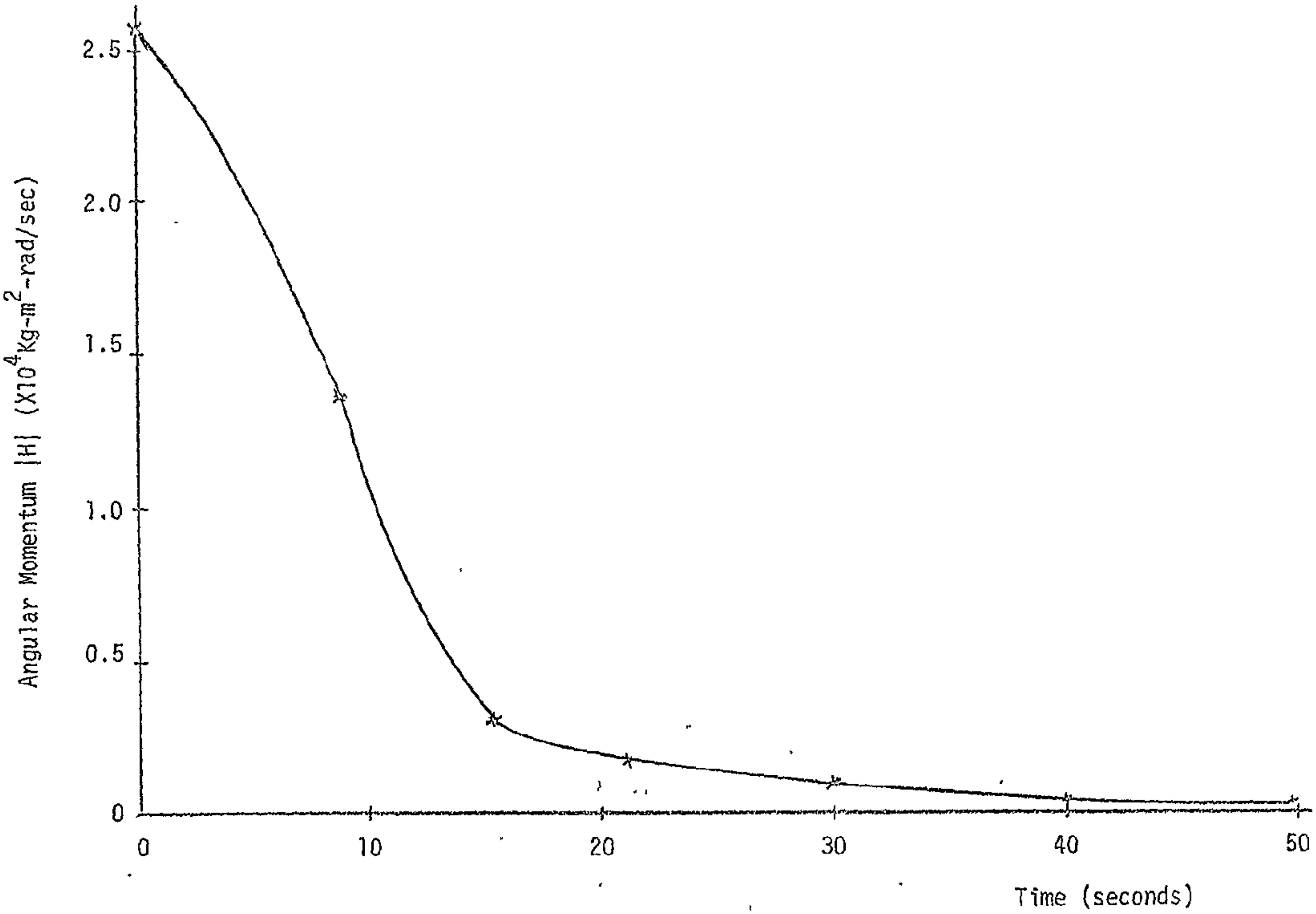

Figure 4-13. Angular Momentum of Satellite

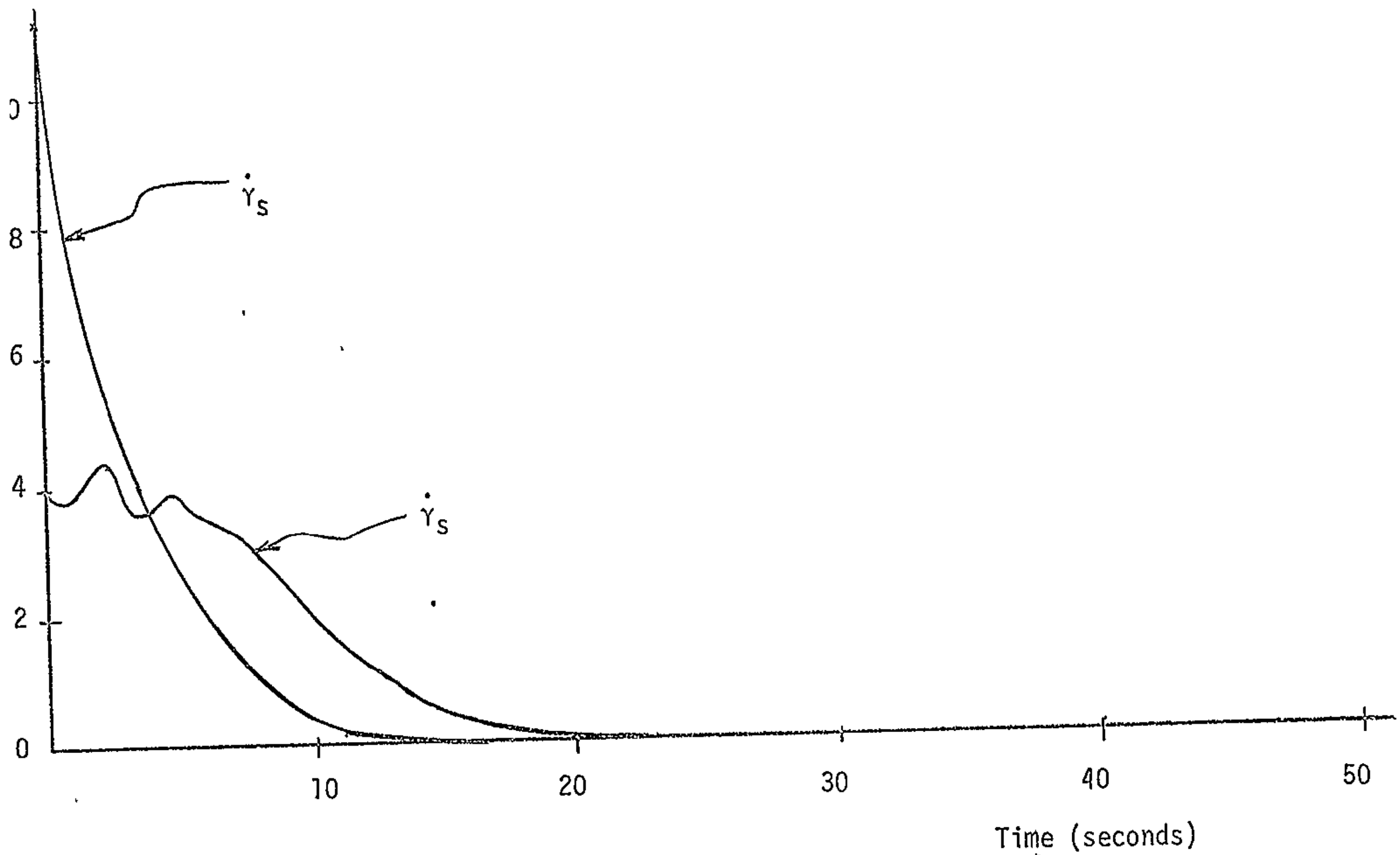

Figure 4-14. Relative Angular Rates Versus Time

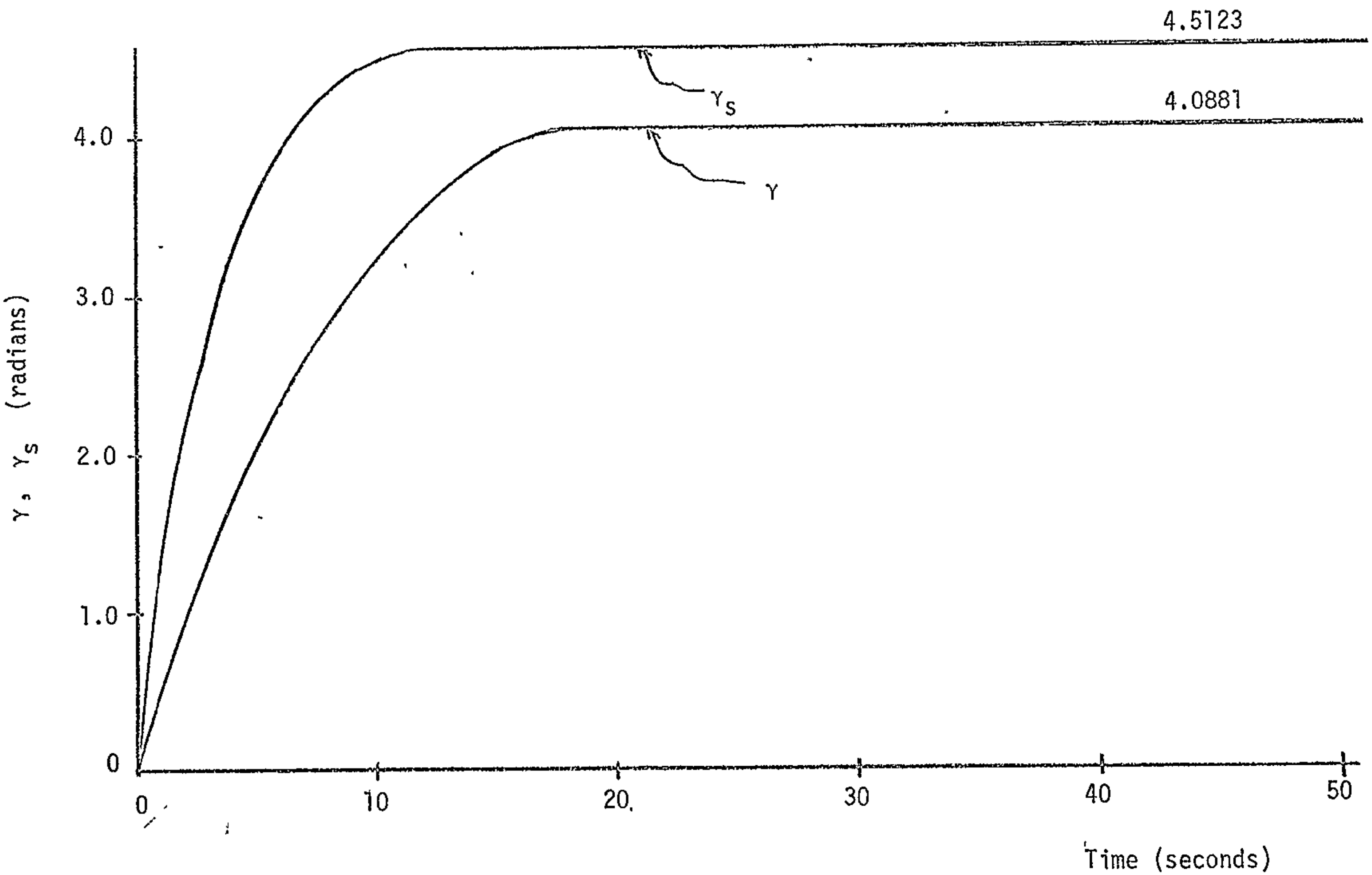

Figure 4-15. Relative Angles Versus Time

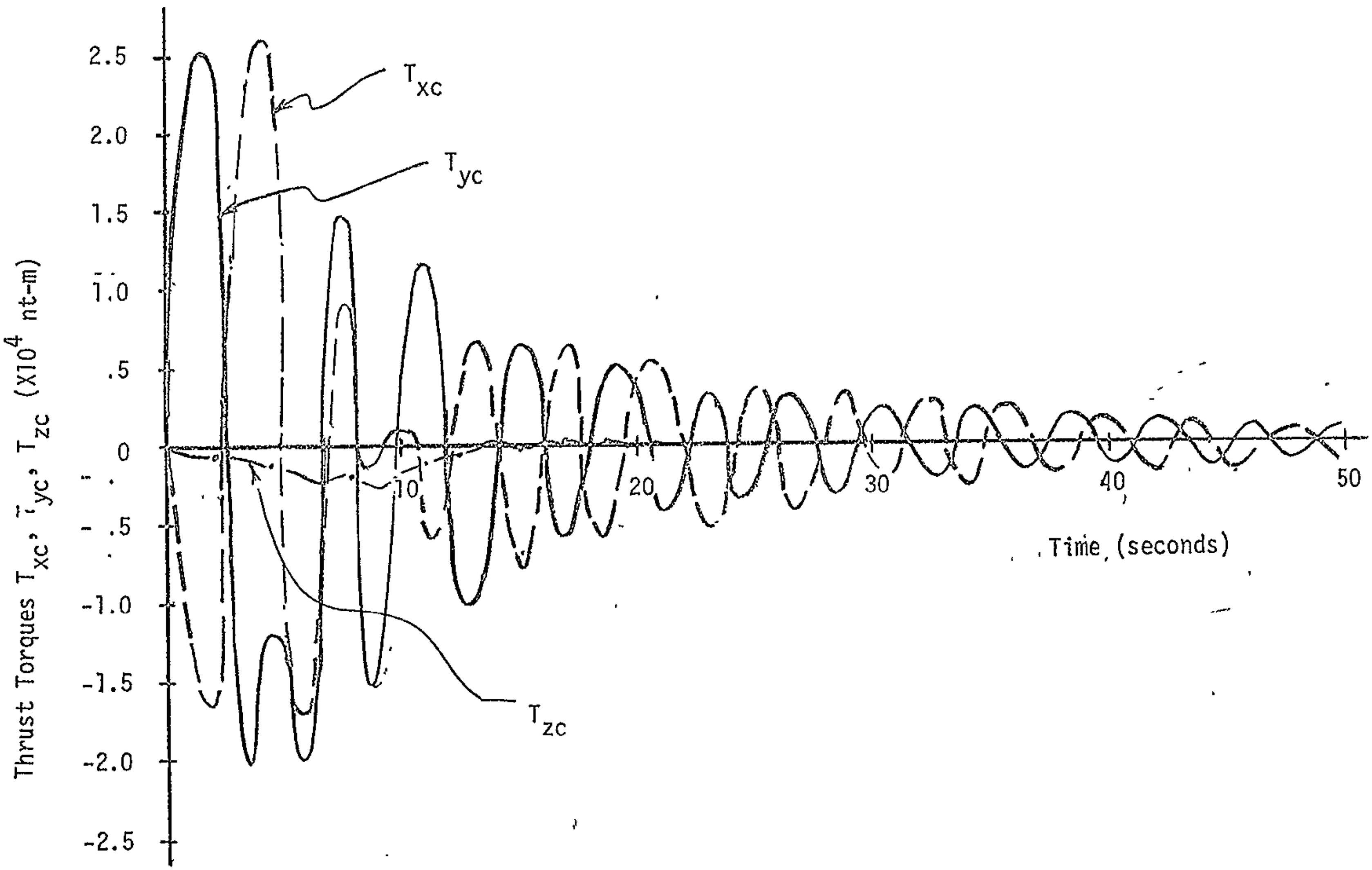

Figure 4-16. Thrust Torques Versus Time

CHAPTER 5

SUMMARY AND RECOMMENDATIONS

This study resulted in three kinds of equations of motion for the free-flying teleoperator system. The first kind is a set of kinematic equations for the FFTO's manipulator. They describe the positions and velocities of the manipulator hand with respect to various coordinate systems. These equations are useful in generating the reference signals for the control of the position and velocity of the hand, especially for catching an object which is within the reach of the arm.

The second kind of equations of motion are two sets of equations which describe the dynamics of a satellite under an ideal detumble and/or despin operation. The idealized assumption is that the FFTO is fixed in space. The objective of this study is to obtain some understanding about the satellite dynamics, paving a way for the study of more realistic cases later. The first set of equations is for the case where the body of a satellite is axially symmetrical. Computer simulations were obtained for this case. The second set of equations is for a general body configuration. The analytic expression for this case is very complex. No simulation was performed for this case.

The third kind of equations of motion is a model describing the combined dynamics of a FFTO and a satellite during detumble and despin operation. The FFTO is not assumed fixed. The motion of FFTO is due to the reaction torque and force exerted by a dynamic satellite. The set of equations are highly nonlinear. For the convenience of observation, the joint dynamic of the FFTO-satellite system is quieted down by the use of a FFTO stabilization. A direction cosine control law is arbitrarily selected for this purpose. Simulation was performed to test the model. The result confirms the adequacy of the model.

All the computer simulations were written in CSMP. They are included in the appendices. The parameters in these programs can be changed to simulate different conditions.

The development of the above models has allowed us to gain a deep understanding of the motion of a FFTO, a satellite, and their combination. Momentum and competence now exist enabling further research to the problem. The following areas are recommended for further study.

Thrust Level Requirement. To obtain a good stabilization of the joint FFTO-satellite system the thrust level was not limited in the simulation. The maximum thrust value was about 2.5×10^4 newton-meters along x or y axis, and about 2.2×10^3 newton-meters along z-axis. These values seem large. It is important to find out if the detumble-despin operation can be accomplished using a more realistic thrust level.

Effect of Arm Mass. In the present study, the arm mass has been neglected. Inclusion of arm mass will complicate the analytic formulation a good deal. However, knowledge of effects of arm mass on the total system dynamics and on the control effort is important. A study of these effects should be made.

Variable Arm Angles. Arm angles α_1 and α_2 were made constant for the present study. It is not known yet if there is any advantage to be gained by allowing α_1 and α_2 to vary. Permitting variable α_1 and α_2 will also increase the complexity of the equations of motion. But based on the results obtained in the present study, this generalization can be made without too much difficulty.

Desired Control Law. The control law governs brake forces and thrust levels. The control law used in this study is arbitrarily chosen. A study should be made to arrive at a simple but effective control. Due to the nonlinearity and the high dimensionality of the system, this task is not a simple one, although the results of the present study will make it easier. One important consideration is the advantage of exerting a preferred combination of despin and decone torques to maintain the angular momentum vector of the satellite as stationary as possible in space. It is believed that this will help in reducing the need of high stabilization torques for FFTO. The result obtained in Chapter 3 can help to accomplish this.

Additional Simulations. Due to the limitation in time many desired simulations could not be performed. With the model already developed, it will be very worthwhile to continue the desired simulations.

REFERENCES

1. Bell Aerospace Company, "Shuttle Free-Flying Teleoperator System Experiment Definition," Report No. D7425-953008, Final Report for NASA Contract NAS8-29153, February, 1973.

2. G. T. Onego and J. H. Clingman, "Free-Flying Teleoperator Requirements and Conceptual Design," Proceedings of the First National Conference on Remotely Manned Systems, California Institute of Technology, September, 1972.

3. H. Fornoff and W. G. Thornton, "Experimental Evaluation of Remote Manipulator Systems," Proceedings of the First National Conference on Remotely Manned Systems, California Institute of Technology, September, 1972.

4. G. C. Faile, D. N. Counter, and E. J. Bourgeois, "Dynamic Passivation of a Spinning and Tumbling Satellite Using Free-Flying Teleoperators," Proceedings of the First National Conference on Remotely Manned Systems, California Institute of Technology, September, 1972.

5. A. Sommerfold, Mechanics, Lecture on Theoretical Physics, Volume 1, Academic Press, New York, 1964.

6. H. Goldstein, Classical Mechanics, Addison-Wesley Publishing Company, Reading, Mass., 1950.

7. D. T. Greenwood, Principles of Dynamics, Prentice-Hall, Inc., Englewood Cliffs, N.J., 1965, p. 364.

8. J. C. Slater and N. H. Frank, Introduction to Theoretical Physics, McGraw-Hill Book Co., 1933, p. 100.

9. R. H. Cannon, Jr., Dynamics of Physical Systems, McGraw-Hill Book Company, New York, 1967.

10. R. L. Halfman, Dynamics, Volumes I and II, Addison-Wesley, Reading, Massachusetts, 1962.

APPENDIX 1

CSMP PROGRAMS FOR CHAPTER 3

A. Simultaneous Despin and Decone

```
LABEL DESPINING AND  DECONING WITH A=800
INITIAL
CONSTANT IA1=9529,IT1=212129,PHI10=0,SY0=0,TET1D0=0,M0=0
DYNAMIC
PARAMETER TET10=1.1486,PHI1D0=4.19,SYD0=0.4809,A=800
C=A*TET1
MX=0
MY=-C*SYD*SIN(TET1)
MZ=-C*IA1*(SYD*COS(TET1)+PHI1D)/IT1
TET1D2=(MX-IA1*(PHI1D+SYD*COS(TET1))*SYD*SIN(TET1))/IT1+SYD**2*...
SIN(TET1)*COS(TET1)
SYD2=(MY-2*IT1*SYD*TET1D*COS(TET1)+IA1*(PHI1D+SYD*COS(TET1))*...
TET1D)/(IT1*SIN(TET1))
PHI1D2=MZ/IA1-SYD2*COS(TET1)+SYD*TET1D*SIN(TET1)
H=SQRT(IT1**2*(TET1D**2+SYD**2*SIN(TET1)**2)+IA1**2*(PHI1D+...
SYD*COS(TET1))**2)
ANGL=SQRT((IT1*TET1D)**2+(SYD*SIN(TET1)*COS(TET1)*(IT1-IA1)-IA1*...
PHI1D)**2)/(IA1*(PHI1D+SYD*COS(TET1))*COS(TET1)+IT1*SYD*SIN(TET1)**2)
BETA=ATAN(ANGL)
W12=SQRT(TET1D**2+SYD**2*SIN(TET1)**2)
W3=PHI1D+SYD*COS(TET1)
M=SQRT(MX**2+MY**2+MZ**2)
SYD=INTGRL(SYD0,SYD2)
SY=INTGRL(SY0,SYD)
PHI1D=INTGRL(PHI1D0,PHI1D2)
PHI1=INTGRL(PHI10,PHI1D)
TET1D=INTGRL(TET1D0,TET1D2)
```

```
TET1=INTGRL(TET10,TET1D)
MT=INTGRL(MO,M)
PRINT MT
PRTPLT SYD,PHI1D,TET1,H,BETA,W12,W3
TIMER DELT=0.05,FINTIM=600,OUTDEL=5
FINISH SYD=0.01
PRTPLT SYD,PHI1D,TET1,H,BETA,W12,W3
END
TERMINAL
STOP
ENDJOB
```

B. DETUMBLE THEN DESPIN

```
LABEL DETUMBLING THEN DESPINING WITH A=20
INITIAL
CONSTANT IA1=9529,IT1=212129,PHI10=0,SY0=0,TET1D0=0
DYNAMIC
PARAMETER TET10=1.1486,PHI1D0=4.19,SYD0=0.4809,A=20,...
X=-1,Y=-1,Z=0,M=0.01,N=10,MO=0
B=AND(A,TET1)
C=B*A*TET1
MX=C*X*TET1D
MY=C*Y*SYD*SIN(TET1)
MZ=C*Z
TET1D2=(MX-IA1*(PHI1D+SYD*COS(TET1))*SYD*SIN(TET1))/IT1+SYD**2*...
SIN(TET1)*COS(TET1)
SYD2=(MY-2*IT1*SYD*TET1D*COS(TET1)+IA1*(PHI1D+SYD*COS(TET1))*...
TET1D)/(IT1*SIN(TET1))
PHI1D2=MZ/IA1-SYD2*COS(TET1)+SYD*TET1D*SIN(TET1)
H=SQRT(IT1**2*(TET1D**2+SYD**2*SIN(TET1)**2)+IA1**2*(PHI1D+...
SYD*COS(TET1))**2)
ANGL=SQRT((IT1*TET1D)**2+(SYD*SIN(TET1)*COS(TET1)*(IT1-IA1)-IA1*...
PHI1D)**2)/(IA1*(PHI1D+SYD*COS(TET1))*COS(TET1)+IT1*SYD*SIN(TET1)**2)
```

```
BETA=ATAN(ANGL)
W12=SQRT(TET1D**2+SYD**2*SIN(TET1)**2)
W3=PHI1D+SYD*COS(TET1)
M=SQRT(MX**2+MY**2+MZ**2)
SYD=INTGRL(SYD0,SYD2)
SY=INTGRL(SY0,SYD)
PHI1D=INTGRL(PHI1D0,PHI1D2)
PHI1=INTGRL(PHI10,PHI1D)
TET1D=INTGRL(TET1D0,TET1D2)
TET1=INTGRL(TET10,TET1D)
MT=INTGRL(M0,M)
PRTPLT SYD,PHI1D,TET1,M,BETA,W12,W3
PRINT MT
TIMER DELT=0.05,FINTIM=5000,OUTDEL=25
FINISH W12=0.200
END
TERMINAL
STOP
ENDJOB

LABEL DETUMBLING THEN DESPINING WITH A=200
INITIAL
CONSTANT IA1=9529,IT1=212129,PHI10=0,SY0=0,TET1D0=0
DYNAMIC
PARAMETER TET10=1.1486,PHI1D0=4.19,SYD0=0.4809,A=200,...
X=-1,Y=-1,Z=0,M=0.01,N=10,M0=0
B=AND(A,TET1)
C=B*A*TET1
MX=C*X*TET1D
MY=C*Y*SYD*SIN(TET1)
MZ=C*Z
TET1D2=(MX-IA1*(PHI1D+SYD*COS(TET1))*SYD*SIN(TET1))/IT1+SYD**2*...
SIN(TET1)*COS(TET1)
SYD2=(MY-2*IT1*SYD*TET1D*COS(TET1)+IA1*(PHI1D+SYD*COS(TET1))*...
```

```
TET1D)/(IT1*SIN(TET1))
PHI1D2=MZ/IA1-SYD2*COS(TET1)+SYD*TET1D*SIN(TET1)
H=SQRT(IT1**2*(TET1D**2+SYD**2*SIN(TET1)**2)+IA1**2*(PHI1D+...
SYD*COS(TET1))**2)
ANGL=SQRT((IT1*TET1D)**2+(SYD*SIN(TET1)*COS(TET1)*(IT1-IA1)-IA1*...
PHI1D)**2)/(IA1*(PHI1D+SYD*COS(TET1))*COS(TET1)+IT1*SYD*SIN(TET1)**2)
BETA=ATAN(ANGL)
W12=SQRT(TET1D**2+SYD**2*SIN(TET1)**2)
W3=PHI1D+SYD*COS(TET1)
M=SQRT(MX**2+MY**2+MZ**2)
SYD=INTGRL(SYD0,SYD2)
SY=INTGRL(SY0,SYD)
PHI1D=INTGRL(PHI1D0,PHI1D2)
PHI1=INTGRL(PHI10,PHI1D)
TET1D=INTGRL(TET1D0,TET1D2)
TET1=INTGRL(TET10,TET1D)
MT=INTGRL(M0,M)
PRTPLT SYD,PHI1D,TET1,H,BETA,W12,W3
PRINT MT
TIMER DELT=0.05,FINTIM=800,CUTDEL=5
FINISH W12=0.200
END
TERMINAL
STOP
ENDJOB


LABEL DETUMBLING THEN DESPINING WITH A=800
INITIAL
CONSTANT IA1=9529,IT1=212129,PHI10=0,SY0=0,TET1D0=0
DYNAMIC
PARAMETER TET10=1.1486,PHI1D0=4.19,SYD0=0.4809,A=800,...
X=-1,Y=-1,Z=0,M=0.01,N=10,M0=0
B=AND(A,TET1)
C=B*A*TET1
```

```
MX=C*X*TETlD
MY=C*Y*SYD*SIN(TETl)
MZ=C*Z
TETlD2=(MX-IAl*(PHIlD+SYD*COS(TETl))*SYD*SIN(TETl))/ITl+SYD**2*...
SIN(TETl)*COS(TETl)
SYD2=(MY-2*ITl*SYD*TETlD*COS(TETl)+IAl*(PHIlD+SYD*COS(TETl))*...
TETlD)/(ITl*SIN(TETl))
PHIlD2=MZ/IAl-SYD2*COS(TETl)+SYD*TETlD*SIN(TETl)
H=SQRT(ITl**2*(TETlD**2+SYD**2*SIN(TETl)**2)+IAl**2*(PHIlD+...
SYD*COS(TETl))**2)
ANGL=SQRT((ITl*TETlD)**2+(SYD*SIN(TETl)*COS(TETl)*(ITl-IAl)-IAl*...
PHIlD)**2)/(IAl*(PHIlD+SYD*COS(TETl))*COS(TETl)+ITl*SYD*SIN(TETl)**2)
BETA=ATAN(ANGL)
W12=SQRT(TETlD**2+SYD**2*SIN(TETl)**2)
W3=PHIlD+SYD*COS(TETl)
M=SQRT(MX**2+MY**2+MZ**2)
SYD=INTGRL(SYD0,SYD2)
SY=INTGRL(SY0,SYD)
PHIlD=INTGRL(PHIlD0,PHIlD2)
PHIl=INTGRL(PHIl0,PHIlD)
TETlD=INTGRL(TETlD0,TETlD2)
TETl=INTGRL(TETl0,TETlD)
MT=INTGRL(M0,M)
PRTPLT SYD,PHIlD,TETl,H,BETA,W12,W3
PRINT MT
TIMER DELT=0.05,FINTIM=800,CUTDEL=5
FINISH W12=M,W3=N
CONTINUE
TIMER DELT=0.05,FINTIM=700,CUTDEL=5
PARAMETER TETl0=1.1486,PHIlD0=4.19,SYD0=0.4809,A=800,...
X=0,Y=0,Z=-1,M=10,N=0.01
END
TERMINAL
STOP
ENDJOB
```

```
LABEL DETUMBLING THEN DESPINING WITH A=1600
INITIAL
CONSTANT IA1=9529,IT1=212129,PHI10=0,SY0=0,TET1D0=0
DYNAMIC
PARAMETER TET10=1.1486,PHI1D0=4.19,SYD0=0.4809,A=1600,...
X=-1,Y=-1,Z=0,M=0.01,N=10,MO=0
B=AND(A,TET1)
C=B*A*TET1
MX=C*X*TET1D
MY=C*Y*SYD*SIN(TET1)
MZ=C*Z
TET1D2=(MX-IA1*(PHI1D+SYD*COS(TET1))*SYD*SIN(TET1))/IT1+SYD**2*...
SIN(TET1)*COS(TET1)
SYD2=(MY-2*IT1*SYD*TET1D*COS(TET1)+IA1*(PHI1D+SYD*COS(TET1))*...
TET1D)/(IT1*SIN(TET1))
PHI1D2=MZ/IA1-SYD2*COS(TET1)+SYD*TET1D*SIN(TET1)
H=SQRT(IT1**2*(TET1D**2+SYD**2*SIN(TET1)**2)+IA1**2*(PHI1D+...
SYD*COS(TET1))**2)
ANGL=SQRT((IT1*TET1D)**2+(SYD*SIN(TET1)*COS(TET1)*(IT1-IA1)-IA1*...
PHI1D)**2)/(IA1*(PHI1D+SYD*COS(TET1))*COS(TET1)+IT1*SYD*SIN(TET1)**2)
BETA=ATAN(ANGL)
W12=SQRT(TET1D**2+SYD**2*SIN(TET1)**2)
W3=PHI1D+SYD*COS(TET1)
M=SQRT(MX**2+MY**2+MZ**2)
SYD=INTGRL(SYD0,SYD2)
SY=INTGRL(SY0,SYD)
PHI1D=INTGRL(PHI1D0,PHI1D2)
PHI1=INTGRL(PHI10,PHI1D)
TET1D=INTGRL(TET1D0,TET1D2)
TET1=INTGRL(TET10,TET1D)
MT=INTGRL(MO,M)
PRTPLT SYD,PHI1D,TET1,H,BETA,W12,W3
PRINT MT
TIMER DELT=0.05,FINTIM=600,OUTDEL=0.5
FINISH W12=0.200
```

```
END
TERMINAL
STOP
ENDJOB
```

```
LABEL DETUMBLING THEN DESPINING WITH A=3000
INITIAL
CONSTANT IA1=9529,IT1=212129,PHI10=0,SY0=0,TET1D0=0
DYNAMIC
PARAMETER TET10=1.1486,PHI1D0=4.19,SYD0=0.4809,A=3000,...
X=-1,Y=-1,Z=0,M=0.01,N=10,M0=0
B=AND(A,TET1)
C=B*A*TET1
MX=C*X*TET1D
MY=C*Y*SYD*SIN(TET1)
MZ=C*Z
TET1D2=(MX-IA1*(PHI1D+SYD*COS(TET1))*SYD*SIN(TET1))/IT1+SYD**2*...
SIN(TET1)*COS(TET1)
SYD2=(MY-2*IT1*SYD*TET1D*COS(TET1)+IA1*(PHI1D+SYD*COS(TET1))*...
TET1D)/(IT1*SIN(TET1))
PHI1D2=MZ/IA1-SYD2*COS(TET1)+SYD*TET1D*SIN(TET1)
H=SQRT(IT1**2*(TET1D**2+SYD**2*SIN(TET1)**2)+IA1**2*(PHI1D+...
SYD*COS(TET1))**2)
ANGL=SQRT((IT1*TET1D)**2+(SYD*SIN(TET1)*COS(TET1)*(IT1-IA1)-IA1*...
PHI1D)**2)/(IA1*(PHI1D+SYD*COS(TET1))*COS(TET1)+IT1*SYD*SIN(TET1)**2)
BETA=ATAN(ANGL)
W12=SQRT(TET1D**2+SYD**2*SIN(TET1)**2)
W3=PHI1D+SYD*COS(TET1)
M=SQRT(MX**2+MY**2+MZ**2)
SYD=INTGRL(SYD0,SYD2)
SY=INTGRL(SY0,SYD)
PHI1D=INTGRL(PHI1D0,PHI1D2)
PHI1=INTGRL(PHI10,PHI1D)
```

```
TET1D=INTGRL(TET1D0,TET1D2)
TET1=INTGRL(TET10,TET1D)
MT=INTGRL(M0,M)
PRTPLT SYD,PHI1D,TET1,H,BETA,W12,W3
PRINT MT
TIMER DELT=0.05,FINTIM=600,CUTDEL=5
FINISH W12=0.200
END
TERMINAL
STOP
ENDJOB
```

C. DESPIN THEN DETUMBLE

```
LABEL DESPINING THEN DECONING WITH A=800
INITIAL
CONSTANT IA1=9529,IT1=212129,PHI10=0,SY0=0,TET1D0=0
DYNAMIC
PARAMETER TET10=1.1486,PHI1D0=4.19,SYD0=0.4809,A=800,...
X=0,Y=0,Z=-1,M=10,N=0.01,M0=0
B=AND(A,TET1)
C=B*A*TET1
MX=C*X*TET1D
MY=C*Y*SYD*SIN(TET1)
MZ=C*Z
TET1D2=(MX-IA1*(PHI1D+SYD*COS(TET1))*SYD*SIN(TET1))/IT1+SYD**2*...
SIN(TET1)*COS(TET1)
SYD2=(MY-2*IT1*SYD*TET1D*COS(TET1)+IA1*(PHI1D+SYD*COS(TET1))*...
TET1D)/(IT1*SIN(TET1))
PHI1D2=MZ/IA1-SYD2*COS(TET1)+SYD*TET1D*SIN(TET1)
H=SQRT(IT1**2*(TET1D**2+SYD**2*SIN(TET1)**2)+IA1**2*(PHI1D+...
SYD*COS(TET1))**2)
```

```
ANGL=SQRT((IT1*TET1D)**2+(SYD*SIN(TET1)*COS(TET1)*(IT1-IA1)-IA1*...
PHI1D)**2)/(IA1*(PHI1D+SYD*COS(TET1))*COS(TET1)+IT1*SYD*SIN(TET1)**2)
BETA=ATAN(ANGL)
W12=SQRT(TET1D**2+SYD**2*SIN(TET1)**2)
W3=PHI1D+SYD*COS(TET1)
M=SQRT(MX**2+MY**2+MZ**2)
SYD=INTGRL(SYD0,SYD2)
SY=INTGRL(SY0,SYD)
PHI1D=INTGRL(PHI1D0,PHI1D2)
PHI1=INTGRL(PHI10,PHI1D)
TET1D=INTGRL(TET1D0,TET1D2)
TET1=INTGRL(TET10,TET1D)
MT=INTGRL(M0,M)
PRTPLT SYD,PHI1D,TET1,H,BETA,W12,W3
PRINT MT
TIMER DELT=0.05,FINTIM=150,OUTDEL=5
FINISH W12=M,W3=N
CONTINUE
TIMER DELT=0.05,FINTIM=600,OUTDEL=5
PARAMETER TET10=1.1486,PHI1D0=4.19,SYD0=0.4809,A=800,...
X=-1,Y=-1,Z=0,M=0.01,N=10
PRTPLT SYD,PHI1D,TET1,H,BETA,W12,W3
END
TERMINAL
STOP
ENDJOB
```

APPENDIX 2

CSMP PROGRAM FOR CHAPTER 4

```
TITLE CSMP SIMULATION OF THE SATELLITE-FFTO SYSTEM
INITIAL
          D1=M*MS*LSF/(M+MS)
  CONSTANT K1=10000.,K2=100000.,K3=10000.,K4=100000.,...
      K5=10000.,K6=100000.,L1=5.223,L5=0.75,LSF=7.0,...
      L=3.6385,I11=48.17,I22=61.5,I33=34.67,...
      J11=65016.7,J22=65016.7,J33=10000.0,M=200.0,...
      MS=6600.0,SINO=0.866,COSO=0.5
DYNAMIC
      K=1000.0*RAMP(0.0)
      KS=1000.0*RAMP(0.0)
      WX=INTGRL(0.0,WXDOT)
      WY=INTGRL(0.0,WYDOT)
      WZ=INTGRL(0.0,WZDOT)
      VXS=INTGRL(-0.3464,VXSDOT)
      VYS=INTGRL(0.0,VYSDOT)
      VZS=INTGRL(1.300334,VZSDOT)
      C11=INTGRL(1.0,C11DOT)
      C12=INTGRL(0.0,C12DOT)
      C13=INTGRL(0.0,C13DOT)
      C21=INTGRL(0.0,C21DOT)
      C22=INTGRL(1.0,C22DOT)
      C23=INTGRL(0.0,C23DOT)
      C31=INTGRL(0.0,C31DOT)
      C32=INTGRL(0.0,C32DOT)
      C33=INTGRL(1.0,C33DOT)
      RS=INTGRL(0.0,RSDOT)
      R=INTGRL(0.0,RDOT)
      C11DOT=C12*WZ-C13*WY
      C12DOT=C13*WX-C11*WZ
      C13DOT=C11*WY-C12*WX
      C21DOT=C22*WZ-C23*WY
      C22DOT=C23*WX-C21*WZ
      C23DOT=C21*WY-C22*WX
      C31DOT=C32*WZ-C33*WY
      C32DOT=C33*WX-C31*WZ
      C33DOT=C31*WY-C32*WX
      SINR,COSR,SINRS,COSRS=SINCOS(R,RS)
      TXC=-K1*WX+K2*C11*(C23-C32)
      TYC=-K3*WY+K4*C22*(C31-C13)
      TZC=-K5*WZ+K6*C33*(C12-C21)
      H=SQRT((J11*VXS)**2+(J22*VYS)**2+(J33*VZS)**2)
      WZDOT=(K*RDOT+TZC-(I22-I11)*WX*WY)/I33
      VZSDOT=-KS*RSDOT/J33
      RDOT=-WZ+(WX*COSR+WY*SINR)*COSO/SINO-(VXS*COSRS-...
           VYS*SINRS)/SINO
      RSDOT=VZS-(WX*COSR+WY*SINR)/SINO+(VXS*COSRS-...
            VYS*SINRS)*COSO/SINO
```

```
      D2=C11DOT*WY-C12DOT*WX
      D3=C21DOT*WY-C22DOT*WX
      D4=C31DOT*WY-C32DOT*WX
      D5=(C11*COSR+C12*SINR)*D2+(C21*COSR+C22*SINR)*D3...
         +(C31*COSR+C32*SINR)*D4
      D6=(-C11*SINR+C12*COSR)*D2+(-C21*SINR+C22*COSR)*...
         D3+(-C31*COSR+C32*COSR)*D4
      D7=C13*D2+C23*D3+C33*D4
      D8=D1*(L+L1*COSO)

      D9=D8*COSR
      D10=D8*SINR
      D11=D6*D8+KS*RSDOT/SINO-K*RDOT*COSO/SINO
      D12=L*D1*D5+L1*D1*D7*SINO
      D13=-L1*D1*D6+(K*RDOT-KS*RSDOT*COSO)/SINO
      D14=(J33-J22)*VYS*VZS*SINRS+(J11-J33)*VXS*VZS*...
          COSRS+L1*D1*(D5*COSO-D7*SINO)
      D15=D8*SINR
      D16=D8*COSR
      B1=-(I33-I22)*WY*WZ+D11*COSR+L5*D1*D6*COSR+...
         (D12+D14)*SINR+D1*L5*D5*SINR+TXC
      B2=-(I11-I33)*WX*WZ+D11*SINR+L5*D1*D6*SINR-...
         (D12+D14)*COSR-D1*L5*D5*COSR+TYC
      B3=D13+L1*D1*D6-(J33-J22)*VYS*VZS*COSRS+(J11-...
         J33)*VXS*VZS*SINRS
      B4=VXS*COSRS*RSDOT-VYS*SINRS*RSDOT+WX*COSR*RDOT...
         +WY*SINR*RDOT
      A11=I11+D9*COSR+D1*L5+D15*SINR
      A12=D10*COSR-D16*SINR
      A13=-J11*SINRS*SINR
      A14=-J22*COSRS*SINR
      A21=D9*SINR-D15*COSR
      A22=I22+D1*L5+D10*SINR+D16*COSR
      A23=J11*SINRS*COSR
      A24=J22*COSRS*COSR
      A33=J11*COSRS
      A34=-J22*SINRS
      A41=-SINR
      A42=COSR
      A43=-SINRS
      A44=-COSRS
      WXDOT,WYDOT,VXSDOT,VYSDOT=SUBXYZ(B1,B2,B3,B4,...
          A11,A12,A13,A14,A21,A22,A23,A24,A33,A34,...
          A41,A42,A43,A44)
TIMER FINTIM=100.0,OUTDEL=0.8
PRTPLT WX,WY,WZ,VXS,VYS,VZS,C11,C22,C33,RSDOT,RDOT,...
       RS,R,TXC,TYC,TZC,H
LABEL CSMP SIMULATION OF THE SATELLITE-FFTO SYSTEM
END
STOP
```

```
C THIS SUBROUTINE IS USED TO CHANGE THE ARGUMENT TO BE
C LESS THAN 18*2*PI BEFORE CALL 'SIN' AND 'COS'
C (ARGUMENT OF LIBRARY SUBROUTINES 'SIN' AND 'COS' IS
C LIMITED TO 18*2*PI)
C
      SUBROUTINE SINCOS(R,RS,SINR,COSR,SINRS,COSRS)
      REAL LIMIT
      LIMIT=2.0*18.0*3.141592653
      IR=R/LIMIT
      AR=R-IR*LIMIT
      SINR=SIN(AR)
      COSR=COS(AR)
      IRS=RS/LIMIT
      ARS=RS-IRS*LIMIT
      SINRS=SIN(ARS)
      COSRS=COS(ARS)
      RETURN
      END
```

```
C THIS FORTRAN SUBROUTINE IS USED TO CHANGE THE
C UNSUBSCRIPTED ARRAY INTO SUBSCRIPTED ONE BEFORE
C CALL SUBROUTINE 'SIMQ' (SUBSCRIPTED ARRAY IS NOT
C PERMITTED IN CSMP)
C
      SUBROUTINE SUBXYZ(B1,B2,B3,B4,A11,A12,A13,A14,A21,
     C   A22,A23,A24,A33,A34,A41,A42,A43,A44,WXDOT,WYDOT,
     C   VXSDOT,VYSDOT)
      DIMENSION A(4,4),B(4)
      N=4
      A(1,1)=A11
      A(1,2)=A12
      A(1,3)=A13
      A(1,4)=A14
      A(2,1)=A21
      A(2,2)=A22
      A(2,3)=A23
      A(2,4)=A24
      A(3,1)=0.0
      A(3,2)=0.0
      A(3,3)=A33
      A(3,4)=A34
      A(4,1)=A41
      A(4,2)=A42
      A(4,3)=A43
      A(4,4)=A44
      B(1)=B1
      B(2)=B2
      B(3)=B3
      B(4)=B4
      CALL SIMQ(A,B,N,KS)
```

```
      WXDOT=B(1)
      WYDOT=B(2)
      VXSDOT=B(3)
      VYSDOT=B(4)
      RETURN
      END
```

```
C THIS SUBROUTINE IS USED TO SOLVE A SET OF SIMULTANEOUS
C LINEAR EQUATIONS
C
      SUBROUTINE SIMQ(A,B,N,KS)
      DIMENSION A(1),B(1)
C
C        FORWARD SOLUTION
C
      TOL=0.0
      KS=0
      JJ=-N
      DO 65 J=1,N
      JY=J+1
      JJ=JJ+N+1
      BIGA=0
      IT=JJ-J
      DO 30 I=J,N
C
C        SEARCH FOR MAXIMUM COEFFICIENT IN COLUMN
C
      IJ=IT+I
      IF(ABS(BIGA)-ABS(A(IJ))) 20,30,30
   20 BIGA=A(IJ)
      IMAX=I
   30 CONTINUE
C
C        TEST FOR PIVOT LESS THAN TOLERANCE
C
      IF(ABS(BIGA)-TOL) 35,35,40
   35 KS=1
      RETURN
C
C        INTERCHANGE ROWS IF NECESSARY
C
   40 I1=J+N*(J-2)
      IT=IMAX-J
      DO 50 K=J,N
      I1=I1+N
      I2=I1+IT
      SAVE=A(I1)
      A(I1)=A(I2)
      A(I2)=SAVE
```

```
C
C         DIVIDE EQUATION BY LEADING COEFFICIENT
C
   50 A(I1)=A(I1)/BIGA
      SAVE=B(IMAX)
      B(IMAX)=B(J)
      B(J)=SAVE/BIGA
C
C         ELIMINATE NEXT VARIABLE
C
      IF(J-N) 55,70,55
   55 IQS=N*(J-1)
      DO 65 IX=JY,N
      IXJ=IQS+IX
      IT=J-IX
      DO 60 JX=JY,N
      IXJX=N*(JX-1)+IX
      JJX=IXJX+IT
   60 A(IXJX)=A(IXJX)-(A(IXJ)*A(JJX))
   65 B(IX)=B(IX)-(B(J)*A(IXJ))
C
C         BACK SOLUTION
C
   70 NY=N-1
      IT=N*N
      DO 80 J=1,NY
      IA=IT-J
      IB=N-J
      IC=N
      DO 80 K=1,J
      B(IB)=B(IB)-A(IA)*B(IC)
      IA=IA-N
   80 IC=IC-1
      RETURN
      END
```